

Synthesis of Novel Ligands for Extraction of Metal Ions from Aqueous Medium and Theoretical Investigation for the Extraction Mechanism

By

AMRITA DAS

CHEM01201104009

BHABHA ATOMIC RESEARCH CENTRE

*A thesis submitted to the
Board of Studies in Chemical Science*

*In partial fulfillment of requirements
For the degree of*

DOCTOR OF PHILOSOPHY

of

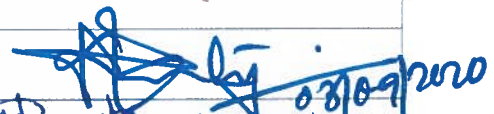
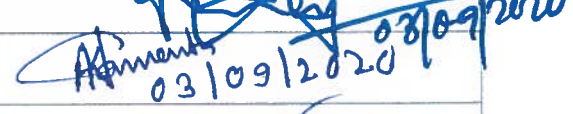
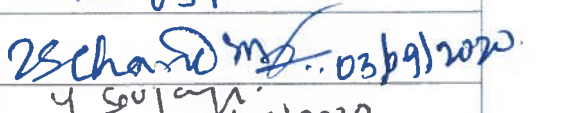
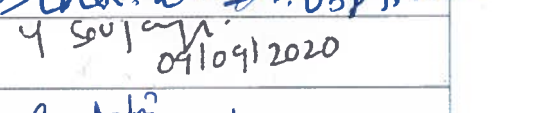
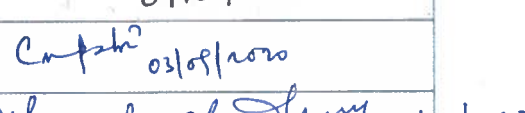
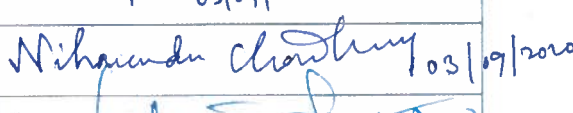
HOMI BHABHA NATIONAL INSTITUTE



February, 2020

Recommendations of the Viva Voce Board

As members of the Viva Voce board, we certify that we have read the dissertation prepared by AMRITA DAS entitled "Synthesis of Novel Ligands for Extraction of Metal Ions from Aqueous Medium and Theoretical Investigation for the Extraction Mechanism" and recommend that it may be accepted as fulfilling the dissertation requirement for the Degree of Doctor of Philosophy.

Doctoral Committee	Present Members	Signature with Date
Chairman	Dr. D. K. Maity	 03/09/2020
Convener (Guide)	Dr. A. K. Samanta	 03/09/2020
Co-Guide	Dr. K. R. S. Chandrakumar	 03/09/2020
External Examiner	Dr. Y. Soujanya (through VC)	 04/09/2020
Member-1	Dr. C. N. Patra	 03/09/2020
Member-2	Dr. N. Choudhury	 03/09/2020
Member-3	Dr. C. Majumder (through VC)	 03/09/2020

Final approval and acceptance of this dissertation is contingent upon the candidate's submission of the final copies of the dissertation to HBNI.

We hereby certify that we have read this dissertation prepared under my direction and recommend that it may be accepted as fulfilling the dissertation requirement.

Guide:



Dr. A. K. Samanta

Date: 03/09/2020

Place: Mumbai

Co-Guide:



Dr. K. R. S. Chandrakumar

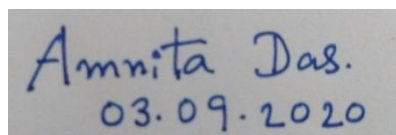
Date: 03/09/2020

Place: Mumbai

STATEMENT BY AUTHOR

This dissertation has been submitted in partial fulfillment of requirements for an advanced degree at Homi Bhabha National Institute (HBNI) and is deposited in the Library to be made available to borrowers under rules of the HBNI.

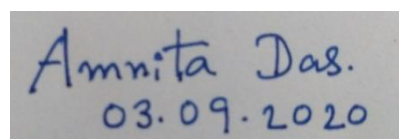
Brief quotations from this dissertation are allowable without special permission, provided that accurate acknowledgement of source is made. Requests for permission for extended quotation from or reproduction of this manuscript in whole or in part may be granted by the Competent Authority of HBNI when in his or her judgment the proposed use of the material is in the interests of scholarship. In all other instances, however, permission must be obtained from the author.

A rectangular box containing handwritten text in blue ink. The text reads "Amrita Das." on the first line and "03.09.2020" on the second line.

Amrita Das

DECLARATION

I, hereby declare that the investigation presented in the thesis has been carried out by me. The work is original and has not been submitted earlier as a whole or in part for a degree /diploma at this or any other Institution / University.

A rectangular box containing handwritten text in blue ink. The text reads "Amrita Das." on the first line and "03.09.2020" on the second line.

Amrita Das

List of Publications arising from the thesis

Journal

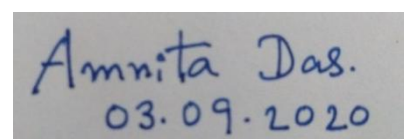
1. Assessment of phosphate functionalised silica gel (PFSG) for separation and recovery of uranium from simulated silicide fuel dissolver solution, A.Das, M.Sundararajan, B.Paul, S.chopade, A.K.Singh, V. Kain, Colloids and Surfaces A, 530(2017)124-133.
2. Evaluation of novel ligand dithiodiglycolamide (DTDGA) for separation and recovery of palladium from simulated spent catalyst dissolver solution, A. Das, R. Ruhela, A.K. Singh, R.C. Hubli, Separation and Purification Technology 125 (2014) 151-155.
3. Carrier mediated transport of Pd(II) from nitric acid medium using Dithiodiglycolamide (DTDGA) across a supported liquid membrane (SLM), S. Panja, R. Ruhela, A. Das, S. C. Tripathi, A. K. Singh, P. M. Gandhi, R. C. Hubli, Journal of Membrane Science 449 (2014) 67-73.
4. Enhanced adsorption and separation of zirconium and hafnium under mild conditions by phosphoric acid based ligand functionalized silica gels: Insights from experimental and theoretical investigations, A. Das, K. R. S. Chandrakumar, B. Paul, S.M. Chopade, S. Majumdar, A. K. Singh, V. Kain, Separation and Purification Technology 239 (2020) 116518.
5. Sorption of uranium from aqueous medium by functionalised silica gels: Effect of anions, A. Das, K. R. S. Chandrakumar, R. Banerjee, R. S. Dutta, B. Paul, S. M. Chopade, S. Majumdar, A. K. Singh, V. Kain. (Communicated)
6. Separation of uranium and rare earths by DHAFSG, A. Das, K.R.S. Chandrakumar, R. Banerjee, R.S. Dutta, B. Paul, S. M. Chopade, S. Majumdar, A. K. Singh, V. Kain. (Communicated)

Conference/Symposium

1. Recovery of uranium from uranium bearing black shale, A.Das, M.Yadav, A. K. Singh, ISMC-2016.
2. Evaluation of novel ligand dithiodiglycolamide (DTDGA) for separation and recovery of palladium from simulated spent catalyst dissolver solution, A. Das, R. Ruhela, N. Iyer, A.K. Singh, R.C. Hubli, SESTEC 2014.

Other Publications:

1. Novel imino diacetamide styrene divinyl benzene resin for separation of 99molybdenum from irradiated uranium–aluminium alloy , R. Ruhela, A. Rao, N. Iyer, A. Das, P. Kumar, A. K. Singh, B. S. Tomar, R. C. Hubli, RSC Adv., 2014, 4, 62654.
2. Separation and recovery of palladium from spent automobile catalyst dissolver solution using dithiodiglycolamide encapsulated polymeric beads, K. K. Singh, R. Ruhela, A. Das, M. Kumar, A. K. Singh, R. C. Hubli, P. N. Bajaj, Journal of Environmental Chemical Engineering 3 (2015) 95–103 .
3. Solvation energy of multiply charged anions and dielectric constant for finite system: a microscopic theory based bottom-up and top-down approach, A. K. Pathak, M. Tripathy, A.Das, A.K.Samanta, Molecular Physics, 2013, Vol. 111, No. 8, 975–982.



Amrita Das.
03.09.2020

Amrita Das

Dedicated to

My Son & Soumitra

Acknowledgment

I am extremely indebted to **Dr. Swapan. K. Ghosh**, former Head, Theoretical Chemistry Section, Chemistry Group, Bhabha Atomic Research Centre, Mumbai, my guide, **Dr. Alok. K. Samanta** and chairman of my PhD committee, **Dr. Dilip. K. Maity**, Associate Dean, HBNI, for giving me an opportunity to pursue my PhD work. I sincerely thank them for their crucial comments and precious suggestions in elevating my knowledge and improving the quality of work during this course of time. I am very fortunate to take this chance to declare that their enthusiastic interest and precious suggestions were of immense help during planning, implementation of the work and elucidation of the results. Their priceless guidance and continuous encouragement during the whole course of this study are immutable.

The thesis would not have been achievable without the guidance, assistance, support, decisive scrutiny and priceless suggestions from my co-guide **Dr. K. R. S. Chandrakumar** who has been actually important to me in completion of the work, for which I am tremendously thankful. I am also grateful to him for sharing his exceptional knowledge and scientific perceptiveness with me. His enthusiasm, profound commitment in research and significant investigation strategy of experimental and theoretical data has made an immense impression on me.

I am highly thankful to all of my doctoral committee members, **Dr. Chandra Nath Patra**, **Dr. Nihar Choudhury** and **Dr. Chiranjib Majumder** for their constant encouragement, support, critical review and suggestions during the annual progress review and also in pre-synopsis viva-voce.

I am very thankful to **Shri Ajoy K. Singh**, Head, Hydrometallurgy Section, Materials Processing and Corrosion Engineering Division, BARC, **Dr. Vivekanand Kain**, Head, Materials Processing Division, Materials Group, BARC for their

immense support and scientific discussion in pursuing this work. I am extremely thankful to **Dr. M. Krishnan**, Head, Materials Group, **Dr. R. C. Hubli**, former Head, Materials Processing Division for their immense support in carrying out this work. I eagerly thank to **Dr. M. Sundararajan**, Theoretical Chemistry Section, **Dr. Ritesh Ruhela**, Hydrometallurgy Section, for their enormous support and scientific discussion in carrying out this work.

I sincerely recognize the enormous support rendered to my research work by **Dr. Bhaskar Paul** and **Dr. Sanjib Majumdar**, Materials Processing and Corrosion Engineering Division, Materials Group, **Dr. R. S. Dutta**, Head, Surface Characterization Section, Materials Science Division, **Mrs. Rumu Halder Banerjee**, Surface Characterization Section, **Shri Suresh M. Chopade** and **Shri P. Sonawane**, Chemistry Division, without which the thesis would not have been possible.

I am glad to express my gratefulness towards my parents for their love and care for me. I couldn't have accomplished this without them. I am most grateful to my husband, **Dr. Soumita Das**, for his love, suggestion, support and patience that permitted me to complete this work.

CONTENTS

	<u>Page no</u>
Synopsis	xvii-xxv
List of Figures	xxvi-xxx
List of Tables	xxxi
Chapter 1 Introduction	
1.1. Solvent Extraction Method.....	2
1.1.1. Limitations of Solvent Extraction.....	4
1.2. Solid Phase Extraction (SPE) Method.....	5
1.2.1. Limitations of SPE.....	5
1.3. Membrane Extraction Method.....	6
1.3.1. Limitations of Membrane Technique.....	7
1.4. Types of Extractants	7
1.4.1. Phosphorus based Ligands.....	8
1.4.2. Nitrogen based Ligands.....	8
1.4.3. Sulfur based Ligands.....	9
1.4.4. Other Ligands.....	10
1.5. Extraction of Important Metal Ions from Aqueous Medium.....	10
1.5.1. Applications of Important Metal Ions.....	11
1.5.1.1. Applications and Health Impact of Uranium	11
1.5.1.2. Applications of Zirconium.....	11
1.5.1.3. Applications of Rare Earth Elements.....	12
1.5.1.4. Applications of Palladium.....	12
1.5.1.5. Applications and Health Impact of Other Heavy Elements.....	13
1.5.2. Sources of Metal Ions of Importance.....	14

1.5.2.1.	Sources of Uranium.....	14
1.5.2.2.	Sources of Zirconium	16
1.5.2.3.	Sources of Rare Earth Elements.....	16
1.5.2.4.	Sources of Palladium.....	17
1.5.2.5.	Sources of Heavy Metals.....	18
1.6.	Theoretical Investigation on Metal-Ligand Binding	18
1.7.	Objective of Present Work.....	20
	References.....	21

Chapter 2 Synthesis, Characterisation and Experimental Techniques

2.1.	Synthesis and Characterisation of Functionalised Silica Gels.....	30
2.1.1.	Synthesis & Characterisation of Single Phosphate Functionalised Silica Gel (SPFSG).....	30
2.1.1.1.	Synthesis of Single Phosphate Functionalised Silica Gel (SPFSG).....	30
2.1.1.2.	Characterization Studies for SPFSG.....	30
2.1.1.2.1.	FT-IR Study for SPFSG.....	30
2.1.1.2.2.	SEM and EDS Study for SPFSG.....	31
2.1.1.2.3.	TGA Study for SPFSG.....	32
2.1.1.2.4.	XPS Study for SPFSG.....	33
2.1.2.	Synthesis & Characterisation of Mono-Phosphate Functionalised Silica Gel (MPFSG).....	34
2.1.2.1.	Synthesis of MPFSG.....	34
2.1.2.2.	Characterization Studies for MPFSG.....	34
2.1.2.2.1.	FT-IR Spectra of MPFSG.....	34
2.1.2.2.2.	EDS Spectra of MPFSG.....	35

2.1.3. Synthesis and Characterisation of Bi-Phosphate Functionalised Silica Gel (BPFSG).....	35
2.1.3.1. Synthesis of BPFSG.....	35
2.1.3.2. Characterisation of BPFSG.....	36
2.1.3.2.1. FT-IR Study for BPFSG.....	36
2.1.3.2.2. XPS Study for BPFSG.....	37
2.1.4. Synthesis and Characterisation of Tri-Phosphate Functionalised Silica Gel (TPFSG).....	37
2.1.4.1. Synthesis of TPFSG.....	37
2.1.4.2. Characterisation of TPFSG.....	38
2.1.4.2.1. FT-IR Spectra of TPFSG.....	38
2.1.4.2.2. SEM-EDS Study of TPFSG.....	38
2.1.4.2.3. XPS Study of TPFSG.....	39
2.1.5. Synthesis and Characterisation of Amine and AmidoPyridyl Phosphate Functionalised Silica Gel (AAPPFSG).....	39
2.1.5.1. Synthesis of AAPPFSG.....	39
2.1.5.2. Characterisation of AAPPFSG	40
2.1.5.2.1. FT-IR Spectra of AAPPFSG	40
2.1.5.2.2. SEM-EDS Spectra of AAPPFSG	42
2.1.5.2.3. XPS Spectra of AAPPFSG	42
2.1.6. Synthesis and Characterisation of 1,8-dihydroxy anthraquinone Functionalised Silica Gel (DHAFSG)	43
2.1.6.1. Synthesis of DHAFSG.....	43
2.1.6.2. Characterisation of DHAFSG.....	43
2.1.6.2.1. FT-IR Spectra of DHAFSG.....	43

2.1.6.2.2. SEM-EDS Study of DHAFSG.....	44
2.1.7. Synthesis and Characterisation of AmidoPyridylAmine Functionalised Silica Gel (APAFSG).....	44
2.1.7.1. Synthesis of APAFSG	44
2.1.7.2. Characterisation of APAFSG	45
2.1.8. Synthesis and Characterisation of Butanol Functionalised Silica Gel (BFSG)	46
2.1.8.1. Synthesis of BFSG	46
2.1.8.2. Characterisation of BFSG	47
2.2. Experiments and Analysis.....	47
2.2.1. Reagents and Solution Preparations.....	47
2.2.1.1. Reagents.....	47
2.2.1.2. Preparation of Solutions and Analysis.....	48
2.2.2. Solid Phase Extraction (SPE) Method: Sorption Experiments.....	50
2.2.2.1. Sorption Equilibration.....	50
2.2.2.2. Sorption Extraction.....	50
2.2.2.3. pH Variation of Feed Solution	51
2.2.2.4. Sorption Kinetics Studies	51
2.2.2.4.1. Pseudo 1 st -Order Kinetic Model.....	51
2.2.2.4.2. Pseudo 2 nd -Order Kinetic Model.....	51
2.2.2.5. Sorption Isotherm Studies.....	52
2.2.2.5.1. Langmuir Isotherm Model.....	52
2.2.2.5.2. Freundlich Isotherm Model.....	52
2.2.2.6. Determination of Loading Capacity.....	52
2.2.2.7. Thermodynamic Studies.....	53

2.2.2.8. Effect of the Metal Ions on Sorption.....	54
2.2.2.9. Desorption and Re-usability.....	54
2.2.2.10. Column Studies.....	55
2.2.3. Liquid-Liquid Extraction Studies.....	55
2.2.3.1. Solvent Extraction Studies.....	55
2.2.3.2. Supported Liquid Membrane (SLM) Studies.....	56
References.....	56

Chapter 3 Selective Separation of Uranium with Phosphate Functionalised Silica Gels

3.1 Introduction.....	60
3.2 Results and Discussion	62
3.2.1 Kinetics Studies.....	62
3.2.2 Effect of pH of Feed Solution on Uranium Sorption.....	64
3.2.3 Sorption Isotherm Studies.....	66
3.2.4 Effect of other Metal Ions on Uranium Sorption	67
3.2.5 Desorption Studies and Reusability of Sorbents.....	68
3.2.6 Separation and Recovery of Uranium from SSFSDS.....	69
3.2.7 Quantum Chemical Studies on the Binding Ability of Uranyl Ion with the Ligand.....	70
3.3 Conclusions.....	70
References.....	71

Chapter 4 Effect of Amido Pyridyl Functional Group in Phosphate Functionalised Silica Gels on the Enhanced Separation of Zirconium from Hafnium

4.1. Introduction.....	79
4.2. Results and Discussion.....	81
4.2.1. Effect of pH of Feed Solution on Zr and Hf Sorption.....	81
4.2.2. Kinetics Studies.....	82

4.2.3. Sorption Isotherm Studies.....	84
4.2.4. Loading Capacities (mg/g) of Zirconium and Hafnium on to Loaded Functionalised Silica Gels.....	85
4.2.5. Desorption Studies for Zirconium and Hafnium from Loaded Functionalised Silica Gels.....	86
4.2.6. Column Studies.....	87
4.2.7. Quantum Chemical Studies on the Sorption Behaviour of Zr and Hf with Phosphate Functionalised Silica Gel.....	87
4.3 Conclusions.....	89
References.....	89

Chapter 5 Separation of Actinides from Rare Earth Metals by Dihydroxy Anthraquinone and Ethyl-Bis-Triazinylpyridine Based Ligands

5.1 Introduction.....	96
5.2. Results & Discussion.....	98
5.2.1. Sorption Studies of Rare Earths and Uranium using 1,8-Dihydroxy Anthraquinone Functionalised Silica Gel (DHAFSG) by Solid Phase Extraction (SPE) Technique.....	98
5.2.1.1. pH Variation of Feed Solution.....	98
5.2.1.2. Sorption Kinetics Studies.....	99
5.2.1.3. Sorption Isotherm Studies.....	100
5.2.1.4. Studies for Loading Capacities of Rare Earths and Uranium on DHAFSG.....	101
5.2.1.5. Separation of Rare Earths and Uranium from Loaded DHAFSG.....	102
5.2.1.6. Theoretical Studies on the Complexation Behaviour of Rare Earths and Uranium with DHAFSG.....	102

5.2.2. Separation Studies of Rare Earths and Actinides using Ethyl-Bis-Triazinyl Pyridine (Et-BTP) by Solvent Extraction Technique	104
5.2.2.1. Choice of Appropriate Diluents for Et-BTP solvent.....	105
5.2.2.2. Role of Alpha-Bromo Carboxylic Acids and Chlorinated Cobalt Dicarbolide (CCD) as Auxiliary Lligands.....	106
5.2.2.3. Effect of Variation of CCD Concentration.....	107
5.2.2.4. Effect of Variation of Et-BTP Concentration.....	108
5.2.3. Separation Studies of Rare Earths and Actinides using Ethyl-Bis-Triazinyl Pyridine (Et-BTP) by Supported Liquid Membrane (SLM) Technique	109
5.3. Conclusion.....	110
References.....	111

Chapter 6 Separation and Enhanced Recovery of Palladium using Dithio Diglycol Amide (DTDGA) Ligand

6.1 Introduction.....	113
6.2. Results and Discussion.....	115
6.2.1. Solvent Extraction Studies with DTDGA Ligand.....	115
6.2.1.1. Extraction Kinetics.....	115
6.2.1.2. Effect of Feed Acidity.....	115
6.2.1.3. Effect of DTDGA Ligand Concentration	117
6.2.1.4 Effect of Diluents.....	117
6.2.1.5 Back Extraction of Palladium from Loaded DTDGA.....	118
6.2.1.6 Extraction Behavior of DTDGA from SSCD Solution.....	119
6.2.2. Membrane Studies with DTDGA Ligand.....	119
6.2.2.1. Effect of Feed Nitric Acid Concentration.....	119
6.2.2.2 Effect of DTDGA Concentration.....	121
6.2.2.3 Effect of Membrane Pore Size	122

6.2.2.4. Membrane Thickness.....	123
6.2.2.5. Selectivity over other Fission Products.....	125
6.2.2.6. Stability of Membrane.....	126
6.3. Conclusion.....	127
References.....	127
Chapter 7 Separation of Lead, Zinc, Copper, Chromium from Aqueous Medium	
7.1. Introduction.....	131
7.2. Results and Discussion.....	132
7.2.1. Sorption Extraction of Lead, Zinc, Copper and Chromium	132
7.2.2. Loading Capacities.....	134
7.2.3. Comparison of Extraction with Other Sorbents.....	135
7.2.4. Thermodynamic Studies.....	136
7.3. Conclusion.....	138
References.....	139
Chapter 8 Summary and Conclusion.....	146

SYNOPSIS

Extraction is a method used for the separation, pre-concentration and removal of metal ions from different industrial process streams like mining industry, leather industry, nuclear industry, chemical production industry etc. The metal ions generated in the process streams are required to be separated for their valuable re-usage as well as safe disposal of the process streams into the environment as they are hazardous to human health. Different methods have so far been adopted for the extraction and separation of metal ions from aqueous streams like precipitation, solvent extraction, membrane separation and solid phase extraction (SPE) etc. Solvent extraction method is used when the metal ion concentration in the aqueous phase is $>1\text{gL}^{-1}$. This method is a liquid-liquid separation technique where the aqueous phase (liquid phase) containing the metal ions is equilibrated with an organic solvent phase (liquid phase). The metal ions present in the aqueous phase distribute itself into the organic solvent (chosen as selective towards the metal ion of interest) phase and the aqueous phase after equilibration. The metal ions are then extracted back into another aqueous phase containing suitable reagent (strip solution). Thus, the metal ions are extracted and separated as per the requirement. Solvent extraction method has major limitations like i) it uses large volume of organic solvent and therefore, not wise to use at low concentrations of metal ions, ii) solvent loss due to aqueous solubility of the valuable organic solvent, iii) degradation of solvent due to chemical and radiation effect etc.

In case of SPE method, metal ions distribute itself into the solid sorbent and the aqueous medium. SPE method is used when the concentration of metal ions in the solution is $<1\text{gL}^{-1}$. SPE method has some advantages like i) it is easy to operate, ii) economically viable, ii) no aqueous solubility of the sorbent support material. In the SPE method, the sorbents are of different types e.g., i) inorganic sorbents namely,

zeolite, bentonite, clay, silica, titanium dioxide etc., ii) chemically modified solid materials like polymers, silica gel, carbon-nanotubes, etc. Chemically modified sorbents provide a better selectivity towards the metal ion of interest.

Membrane technique also consists of one aqueous feed solution containing the metal ions, an organic phase where the metal ions are extracted from the feed solution and the strip solution where the metal ions are back extracted into the aqueous phase from the loaded organic phase. Membrane technique is also applicable till now to low concentration of metal ions ($\leq 0.5 \text{gL}^{-1}$).

Choice of the ligands suitable for the extraction of metal ions is vital for all these techniques discussed above. The ligands can be a cation exchanger, anion exchanger or, a chelating ligand depending upon the speciation of the metal ions present in the aqueous phase. There are many types of ligands reported for the extraction of metal ions from the aqueous phase. Cation exchanger like di(2-ethyl hexyl phosphoric acid) (DEHPA); neutral O-donor ligands like tributyl phosphate (TBP), octyl phenyl acid phosphate (OPAP), trioctyl phosphine oxide (TOPO), methyl-isobutyl ketone (MIBK); ligands with neutral soft donor atoms like 'S' and 'N' e.g. tris-iso-octyl amine (Adogen-364), di-n-octyl sulfide, α -benzoinoxime (ABO) [1] and benzoylmethylene triphenylphosphorane (BMTTP) [2]; Anion exchanger ligands like aliquat-336 are reported for the extraction and separation of various metal ions.

In spite of the fact that different types of ligands and their applications for extraction of various metal ions have been reported in the literature. These ligands have also some issues in their large scale applications. These limitations are primarily due to the different concerns like high aqueous solubility, low organic solubility, choice of proper diluent, degradation of ligand, selectivity towards metal ion, acidity

of aqueous feed solution along with several economical factors, etc. Therefore, demands for the search of new ligands is still in progress. Accordingly, the present work focusses on the extraction and separation of metal ions like uranium, zirconium-hafnium, rare earth elements and actinides, palladium, heavy metals from aqueous medium. In addition, we have also synthesised some novel ligands for the extraction of metal ions of our interest. The metal ions have been chosen as per our priority because of the reasons described below.

Uranium is the essential element in nuclear reactors [3-4]. Demands of the nuclear power are increasing steadily due to the fast decline of the fossil fuel resources and the associated environment pollution. Nuclear energy in this respect is a renewable long term source of energy. At different stages of nuclear fuel cycle, several wastages are generated in solid or, aqueous forms. Aqueous wastes generated from the spent nuclear fuels like high level waste (HLW), low level waste (LLW) etc. contains almost all the elements present in the periodic table in different percentages. Therefore, separation of valuable and required metal ions from these radioactive wastes are extremely important for their safe disposal. Zirconium has a wide application in nuclear industry especially it acts as a cladding material of nuclear fuel [4]. However, the naturally available zirconium always contains hafnium due to their similar physical and chemical properties [5]. Hafnium has a very high neutron absorption cross section which causes problem in nuclear reactor [6]. Thereby, separation of zirconium from hafnium is essential for the significant usage of zirconium in nuclear industry [7-8]. Rare earth elements have enormous applications in metallurgy, petroleum, textiles, agriculture, glass and glass polishing (e.g. erbium-doped fibre amplifiers), ceramics, catalysts, phosphors, magnets (e.g samarium-cobalt and neodymium-iron-boron high-flux rare-earth magnets), superconductors, opto-

electronics applications (e.g Nd-YAG laser). But naturally available rare earth ores contain actinides along with it [9]. High level waste (HLW) generated from nuclear industry also contains rare earth elements along with actinides and these rare earth elements create problem during vitrification of nuclear wastes. Therefore, rare earth elements need to be separated from actinides. Similarly, palladium is also found to have numerous applications in different fields [10]. Recovery of palladium from various secondary resources like high level waste (HLW) solutions [11] and, spent catalysts from automotive and petroleum industries [12] is essential. Heavy elements like lead, copper, zinc and chromium are also found to be one of the most common metal ions in aqueous streams from industrial wastes. These elements are hazardous to human health if inhaled or, ingested because they cause organ failure and permanent damages to human body. Removal of these elements from aqueous streams is essential and beneficial to our society.

In the present work, novel solid phase extractants namely, mono-phosphate functionalised silica gels (PFSGs), bi-phosphate functionalised silica gel (BPFSG), tri-phosphate functionalised silica gel (TPFSG), amine and amido pyridyl phosphate functionalised silica gel (AAPPFSG), 1,8-di-hydroxy anthraquinone functionalised silica gel (DHAFSG), amidopyridylamine functionalised silica gel (APAFSG) have been synthesised, characterised and evaluated for the metal value extraction from aqueous phase by SPE method. In addition to the SPE, we have also focused on the basis of liquid-liquid extraction techniques using the novel ligand N,N,N',N'-tetra(2-ethylhexyl)dithiodiglycolamide (DTDGA) for the separation and recovery of palladium from simulated spent automobile catalyst leach liquor and simulated high level waste. In addition to the experimental works, our work is also focused on the understanding of structure-activity relationship for the metal ion-ligand interactions

by employing quantum chemistry based theoretical investigations. Accordingly, we have carried out extensive theoretical calculations for the metal-ligand complexes using density functional theory (DFT) calculations. In particular, our modeling involves in obtaining the electronic structure of the metal-ligand complexes, ii) calculation of bond vibration frequencies and iii) thermodynamical and kinetical stability of the metal-ligand complexes. All the works reported in this thesis are presented into eight chapters as described below.

In the first chapter, concise introduction for the different extraction methods and novel ligands is presented. We have also focused on the different sources of solid and liquids wastages, primarily for uranium, palladium, zirconium and rare earth metals. The various methods available for separation and recovery of these metals have also been discussed in great detail. The extensive literature available on uranium, zirconium, rare earth metals and palladium recovery from different sources has been reviewed. Further, the possible applications of recovered metal values in nuclear and non-nuclear fields have also been stated. Details of the computational methods used for the elucidation of the complexation behavior of metal ions with suitable ligands have been illustrated. Lastly the motivation for this work has been explained.

In the second chapter, synthesis and characterization of functionalised silica gels using different instrumental techniques have been extensively discussed. Experimental details for the SPE method, solvent extraction and also for supported liquid membrane (SLM) separation methods have been discussed.

In the third chapter, details of uranium extraction from the nuclear wastages using single-phosphate functionalised silica gels (SPFSG), bi-phosphate functionalised silica gel (BPFSG), tri-phosphate functionalised silica gel (TPFSG), amine and amido pyridyl phosphate functionalised silica gel (AAPPFSG) have been

presented. Kinetics of sorption of uranium has been found to be fast using all these ligands and the kinetic data has been modeled well by pseudo second order kinetic model. Isotherm studies for the sorption of uranium have also been carried out. Tests have been carried out for the selectivity of the sorbents (using SPFSG sorbent) towards uranium over other metal ions and it has been found that the ligands have very high extractability and selectivity towards uranium over other metal ions e.g., iron, aluminium, magnesium, calcium etc. Back extraction of uranium from the loaded sorbent has been studied with solutions of varying pH in nitric acid medium. It has been observed that it is possible to extract >99% of uranium in multiple stages. This confirms the re-usability of the sorbents. Thermodynamic studies on the extraction behaviour of uranium from nitric acid medium have also been carried out using BPFSG, TPFSG and AAPPFSG. Theoretical calculations for binding of uranium with these functionalised ligands have also been carried out and these results have been found to be in good agreement with the experimental results.

In chapter four, separation of zirconium from hafnium using functionalised silica gels namely, mono-phosphate functionalised silica gel (MPFSG), bi-phosphate functionalised silica gel (BPFSG), amine and amido pridyl phosphate functionalised silica gel (AAPPFSG), has been discussed in details. Sorption behaviour of zirconium and hafnium with the variation of pH of feed solutions has been investigated. Kinetic studies for zirconium and hafnium are found to follow pseudo second order kinetic model for both zirconium and hafnium. Separation of hafnium from zirconium has been obtained at pH below pH 1.2. It has been observed that as the number of binding sites of the ligands increases, the selectivity towards zirconium increases. Therefore, separation of zirconium from hafnium is best obtained using AAPPFSG which has the

more number of binding sites compared to other ligands namely, MPFSG and BPFSG.

In the fifth chapter, separation of uranium from rare earth elements using 1,8-dihydroxyanthraquinone functionalised silica gel (DHAFSG) by sorption method and also the separation of actinides from lanthanides using ethyl-bis-triazinylpyridine (Et-BTP) by both solvent extraction and supported liquid membrane (SLM) method have been discussed. Sorption studies of uranium and rare earths namely, europium, samarium, ytterbium and yttrium have been carried out using DHAFSG sorbent. Variation of sorption of uranium and rare earths with the variation of pH of the feed solutions has been explored. Kinetics studies for uranium and rare earths have shown that sorption equilibrium takes place within 30 minutes. Desorption studies show that separation of uranium from rare earths is possible using DHAFSG sorbent. Et-BTP ligand has shown the selectivity towards americium over lanthanides with a combination with chlorinated cobalt dicarbollide (CCD) in nitrobenzene diluent in both solvent extraction and SLM techniques.

The sixth chapter deals with the extraction of palladium by solvent extraction as well as membrane techniques using the novel ligand namely N,N,N',N'-tetra-(2-ethylhexyl) dithiodiglycolamide (DTDGA). Separation of palladium using DTDGA ligand from simulated spent catalyst dissolver (SSCD) solution prepared in hydrochloric acid medium and high level waste (HLW) in nitric acid medium obtained from nuclear industry have been described. Very high extractability and selectivity are obtained for palladium over other metal ions present in SSCD solution. It has been observed that more than 99% back extraction of palladium is possible in a single stage with 0.1M thiourea in 0.1M hydrochloric acid medium. In membrane separation technique, DTDGA has been impregnated on supported microporous

membrane and tested for the extraction of palladium from high level liquid waste (HLW) in nitric acid medium. Various parameters like feed acidity, DTDGA concentration in membrane phase, membrane porosity etc. have been optimized to achieve maximum transport rate of palladium. Reusability of the membrane has also been tested.

In the seventh chapter, we present our results obtained for the sorption and removal of lead, zinc, copper and chromium from aqueous medium using butanol functionalised silica gel (BFSG) and amidopyridylamine functionalised silica gel (APAFSG). It has been observed that at neutral pH (i.e. pH 7), all the metals get sorbed as neutral species e.g., lead nitrate, zinc chloride, copper sulphate and potassium dichromate and therefore, the anions also play a major role in the complexation reactions. Details of the sorption thermodynamics of these hazardous metals have been studied and discussed in this chapter.

In the last chapter, a summary of the results and important conclusions drawn from all the above studies have been discussed broadly.

References

1. Separation of palladium from high level liquid waste of PUREX origin by solvent extraction and precipitation methods using oximes, A. Dakshinamoorthy, P. S. Dhani, P. W. Naik, S.K. Dudwadkar, S. K. Munshi, P. K. Dey, V. Venugopal, *Desalination*, 2008, 232, 26-36.
2. Extraction of fission palladium(II) from nitric acid by benzoylmethylenetriphenylphosphorane (BMTTP), M. M. Raj, A. D. Panchanatheswaran, K. A. Venkatesan, T. G. Srinivasan, P. R. V. Rao, *Hydrometallurgy*, 2006, 84, 118-124.
3. Source book of Atomic Energy, S. Glasstone, US Atomic Energy Commission, 1979.
4. Low enrichment dispersion fuels for research and test reactors, S. Nazare, *J. Nucl. Mater.*, 1984, 124, 14-24.

5. Zirconium and Hafnium Separation, Part 1. Liquid/Liquid Extraction in Hydrochloric Acid Aqueous Solution with Aliquat 336, L. Poriel, A. Favre-Re'guillon, S. Pellet-Rostaing, M. Lemaire, Separation Science and Technology, 2006, 41, 1927-1940.
6. Zirconium and hafnium metallurgy, B. K. Xiong, W. G. Wen, X. M. Yang, H. Y. Li, F.C. Luo, W. Zhang, J. M. Guo, Metallurgical Industry Press, Beijing, 2006.
7. Ferrocyanide method for separation of hafnium from zirconium, W. Schumb, F. Pittman, Ind. Eng. Chem. Anal. Ed., 2002, 14, 512-515.
8. Anion exchange of complex ions of hafnium and zirconium in HCl-HF mixtures, E. H. Huffman, R. C. Lilly, J. Am. Ceram. Soc., 1951, 73, 2902-2905.
9. A critical review on solvent extraction of rare earths from aqueous solutions, F. Xie, T. A. Zhang, D. Dreisinger, F. Doyle, Minerals Engineering, 2014, 56, 10-28.
10. Platinum Today, A. Cowley, M. Steel, Johnson Matthey Reports, London, 2007.
11. N,N,N',N'-tetra-(2-ethylhexyl)-thiodiglycolamide (T(2EH)TDGA): A novel ligand for the extraction of palladium from high level liquid waste (HLLW), R. Ruhela, J.N. Sharma, B.S. Tomar, S. Panja, S.C. Tripathi, R.C. Hubli, A.K. Suri, Radiochim. Acta, 2010, 98, 209-214.
12. Recovery and separation of palladium from spent catalyst, M. A. Barakat, M. H. H. Mahmoud, Y. S. Mahrous, Appl. Catal. A: Gen., 2006, 301, 182-186.

LIST OF FIGURES

	Page No
Figure 1.1 Supported liquid membrane set up.....	7
Figure 1.2 General processing of uranium from ores.....	14
Figure 1.3 Nuclear fuel cycle.....	15
Fig.2.1 Synthesis route of SPFSG.....	30
Fig.2.2 FTIR spectra of SPFSG.....	31
Fig.2.3 SEM spectra of SPFSG.....	32
Fig.2.4 EDS spectra of SPFSG (intensity vs. Kinetic energy (keV) plot).....	32
Fig.2.5 TGA spectra of SPFSG.....	32
Fig.2.6 (a) XPS spectra of SPFSG. Peaks at 126.5 eV, 178eV, 306 eV, 347 eV are due to residual impurities of Cu (3s), Ba (4p), Mg (KLL Auger), CaSO ₄ (Ca 2p) respectively which are present in the reagents used in the studies, (b) C1s peak at 284.6 eV in the XPS spectra of SPFSG.....	32
Fig.2.7 Synthesis scheme of MPFSG.....	34
Fig.2.8 FT-IR spectra of MPFSG.....	34
Fig.2.9 EDS spectra of MPFSG (intensity vs. kinetic energy (keV) plot).....	35
Fig.2.10 Synthesis scheme of BPFSG.....	36
Fig.2.11 FT-IR spectra of BPFSG.....	36
Fig.2.12 XPS study of BPFSG.....	37
Fig.2.13 Synthesis scheme of TPFSG.....	37
Fig.2.14 FT-IR spectra of TPFSG.....	38
Fig.2.15 (a) SEM spectra of TPFSG, (b) EDS spectra of TPFSG (intensity vs. kinetic energy (keV) plot).....	38

Fig.2.16 XPS spectra of TPFSG.....	39
Fig.2.17 Synthesis scheme of AAPPFSG.....	40
Fig.2.18 IR spectra of AAPPFSG.....	41
Fig.2.19 (a) SEM spectra of AAPPFSG, (b) EDS spectra of AAPPFSG (intensity vs. kinetic energy (keV) plot).....	42
Fig.2.20 XPS of AAPPFSG.....	42
Fig.2.21 Synthesis scheme of DHAFSG.....	43
Fig.2.22 FT-IR spectra of DHAFSG.....	44
Fig.2.23 (a) SEM spectra of DHAFSG, (b) EDS spectra of DHAFSG (intensity vs. kinetic energy (keV) plot).....	44
Fig.2.24 Synthesis scheme of APAFSG.....	45
Fig.2.25 FT-IR spectra of APAFSG.....	46
Fig.2.26 Synthesis of BFG.....	46
Fig.2.27 EDS spectra of BFG.....	47
Fig.3.1 Sorption kinetics for uranium: % sorption of uranium vs. time using (a) SPFSG, (b) BPFSG, TPFSG and AAPPFSG.....	63
Fig.3.2 Pseudo first order kinetic plots using (a) SPFSG, (b) BPFSG, TPFSG and AAPPFSG; pseudo second order kinetic plots using (c) SPFSG, (d) BPFSG, TPFSG and AAPPFSG for uranium sorption.....	63
Fig.3.3 Effect of feed pH on sorption of uranium on (a) SPFSG, (b) BPFSG, TPFSG and AAPPFSG.....	65
Fig.3.4 Isotherms for uranium sorption on to (a) SPFSG, (b) BPFSG, TPFSG and AAPPFSG.....	66
Fig.3.5 Sorption behaviour of uranium: Langmuir plot for (a) SPFSG, (b) BPFSG, TPFSG, and AAPPFSG	67

Fig.3.6 Sorption behaviour of uranium: Langmuir plot for (a) SPFSG, (b) BPFSG, TPFSG, and AAPPFSG.....	67
Fig.3.7 Effect of metal ions on sorption of uranium.....	68
Fig.3.8 Desorption of uranium vs. eluent pH.....	69
Fig.3.9 Reusability test for SPFSG sorbent: % sorption of uranium vs. no. of cycles plot.....	69
Fig.3.10 Optimized structure of uranyl bound to SPFSG.....	71
Fig.4.1 Effect of pH of feed solution on sorption of zirconium and hafnium.....	82
Fig.4.2 Sorption kinetics for zirconium and hafnium: % sorption vs. time (sec)..	83
Fig.4.3 (a) Pseudo first order and (b) pseudo second order kinetic plots for zirconium and hafnium sorption.....	83
Fig.4.4 Isotherm plot for zirconium and hafnium sorption	84
Fig.4.5 (a) Langmuir isotherm model, (b) Freundlich isotherm model for sorption of zirconium and hafnium	85
Fig.4.6 Desorption studies for zirconium and hafnium	86
Fig. 4.7 Column studies for zirconium and hafnium separation.....	87
Fig.4.8 Optimised geometries of zirconium with (a) MPFSG, (b) BPFSG and (c) AAPPFSG; and of hafnium with (d) MPFSG, (e) BPFSG and (f) AAPPFSG	88
Fig.5.1 Sorption of rare earths and uranium on DHAFSG.....	98
Fig.5.2 Sorption kinetics of rare earths and uranium on DHAFSG.....	99
Fig.5.3 Kinetic models fitting (a) pseudo first order and (b) pseudo second order kinetic model.....	100
Fig.5.4 Isotherm studies of rare earths and uranium on DHAFSG.....	100
Fig.5.5 Isotherm data for rare earths and uranium sorption on DHAFSG: (a) Langmuir plot, (b) Freundlich plot.....	101

Fig.5.6 Binding sites from anthraquinone ring of DHAFSG.....	103
Fig.5.7 DHAFSG complexes with (a) $\text{Eu}(\text{OH})_2 \cdot 4\text{H}_2\text{O}$, (b) $\text{Eu}(\text{OH}) \cdot 5\text{H}_2\text{O}$ and (c) $\text{UO}_2 \cdot 2\text{H}_2\text{O}$	103
Fig.5.8 Effect of variation of CCD concentration on the extraction of Am^{3+}	108
Fig.5.9 Effect of the variation of Et-BTP concentration on the extraction of Am^{3+}	108
Fig.5.10 Am(III) transport studies with i) only EDTA and ii) EDTA+chloroacetate buffer as the stripping agent. Feed: 0.1 M HNO_3 ; Organic phase: 0.02 M Et-BTP+0.005 M CCD in nitrobenzene.....	109
Fig.5.11 Transport of Am^{3+} , La^{3+} , Eu^{3+} , Nd^{3+} and Lu^{3+} using (0.02 M Et-BTP+ 0.005M CCD) ligands in (nitrobenzene + n-dodecane) diluent mixture. Feed: 0.1M HNO_3 ; Strip: 0.01 M EDTA in chloroacetate buffer (pH=3.5).....	110
Fig.6.1 Extraction kinetics of palladium by DTDGA solvent.....	115
Fig.6.2 Extraction of palladium by DTDGA solvent with variation of feed acidity.....	116
Fig.6.3 Variation of D_{Pd} at a fixed ionic strength of chloride ion.....	116
Fig.6.4 Mole ratio plot: variation of concentration of palladium in the organic phase with the change in $\text{DTDGA}/[\text{Pd}]_{\text{aq}}$	117
Fig.6.5 Distribution ratio of elements present in SSCD solution.....	119
Fig.6.6 Effect of nitric acid concentration in feed solution.....	120
Fig.6.7 Effect of DTDGA concentration on the transport of palladium through membrane.....	122
Fig.6.8 Effect of membrane pore size on the transport of palladium through the membrane.....	123

Fig.6.9 Effect of membrane thickness on the transport of palladium through the membrane	125
Fig.6.10 Transport behaviour of different elements using DTDGA carrier.....	126
Fig.6.11 Stability of membrane for Pd (II) transport using DTDGA ligand.....	127
Fig.7.1 Percentage sorption of Pb(II), Cu(II), Cr(VI) and Zn(II) on APAFSG, BFSG and ASG	133
Fig.7.2 Percentage sorption of Pb(II), Cu(II), Cr and Zn(II) on amine functionalised sorbent.....	133
Fig.7.3 Thermodynamic studies of Pb(II), Cu(II), Cr(VI) and Zn(II) on (a) APAFSG, (b) BFSG and (c) ASG.....	137

LIST OF TABLES

	Page No
Table 2.1 Simulated spent catalyst dissolver (SSCD) solution.....	49
Table 3.1 Sorption behaviour of elements present in SSFSDS on to SPFSG.....	70
Table 4.1 Loading capacities of zirconium and hafnium	86
Table 4.2 Geometrical parameter, binding energies and charge of the metal ions complexed with MPFSG, BPFSG and AAPPFSG with zirconium and hafnium.....	88
Table 5.1 Country wise production of rare earths.....	97
Table 5.2 Loading capacities of rare earths and uranium on DHAFSG.....	101
Table 5.3 Optimised bond lengths of Eu(III) and U(VI) complexes with DHAFSG.....	104
Table 5.4 Solubility of Et-BTP in different organic diluents.....	105
Table 5.5 Data of Am ³⁺ and Eu ³⁺ extraction and their separation with 0.02 M Et-BTP+0.4 M α -bromo-octanoic acid for different aqueous feed solutions.....	106
Table 5.6 Distribution ratio (D) of Am ³⁺ and Eu ³⁺ and their separation factors...	106
Table 6.1 Effect of diluents on the extraction of palladium.....	118
Table 6.2 Back extraction studies.....	118
Table 6.3 Permeability co-efficient (P) values for Pd(II) using DTDGA /n-dodecane organic phase.....	124
Table 7.1 Loading capacities of Pb(II), Cu(II), Zn(II) and Cr(VI).....	134
Table 7.2 Sorption of Pb(II), Cu(II), Zn(II) and Cr(VI) by different sorbents.....	135
Table 7.3 Enthalpy values of metal ligand complexes.....	137

Thesis Highlight

Name of the Student: Amrita Das

Name of the CI/OCC: Homi Bhabha National Institute

Enrolment No.: CHEM01201104009

Thesis Title: Synthesis of novel ligands for extraction of metal ions from aqueous medium and theoretical investigation for the extraction mechanism

Discipline: Chemical Sciences

Sub-Area of Discipline: Metal Extraction by Ligands

Date of viva voce: 3rd September, 2020

Metals are of enormous importance in our life. They are extremely required in different industries like nuclear, petroleum, electronics, catalysts, jewellery etc. The metal ions are extracted and separated from their primary sources like ores and also from the secondary resources like industrial aqueous streams, process effluents and disposed waste waters. It is very important to recover the metal values from the different resources for their further usage and safe disposal of the aqueous streams into the environment.

Here, focus was on the extraction and recovery of uranium from aqueous nitric acid medium, separation of zirconium from hafnium from aqueous streams, separation of rare earths from actinides, recovery of palladium from aqueous hydrochloric acid medium, removal of hazardous metals e.g. lead, copper, zinc, chromium from industrial waste waters. For this purpose, solid phase extraction and solvent extraction methods were adopted.

Different novel ligands were synthesised and tested for the extraction, separation and recovery of the metal ions of interest. The complexation and binding of the metal ions with the ligands have been studied at molecular level by molecular modelling studies. Their geometries were optimized, vibrational frequencies were calculated and binding energies were determined. The computational results explained well the

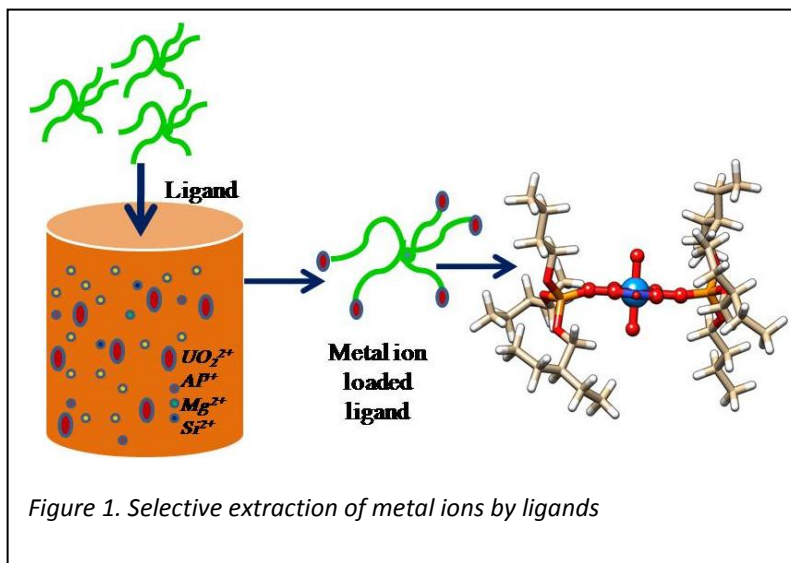


Figure 1. Selective extraction of metal ions by ligands

experimental observations. Phosphate functionalized silica gels has shown a good ability to recover uranium from nitric acid medium. Amine and amido pyridyl phosphate functionalized silica gel has shown ability of moderate separation of zirconium from hafnium under mild conditions. Palladium has been extracted successfully using dithiodiglycolamide from hydrochloric acid medium. Amine based ligands have shown more tendency to bind with the hazardous elements like lead, copper from aqueous medium.

Introduction

Separation and purification of metals have been carried out using different physical and pyrochemical processes for thousands of years. However, the approaches based on selective partitioning of metal ions using chemical means have been rather recent. The method of solvent extraction, for example, was first used at an analytical scale, to partition mercuric chloride from an aqueous solution into ether [1] only about a century ago. Solvent extraction has been extensively used for the separation of plutonium from uranium since 1942, after the importance of the study of their chemical and nuclear properties due to their role in nuclear weapons and nuclear energy was recognised. Research on finding a suitable extractant started in full swing and in 1949, tri-n-butyl phosphate (TBP) was found to be an efficient extractant for uranium and plutonium, and it led to the first PUREX (plutonium-uranium recovery and extraction) processing plant at the United States Savannah River site in 1951 [2]. Thereafter, solvent extraction has been quite successful in the production of high purity metals for nuclear defence and energy programs. A variety of selective metal extractants, has been discovered for extensive use of solvent extraction in nuclear reprocessing, waste treatment as well as other hydrometallurgical separations.

Among the other routes to separation, mention may be made of the use of CaCO_3 in a chromatographic mode [3] by Tswett, for separating biological pigments. This paved the way to the development of ion-exchange resins in 1935 and in fact ion exchange chromatography became quite well developed by the 1950s, which became instrumental in chemical confirmation in the initial report of the discovery of mendelevium [4]. By the 1970s, the field of separation science witnessed considerable

attention paid to the design and synthesis of ligands aiming at extraction of the metal ions. Membrane and supercritical fluid based processes for metal ion extraction also flourished receiving considerable attention even in later years.

Separation science has been of immense importance in different branches in science and technology that involve purification of metal ions, and in particular, their chemical separations have always received attention as an important area of research. However, with the growing demand from technology and societal needs, new priorities are continually being set. Thus, with the current research thrust areas such as environmental remediation, pollution prevention etc, production of ultrahigh pure metals for technological applications and consequently, demand for new and highly selective separation and purification processes are always on the rise. Although chemical separations, as used in almost every major industrial process, have been more or less standardised, there may be regulatory and economic incentives to improve efficiencies, need to implement pollution prevention strategies and minimize adverse environmental impacts etc, which will suggest ongoing attempt for renovation and research. Due to the availability of various techniques to a separation scientist, an evaluation of the factors influencing improved metal ion separations as well as the pros and cons of various available methods need to be discussed before attempting to discover newer strategies.

1.1.Solvent Extraction Method

Solvent extraction is a method used to separate metal ions based on their different solubility in to two immiscible liquid phases, usually water and an organic solvent. This method is also called a liquid-liquid extraction method. The aqueous phase containing the metal ions before extraction is called the feed solution. During solvent extraction process, the metal ions are transferred from the aqueous phase in to the

immiscible organic solvent. The two phases are then separated when the metal extraction is over. The remaining aqueous phase after extraction, depleted in the content of metal ions, is called the raffinate. The loaded organic solvent after extraction is then contacted with an aqueous phase containing suitable reagents to back-extract the metal ions in to the aqueous phase from the organic phase. Back-extraction of metal ions from the loaded solvent is termed as stripping. Successful solvent extraction process depends upon the choice of appropriate organic solvent which again depends upon the metal species present in the feed solution. There are four broad categories of solvents or, ligands used in the solvent extraction technique named as

- i) Solvating ligands
- ii) Cation exchangers
- iii) Anion exchangers
- iv) Chelating ligands

Solvating ligands which solvate the metal ions in their neutral form during extraction. Tributyl phosphate (TBP) [5], trioctyl phosphine oxide (TOPO) [6], methyl isobutyl ketone (MIBK) [7] are the solvating ligands commonly used for the extraction of uranium, plutonium, zirconium, hafnium, lead, zinc, iron, cadmium, etc. metal species from aqueous medium. Cation exchangers extract the metal ions present in the aqueous medium in their cationic form. Di-2-ethyl hexyl phosphoric acid (D₂EHPA) [8], naphthenic acid, versatic acid [9] etc. are the commonly used cation exchangers used for the extraction of copper, zinc, nickel, cobalt and silver present in the aqueous solution in their cationic forms. Anion exchangers can extract the metal ions present in their anionic form in the aqueous phase. Commonly used anion exchangers are alamine-336 and aliquat-336 [8] which are quarternary ammonium

salts used for the extraction of uranium, thorium, vanadium, cobalt complexes etc. present in anionic forms in the aqueous solutions. Chelating extractants form chelate with the metal ions present in the aqueous phase and extract them in to the organic phase. Commonly used chelating ligands are lix-63, lix-65 and kelex 100 [10] which are used to extract copper, nickel and cobalt from their aqueous solutions.

Solvent extraction method is used when the metal ion concentration in the aqueous solution is $>1\text{g/L}$. For the application of solvent extraction technique, the following criteria should be fulfilled.

- (i) The solvent should be highly selective for the metal ion of interest.
- (ii) Loading capacity of the solvent should be high for the metal ion so that metal ion can be recovered quantitatively using minimum number of extraction steps.
- (iii) For the re-use of the solvent, strip solution for the back extraction of metal ion from the loaded organic solvent should be easily available.
- (iv) Good solubility of the solvent in paraffinic diluents is important as it provides its user-friendly applicability under non-hazardous environments.
- (v) Solvent should have good chemical stability for its long usage.
- (vi) Solvent should have high flash point and also high boiling point to avoid fire-hazards.
- (vii) It should be easily synthesised easily at a large scale and at low cost.

1.1.1. Limitations of Solvent Extraction

- i) Since the solvent inventory used is high, operational cost is high. Degradation of solvent after repeated use also increases the cost.
- ii) Aqueous solubility of some solvents causes loss of solvent.
- iii) Flammability of organic solvent causes operational work-hazard.

1.2. Solid Phase Extraction (SPE) Method

Solid phase extraction (SPE) method is a tool for treating solutions containing less concentrated solution of metal ions, generally $<1\text{g/L}$. In this method, the metal ion present in the solution distributes itself among the solid phase and the aqueous solution. For large scale applications, SPE are used in columns. Process efficiency is then governed by the solid phase metal loading capacity, flow rate of the aqueous metal ion bearing solution, bed volume in the column etc. SPE can be broadly classified as

- i) Ion Exchange
- ii) Sorption

In ion exchange method, metal ions get attached to the solid phase by coulombic interaction with the solid material which acts as an ion exchanger. Ion exchangers are also of two types i) cation exchanger, ii) anion exchanger. Type of ion exchanger is selected based on the metal species (cationic form /anionic form) present in the aqueous solution.

Sorption of metals can be classified as i) physisorption (caused by van der Waals forces), ii) chemisorption (caused by chemical bonding between metal species and the sorbent). Different structural materials are used for sorption e.g. activated carbons, inorganic extractants, silica gels, polymers etc. These materials are used directly or, modified chemically to enhance sorption and also selectivity of the metal ions of interest. Different chemically modified structural materials are reported in this regard. SPE technique is also used in chromatographic separation, high pressure liquid chromatography (HPLC) for versatile applications.

1.2.1. Limitations of SPE

- i) Long time of operation is required.

- ii) Modelling of metal-ligand complex is difficult.

1.3. Membrane Extraction Method

Membrane extraction technique is also used for the extraction of metal ions from the aqueous solution where the organic phase is entrained in the membrane. In this method also the metal ion distributes itself between two immiscible phases according to its different solubility in these two phases. Metal ion thus gets extracted from the aqueous phase into the organic phase. The extraction is governed by the diffusion of the metal ions from the aqueous phase into the organic phase and also inside the organic phase. Membrane extraction and separation process has its importance because of its low cost, low energy and solvent consumption, high concentration factors. There are two types of liquid membrane extraction techniques, viz.,

- i) Supported liquid membrane
- ii) Emulsion liquid membrane

In supported liquid membrane (SLM), the thin layer of organic phase is immobilized onto a suitable inert microporous support, and then interposed in between two aqueous solutions i.e. the feed solution and the strip solution (Fig.1.1) [11]. In this three-phase extraction technique metal ions are extracted from the aqueous feed solution through the organic liquid phase into the strip solution as shown in the figure. In supported liquid membrane, microporous films are used as the solid support where the membrane thickness generally used is 20-150 μm .

In emulsion liquid membrane, liquid droplets (droplet size 0.5-10 μm) consisting of the organic phase are dispersed into aqueous phase where the metal ions are present. The emulsion liquid membrane is a non-supported liquid membrane whereas, flat sheet liquid membrane and hollow fibre liquid membranes are supported liquid membranes.

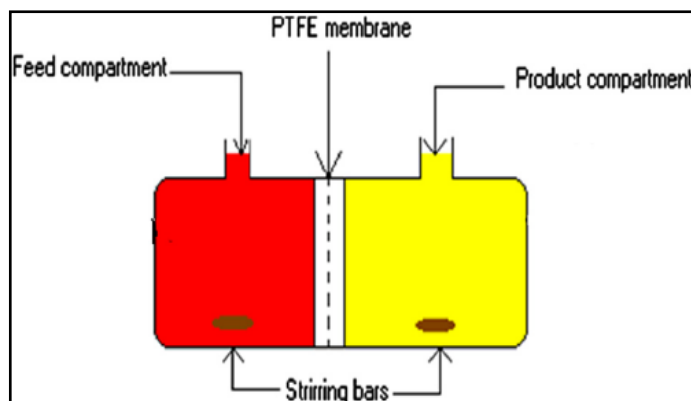


Fig. 1.1 Supported liquid membrane set up

1.3.1. Limitations of Membrane Technique

- i) Stability of the membrane is less.
- ii) Leakage of organic solvent from the membrane pores in case of SLM.

1.4. Types of Extractants

Depending upon the binding mode of the extractants with the metal ions, extractants can be classified as i) Ion exchangers, ii) Complexing ligands. Ion exchangers bind to the metal species by Coulombic interaction. The extractant is either a cation exchanger or, an anion exchanger in this case. Cation exchangers bind with the cations and generally contains $-\text{SO}_3\text{H}$ or, $-\text{COOH}$ group where the proton gets exchanged with the cation. Anion exchangers bind with the anions and generally contain a tertiary amine group. Complexing ligands bind to the metal ion species by co-ordination bonding. Complexing ligands can be classified as i) hard donor ligands which contain a more concentrated, less polarizable electron pair on the binding atom like oxygen and nitrogen atoms, oxide ion etc. at the donor site and ii) soft donor ligands which contain less concentrated and more polarizable electron pair at the co-ordinating atom which are mainly based on sulphur donor atom at the binding site. Different ion exchangers and complexing ligands which are categorised according to the important element present in the binding group such as phosphorus based,

nitrogen based, sulphur based ligands and also other ligands have been described elaborately below.

1.4.1. Phosphorus based Ligands: Different phosphorus based extractants containing oxygen atom at the donor site or, oxide ion at the binding site have been reported so far. Commonly used phosphorus based ligands are tributyl phosphate (TBP) [12], di-(2-ethylhexyl) phosphoric acid (D₂EHPA) [8], 2-ethylhexyl phosphonic acid (PC88A) [13], bis(2,4,4-trimethylpentyl)phosphinic acid (cyanex 272), tri-octyl phosphine oxide (TOPO) [6], tetra-butyl-pyrophosphate (TBPP) [14], di-n-butyl phosphate (DBP) [15], bis(2-ethylhexyl)-1-(2-ethylhexylamino)propyl phosphonate (BEAP) [16], tris(2-ethylhexyl)phosphate (TEHP) [17], di(1-methylheptyl)methyl phosphonate (DMHMP) [18], mixture of tri-alkyl phosphine oxides (cyanex 923), 2-ethylhexyl phosphoric acid mono-2-ethylhexyl ester (EHEHPA) [19], carbamoyl methyl phosphine oxide (CMPO), phosphorylated calixarenes, benzoylmethylene triphenyl phosphorane (BMTPP) [20]. Sorbents like bis-(2,4,4-trimethylpentyl)-monothio phosphinic acid (cyanex-302) encapsulated in to calcium alginate gel, chitosan-tripolyphosphate (CTPP) [21] are also reported.

1.4.2. Nitrogen based Ligands: Tri(iso-octyl)amine, di-n-decylamine sulphate, tri-n-octylamine [22], tertiary amines [23], tri-isodecylamine (alamine 310) [24], N,N,N',N'-tetraalkyl-2 alkyl propane-1,3 diamides [25], N,N'-dimethyl-N,N'-dibutylmalonamide, N,N-dihexyl substituted amides, N,N,N',N'-tetrabutylsuccinamide (TBSA) [26], N,N,N',N' tetrabutyladipicamide, N,N-dibutyldecanamide (DBDEA) [27], N-octanoylpyrrolidine (OPOD) [28], aliquat 336, alamine 336, alamine 308 (tri isooctyl amine), alamine 304 (tri-dodecylamine) [29], alamine 300 [30], N-cyclohexyl-2- pyrrolidone [31], N-octyl aniline [32], tertiary pyridine [33], tris (2-ethylhexyl) amine (TEHA) [34], 5,8-diethyl-7-hydroxy-6-

dodecanone oxime (LIX 63) [35], 2-hydroxy-5-nonylacetoephoneoxime (LIX 84), adogen 464 [36], N-alkyl carboxylic acid amides, N,N'-dimethyl-N,N'-dibutyl-2-tetradecylmalonamide (DMDBTDMA) [37], N,N,N',N'-tetraoctyl diglycolamide (TODGA) [38], N,N,N',N'-tetraoctyl-3,6-dioxo-1,8-diamide (DOODA) [39], dicarboxypyridine diamide (DCPDA) have been reported as the nitrogen based solvents for the extraction of metal ions. Solid phase extractants like modified silica gel with 3-(2-aminoethylamino)propyl group, dipyridyl amide functionalized polymers [40], 2,6-diacetylpyridine functionalized amberlite XAD-4 [41], tertiary pyridine resin, polypyrrole-polythiophene, quaternary ammonium anion exchange resin [42], diethylenetriamine (DETA) grafted onto poly (glycidyl methacrylate) (PGMA) [43], dowex A-1, tetrabutyl ammonium iodide (TBAI) immobilised on the surface of activated carbon [44], 1-(2-pyridylazo) 2-naphthol (PAN) immobilised on resin are also reported for the extraction of various metal ions.

1.4.3. Sulfur based Ligands: Di-n-butyl sulfoxide (DBSO) [45], bi-functional carbamoyl methyl sulfoxides [46], dihexyl sulfoxide (DHSO), bis-2-ethylhexylsulfoxide (BEHSO), bis(2,4,4-trimethylpentyl) monothiophosphinic acid (cyanex 302), cyanex 471x [47], dioctyl sulphide [48], dihexyldithioether, dioctyl sulphoxides (DOSO), bis-(2-ethylhexyl) sulphoxide (BESO), triisobutyl phosphine sulphide (TIPS), 2-octyl-1,4,7-trithiacyclononane (2-octyl-9S3), 1,4,7-trithiacyclodecane (10S3), dinonyl naphthalene sulfonic acid (HDNNS) solvents are reported as the sulphur based extractants. Tri-isobutyl phosphine sulphide (cyanex-471X) permeated in chromosorb-102, dithiooxamide functionalized resin, melamine-formaldehyde-thiourea (MFT) resin, dimercaptosuccinic acid (DMSA) functionalised iron nanoparticles [49], 2-acrylamido-2-methylpropanesulfonic acid (AMPS) grafted on silica surface [50], 5,5-diphenylimidazolidine-2-thione-4-one (thiophenytin)

(DFID) and 2-(4'-methoxy-benzylideneimine) thiophenole (MBIP) [51] are the sulphur based solid phase extractants for the extraction of metal ions.

1.4.4. Other Ligands: 1-(4-Tolyl)-2-methyl-3-hydroxy-4-pyridone [52], dicyclohexano-18-crown-6 (DC18C6) [53], methyl isobutyl ketone (MIBK), naphthenic acids, versatic acids (versatic10, versatic 911), lix 54, hosterex DK-16 are the reported solvents for the extraction of metal ions. Sorbents like goethite, amorphous ferric oxyhydroxide, hematite, akaganeite-type nanocrystals, polypyrrole, activated carbon [54], amberlite IRA-900, amberlite IRN-78, dowex 1x8-400, dowex 2x8-400, amino carboxylic resins like ANKB-2, ANKB-35, MS-5; carbon nanotubes, acrylic acid (AA) incorporated into poly(N-isopropylacrylamide) (PNIPAM) [55], 1-nitroso-2-naphthol immobilised on alumina, 5,5-diphenylimidazolidine-2,4-dione (phenytoin) (DFTD) are reported for the solid phase extraction of metal ions.

A number of biosorbents like chitosan, saw-dust, rice husk have also been applied for the sorption of metal ions [56]; Different bacteria like bacillus cereus, B. subtilis, escherichia coli, pseudomonas aeruginosa and rhodococcus opacus also have been used for the bio-sorption of heavy elements from aqueous medium [57-58].

1.5. Extraction of Important Metal Ions from Aqueous Medium

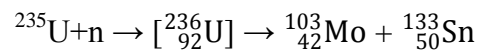
Uranium, zirconium-hafnium, rare earth elements, palladium and other heavy elements like lead, chromium, zinc, copper etc. come into aqueous body from the process streams of different industries like nuclear industry, mining industry, materials manufacturing industries, automobile industry, metal plating industry, chloralkali processing industry, tanneries, smelting and alloy industries, radiator manufacturing, inorganic pigment manufacturing industries, storage battery industries, petroleum refining industries etc. These elements need to be extracted from the aqueous streams for their re-use as well as the pollution free discharge of these

aqueous streams into the environment. Applications of these metal ions in different fields have been discussed below and health impacts of heavy elements on human body have also been highlighted.

1.5.1. Applications of Important Metal ions

1.5.1.1. Applications and Health Impact of Uranium

Uranium has its wide applications in electricity generation, military and civilian usage. Fission of each uranium-235 produces 200MeV energy by the following reaction.



Fission of one gram of uranium-235 can produce energy equivalent to the energy produced by consuming 3 tonnes of coal or 2300 litres of fuel oil. Due to the increasing demand of electricity in human civilisation, production of power from nuclear fuels is gaining importance. The power share in total electricity generation is increasing because of depletion in the resources of conventional fuels like coal, oil and gas. Natural radioactivity of uranium causes health impacts like it damages kidney and also accumulates in bone. Therefore, extraction and recovery of uranium is mandatory.

1.5.1.2. Applications of Zirconium

Zirconium and its compounds have wide applications in various fields. The unique properties of zirconium i.e. corrosion resistance and low thermal neutron absorption cross section (0.02barn) [59] has made it highly useful in nuclear industry. Zirconium alloys are used in nuclear fuel cladding, coolant pressure tubes etc. Earlier zircalloys like zircaloy-1 (Zr-1.5% Sn), zircaloy-2 (Zr-1.5% Sn, 0.14%Fe, 0.10% Cr, 0.06% Ni) had been used in pressure tubes. But the low hydrogen uptake of Zr-2.5Nb alloy increases its mechanical stability against corrosion and therefore frequently used

in pressure tubes replacing zircaloy-2 (in boiling water reactors, BWRs) which has less mechanical strength. Zircaloy-4 (which contains a higher Fe content instead of Ni) is used as cladding material in fuel pins in pressurised water reactors (PWRs). Other applications of zirconium, zirconium alloys and its compounds have been mentioned here. Zircon ($ZrSiO_4$) is refractory, hard, and resistant to chemical attack and hence, is used directly in high-temperature applications. Metallic zirconium has a property of excellent resistance to corrosion and hence, is often used as an alloying agent in making materials which are used in surgical appliances, light filaments, and watch cases. Zirconium dioxide (ZrO_2) is also used in laboratory crucibles, metallurgical furnaces, and as a refractory material [13].

1.5.1.3. Applications of Rare Earth Elements

Rare earth has its enormous applications in a number of fields. Its major applications have been mentioned here. Rare earths are used as electric traction drives replacing or supplementing internal combustion engines in hybrids, plug-in, and electric vehicles. Rare earths are used in wind and hydro power generation, in computer disc drives, cordless power tools, handheld wire-less devices etc. Rare earths can produce magnetic field and therefore, is highly useful in medical diagnosis like medical imaging in MRI. High energy efficiency of rare earth elements is also used in X-ray imaging. The unique luminescent property of rare earths is used widely in flat screen display. Rare earths can oxidise CO and ozone to CO_2 and O_2 . This property is used in catalytic converters and other emission reduction technologies.

1.5.1.4. Applications of Palladium

Palladium demonstrates good catalytic and corrosion resistance behaviour. Therefore, palladium is used in making automobile catalysts which can convert harmful gases from the exhaust (e.g. hydrocarbons, carbon monoxide and nitrogen

dioxide) into less harmful materials (nitrogen, carbon dioxide and water vapour). Palladium is also used in electronics, dentistry, medicine, hydrogen purification, chemical applications. Palladium can adsorb high amount of hydrogen gas (800 times its own volume) and hence, is successfully used for making storage material for hydrogen.

1.5.1.5.Applications and Health Impact of Other Heavy Elements

Other heavy elements coming into aqueous body from different industrial streams are lead, chromium, zinc and copper. They have huge health impact on human body when ingested through aqueous streams and cause many disorders. Some of their health impacts have been discussed here [21-22]. Intake of lead causes damage to brain and nervous system. Lead also causes long-term harm in adults, including increased risk of high blood pressure and kidney damage. High intake of zinc causes fever, birth defect (if over exposed). High intake of copper causes liver and kidney damage and even death, Wilson's disease etc. Intake of chromium causes lung, nasal, and sinus cancer, severe dermatitis and usually painless skin ulcers, liver and kidney problems etc. These heavy elements also have their individual applications like lead is used in batteries, cable sheaths, machinery manufacturing, shipbuilding, light industry, lead oxide, radiation protection and other industries. Chromium is used in tanning as mordants, in dye production, as wood preservers, in the production of pigments used against metal corrosion (electroplating), etc. Zinc is used (as zinc oxide) in paints, rubber, cosmetics, pharmaceuticals, plastics, inks, soaps, batteries, textiles and electrical equipment. Copper is used in electrical generators and motors, in electrical wiring, in electronic goods, such as radio and TV sets, in motor vehicle radiators, air-conditioners, home heating systems etc.

1.5.2. Sources of Metal Ions of Importance

Sources of uranium, zirconium, rare earth elements, palladium and other important heavy elements e.g. lead, chromium, zinc and copper is important to locate these metal ions in nature. Different sources of these metal ions of interest have been described below.

1.5.2.1. Sources of Uranium

Uranium (atomic number 92, electronic configuration $[Rn]5f^3 6d^1 7s^2$) is radioactive in nature and has several isotopes like U^{235} , U^{238} , U^{234} , U^{236} , U^{233} and U^{232} [3]. It is obtained from different sources as described here. ^{238}U (99.27%) and ^{235}U (0.72%) are the most common uranium isotopes found in nature. Uranium is found almost everywhere in nature like rock, soil, rivers, and oceans. Pitchblende is the primary ore of uranium. Other ores are coffinite, davidite etc. Phosphate rocks are also a source of uranium. From phosphate rocks uranium is recovered as a by-product from phosphate fertiliser industry. From different ores, uranium is recovered by the following methods.

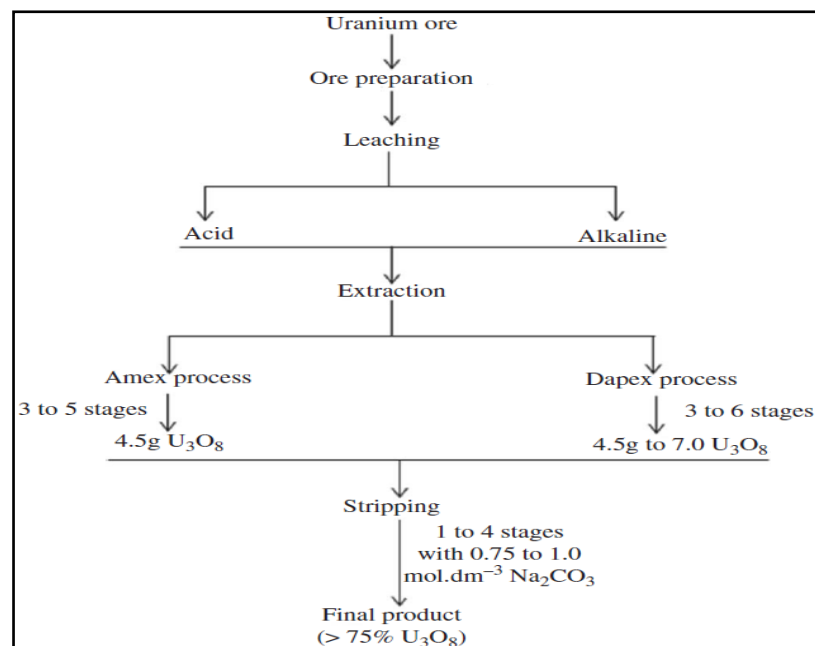


Fig. 1.2 General processing of uranium from ores

The crude product containing uranium is then processed to make uranium fuels for nuclear reactors. In the reactors the fuels are burnt and the remaining uranium present in the spent fuel is reprocessed back for further use. The whole process of uranium cycling is called ‘nuclear fuel cycle’ and is depicted below (Fig.1.3).

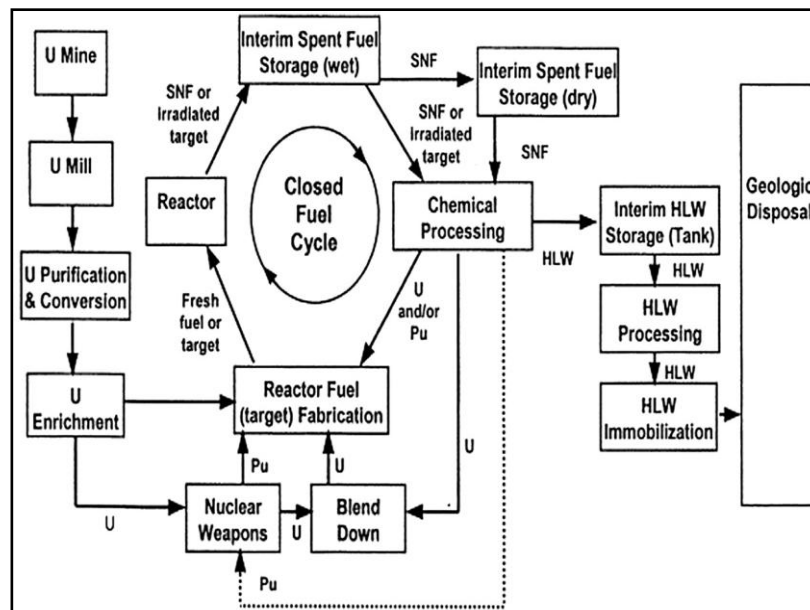


Fig.1.3 Nuclear fuel cycle

Nuclear fuel cycle consists of two main subparts: i) front end and ii) back end. Front end of nuclear fuel cycle consists of uranium mining, milling, enrichment of uranium-235 isotope and fuel fabrication. Wastes and scraps containing uranium are generated during different steps of uranium processing. At the back end, the irradiated fuel is chemically reprocessed for separation and recovery of uranium, plutonium and other precious elements as produced by the fission reaction. Uranium and plutonium are recycled back in the front end of nuclear cycle. Our present work focusses on the extraction and recovery of uranium from fuel scraps and lean aqueous streams produced at the front end of nuclear cycle which are described in chapter 3. Present work also highlights on the extraction of palladium from high level waste (HLW)

(generated at the back end of nuclear fuel cycle) which has been discussed in chapter 6. Rare earth elements have also been tried to remove from HLW as has been described in section 1.5.2.3 below.

1.5.2.2.Sources of Zirconium

Zirconium is a lustrous, grey-white, strong transition metal that resembles hafnium. Zirconium has the atomic number atomic number 40 and the electronic configuration $[\text{Kr}]4d^25s^2$. Zirconium is the ninth most abundant element in the earth's crust. Zircon (ZrSiO_4) is the major source of zirconium. Zirconium is always found in combination with 1-3 wt% hafnium in nature. Separation is very difficult due to their similar chemical properties such as close atomic radii (1.45 Å and 1.44 Å, respectively) and similar valence electron configurations. This makes a concern for the application of zirconium in nuclear industry due to the opposite nature of zirconium and hafnium regarding the absorption of thermal neutrons in the nuclear reactors. Therefore, separation of zirconium from hafnium is mandatory looking into their nuclear applications which has been discussed in chapter 4.

1.5.2.3.Sources of Rare Earth Elements

Rare earths elements are mainly the 14 elements following lanthanum, i.e. from cerium (atomic number 58) to Lutetium (atomic number 71). Yttrium is also considered as a rare earth element (though it does not belong to the lanthanide group) due to its similar properties like lanthanides. The term “rare” is used because these elements occur only rarely in concentrated and economically exploitable mineral deposits in the earth's crust. Monazite is the major source of rare earths in India. Monazite contains 55-60% of rare earths along with uranium. Recovery of rare earth elements from monazite and separation from radioactive uranium is a concern for

their use in public domain. The work focussing on the separation of rare earth elements from uranium has been highlighted in chapter 5.

Rare earth elements are produced after the fission reaction of nuclear fuel and therefore, come into high level waste (HLW) during the reprocessing of spent nuclear fuel. HLW contains both rare earth elements and minor actinides (Np, Am, Cm etc.). HLW is proposed to be vitrified in deep repositories. But the long half lives of minor actinides (10^2 - 10^6 years) increases the risk of glass deformation and radionuclide migration to aquatic environment under natural calamities. Therefore, minor actinides need to be transmuted at accelerator driven subcritical reactor (ADSR) to short-lived or stable nuclides. But the rare earth elements present in HLW creates problem during transmutation due to their high neutron absorption cross sections. Moreover, the rare earth elements also segregate and form a separate phase during vitrification of radioactive wastes. Therefore, separation of minor actinides from rare earth elements is necessary for processing of HLW and this work has been discussed in chapter 5.

1.5.2.4.Sources of Palladium

Palladium (atomic number 46, electronic configuration [Ar] $3d^{10} 4s^2 4p^6 4d^{10}$) is a rare and lustrous silvery-white metal discovered in 1803 by William Hyde Wollaston. Palladium is a rarely available element in nature. It occurs along with the platinum group metals (PGM) in nature. The abundances of PGMs in the primary and secondary ores are 0.7 to 7 ppm respectively [60] where palladium consists of ~0.85% of the total naturally available PGMs. Therefore, separation and recovery of palladium from secondary resources is highly important for its various applications as well as growing demands. Spent automobile catalyst is a good secondary resource of palladium. Therefore, separation and recovery of palladium from spent automobile catalyst has been carried out and discussed in chapter 6.

1.5.2.5.Sources of Heavy Metals

Heavy metals are normally contemplated as those whose density exceeds 5 g/cm³. Most of the components belonging to this grouping are extremely water soluble, popularly-known toxins and carcinogenic agents. Heavy metals e.g. lead, zinc, copper and chromium create environmental pollution largely when they are disposed from industrial wastes like copper comes in the aqueous streams from gold mining industry [61], chromium (VI) comes into aqueous solution from inorganic pigment manufacturing industries and petroleum refining conversion catalysts, lead comes into aqueous solution from plastics, cathode ray tubes, ceramics, alloys like solders, steel and cable reclamation etc. [62]. Removal of heavy elements from aqueous streams is a serious subject for researchers. Extraction and removal of heavy elements from aqueous streams have been discussed in chapter 7.

The selectivity in the extraction of metal ions from the aqueous medium depends upon the selective and strong complexation of the metal species with the ligand. To understand the metal-ligand complexes at molecular level, theoretical investigation and quantum mechanical calculations are required. Theoretical understanding highlights on the electronic states of both of them involved in co-ordination and binding. This gives the idea for design of a more selective ligand based on the co-ordination mode of the ligand and available orbitals and co-ordination number of the metal species. Different quantum chemistry based computational methods as reported for obtaining the equilibrium geometry, binding energy, reaction mechanism etc. have been briefly discussed in section 1.6.

1.6. Theoretical Investigation on Metal-Ligand Binding

Preliminary geometry optimizations can be carried out at the density functional theory (DFT) level employing the PBE functional [63-64] in conjunction

with the def2-TZVP basis set [65-66]. For uranium, zirconium, rare earths etc. the inner-shell core electrons can be replaced by an effective core potential (ECP) generated for a neutral atom by using quasi-relativistic methods [67] and the explicitly treated electrons can be described by standard def-TZVP basis sets. Resolution-of-identity approximation [68-69] is also reported in conjunction with the appropriate auxiliary basis sets to speed up the calculations where empirical dispersion corrections from Grimme (D3) [70] are also incorporated. This provides the basis-set combination which is referred to as def2-TZVP-ECP. Under experimental conditions, the metal ions are extracted from the aqueous phase to the ligand phase after forming complexes with the ligand. The influence of the solvent environment around the metal ion is reportedly considered with the conductor-like screening model (COSMO) [71] during the optimization step. For characterization of the located stationary points as minima on the potential energy hyper surface, gas phase harmonic vibrational frequency calculations can be performed on the gas-phase and solvent-phase optimized geometries, at the same level. The sensitivity of the method implied for the calculations, the RI-PBE-D3/def2-TZVP-ECP geometries can be subjected to additional geometry optimizations at the DFT level employing the BP86 functional [72-73] for which the triple- ζ def2-TZVP(-f) basis sets derived from def2-TZVP can be used by removing the f-polarization functions for the main group elements, for better computational efficiency [65-66]. The calculations can also be corrected for relativistic effects for elements with high atomic numbers using the zero-order regular approximation (ZORA) approach [74-75]. For actinides, the segmented all-electron relativistically contracted (SARC) basis sets [76] are reported, which is specifically developed for scalar relativistic calculations and is individually adapted to ZORA Hamiltonians. The resolution-of-identity (RI) approximation [68-69], as reported, has

also been applied in conjunction with the appropriate auxiliary basis sets for fast computations. Empirical dispersion corrections are also reported to be incorporated using the atom-pairwise dispersion correction with Becke-Johnson damping (D3BJ) [70,77]. ‘Atoms in molecules’ (AIM) [78-79] analysis is reported to be performed to characterize the nature of metal-ligand chemical bonds by evaluating parameters like electron density, the laplacian of the electron density, delocalization indices, and the energy density at bond critical points using the AIMAll program package [80].

1.7. Objective of Present Work

Present thesis work is primarily focused on the separation of different metal ions such as uranium, rare earth elements, zirconium, palladium and heavy elements namely lead, chromium, zinc, copper etc. from various aqueous streams. We have followed three different extraction methods, namely solid phase extraction, solvent extraction and membrane based extraction methods. Since the previously proposed complexing ligands for the separation of metal ions have many limitations, there is a demand for selective and efficient separation of metal ions from various chemical mixture and industrial as well as nuclear reactor wastages. Accordingly, another important aspect of the present thesis work is aimed towards the design of novel ligands for the extraction and separation of metal ions efficiently. For instance, phosphate functionalised silica gels, amine and amido pyridyl phosphate functionalised silica gel have been synthesised, characterised and used for the separation and recovery of uranium from nitric acid medium. These ligands have also been assessed for the separation of zirconium from hafnium. In an another attempt, we have use of another ligand namely 1,8-dihydroxy anthraquinone functionalised silica gel and attempted for the separation and recovery of rare earth elements from uranium.

Separation of rare earth elements from actinides has also been attempted by ethyl bistriazinylpyridine ligand. More importantly, recovery of palladium from spent automobile catalyst and also from high level nuclear waste stream have been carried out a newly proposed complexing ligand namely dithiodiglycolamide (DTDGA) ligand. Similarly, we have also designed other ligands, viz., butanol functionalised silica gel and amido pyridyl amine functionalised silica gels and successfully applied for the removal of heavy metals from aqueous medium. In order to understand the chemical binding pattern of the complexing ligands with different metal ions at the molecular level, quantum chemistry based computational methods have been carried out.

References

1. Solvent Extraction Principles and Practice, Second edition, J. Rydberg, M. Cox, C. Musikas, G. R. Choppin, New York, Basel, pp-9.
2. Sources and Migration of Plutonium in Groundwater at the Savannah River Site, M. Dai, J. M. Kelley, K. O. Buesseler, Environ. Sci. Technol., 2002, 36, 3690-3699.
3. M. S. Tswett and the Discovery of Chromatography II: Completion of the Development of Chromatography (1903-1910), L. S. Ettre, K. I. Sakodynskii, Chromatographia, 1993, 35.
4. Mendeleevium: Divalency and Other Chemical Properties, E. K. Hulet, R. W. Lougheed, J. D. Brady, R. E. Stone, M. S. Coops, Science, 1967, 158, 486-488.
5. The extraction of nitrates by phosphorylated reagents-I The relative extraction rates and solvating mechanisms for uranyl nitrate, T. V. Healy, J. Kennedy, J.Inorg.Nucl.Chem.,1959, 10, 128-136.
6. Transport of silver metal ions through a liquid membrane gel using a solvating extractant (TOPO), N. Taoualit, D.E. H. Boussaad, Desalination, 2006, 193, 321-326.
7. Solvation and Ionic Association of Bis(β -diketonato)(diamine)-cobalt(III) Perchlorates in Alcohols and Ketones, K. Ito, H. Isono, E. Iwamoto, Y. Yamamoto, Bull.Chem.Soc.Jpn., 1988, 61, 4077-4082.

8. Facilitated Cd(II) transport across CTA polymer inclusion membrane using anion (Aliquat 336) and cation (D₂EHPA) metal carriers, O. K. Senhadji, L. Mansouri, S. Tingry, P. Seta, M. Benamor, *Journal of Membrane Science*, 2008, 310, 438-445.
9. Selectivity in solvent extraction of metal ions by organic cation exchangers synergized by macrocycles: Factors relating to macrocycle size and structure, W.J. McDowell, B.A. Moyer, G.N. Case, F.I. Case, *Solvent Extraction and Ion Exchange*, 1986, 4, 217-236.
10. Chelating Reagents in Solvent Extraction Processes: The Present Position, *Coordination Chemistry Reviews*, 1975, 16, 285-307.
11. Modelling of carrier mediated transport of chromium(III) in the supported liquid membrane system with D2EHPA, K. Ochrowicz, W. Apostoluk, *Separation and Purification Technology*, 2010, 72, 112-117.
12. Solvent extraction of uranium (VI) by tributyl phosphate/dodecane from nitric acid medium, M. Alibrahim, H. Shlewit, *Chemical Engineering*, 2007, 51, 57-60.
13. Synergistic extraction of uranium with mixtures of PC88A and neutral oxodonor, S. Biswas, P. N. Pathak, D. K. Singh, S. B. Roy, V. K. Manchanda, *Radioanal Nucl Chem*, 2010, 284, 13-19.
14. Method of Preparing Phosphate Esters, A. Bell, K. Tenn, 1946, 260-461.
15. Some Reactions between Uranium (VI) and Di-n-butyl Phosphate (DBP) in Chloroform and Methyl Isobutyl Ketone (Hexone), D. Dyrssen, F. Krasovec, *Acta Chemica Scandinavica*, 1959, 13, 561-570.
16. Separation of zirconium from hafnium in sulfate medium using solvent extraction with a new reagent BEAP, S. Chen, Z. Zhang, S. Kuang, Y. Li, X. Huang, W. Liao, *Hydrometallurgy*, 2017, 169, 607-611.
17. Extraction and Separation Studies of Uranium (VI) with Tris-2-Ethylhexyl Phosphate, *Radioanal.Nucl.Chem. Letters*, 1990, 144, 439-445.
18. Di-1-methyl heptyl methylphosphonate (DMHMP): A promising extractant in Th-based fuel reprocessing, R. Li, C. Liu, H. Zhao, S. He, Z. Li, Q. Li, L. Zhang, *Separation and Purification Technology*, 2017, 173, 105-112.
19. Synergistic extraction of rare earth by mixtures of 2-ethylhexyl phosphoric acid mono-2-ethylhexyl ester and di-(2-ethylhexyl) phosphoric acid from sulfuric acid medium, H. Xiaowei, L. Jianning, L. Zhiqi, Z. Yongqi, X. Xiangxin, Z. Zhaowu, 410-413.

20. Novel coordination of (benzoylmethylene) triphenylphosphorane in a nickel oligomerization catalyst, W. Kim, F. H. Kowaldt, R. Goddard, C. Kruger, *Angew Chemie*, 1978, 17, 466-467.
21. High performance of phosphonate-functionalized mesoporous silica for U(VI) sorption from aqueous solution, Li-Yong Yuan, Ya-Lan Liu, Wei-Qun Shi, Yu-Long Lv, Jian-Hui Lan, Yu-Liang Zhao, Zhi-Fang Chai, *Dalton Trans.*, 2011, 40, 7446.
22. Vanadium(V) ions transport through tri-n-octyl amine cyclohexane supported liquid membranes, M. A. Chaudry, N. Bukhari, M. Mazhar, F. Tazeen, *Separation and Purification Technology*, 2007, 54, 227-233.
23. The extraction of Pu (IV) nitrate by long chain tertiary amines nitrates, *J.Inorg.Nucl.Chem.*, 1962, 24, 541-546.
24. Extraction of Mo(VI) and U(VI) by alamine 310 and its mixtures from HCl solution, P. Behera, R. Mishra, V. Chakravorty, *Radiochimica Acta*, 1993, 62, 153-158.
25. Extraction chemistry of actinide cations by N,N,N',N'-tetraalkyl-2 alkyl propane-1,3 diamides, L. Nigond, C. Musikas, C. Cuillerdier, 1993, CEA-CONF-11423, 20-23.
26. Extraction of U(IV) and Th(IV) in nitric acid medium with N,N,N',N'-tetrabutyl-succinyl-amide, W. Youshao, L. Yongju, S. Shouli, S. Guoxin, B. Borong, *Uranium Mining and Metallurgy*, 1999, 18, 269-272.
27. The crystal structure of decanamide, J. R. Brathovde, E. C. Lingafelter, *Acta Crystallographica*, 1958, 11, 729.
28. Extraction of uranium (VI) with N-octanoyl pyrrolidine in sulfonated kerosene, L. Zhen, B. Borong, X. Qun, H. Jingtian, 2000, *Nuclear Science and Techniques*, 11, 205-208.
29. Study of gold (III)-HCl-amine alamine 304 extraction equilibrium system, F. J. Alguacil, C. Caravaca, *Hydrometallurgy*, 1993, 34, 91-98.
30. Separation of platinum and palladium from chloride solution by solvent extraction using alamine 300, B. Swain, J. Jeong, S. Kim, J. Lee, *Hydrometallurgy*, 2010, 104, 1-7
31. New uranyl nitrate complex with N-cyclohexyl-2-pyrrolidone: a promising candidate for nuclear fuel reprocessing, T.R. Varga, M. Sato, Zs. Fazekas, M.

- Harada, Y. Ikeda, H. Tomiyasu, *Inorganic Chemistry Communications*, 2000, 3, 637-639.
32. Separation of gallium, indium and thallium by extraction with n-octylaniline in chloroform, S. R. Kuchekar, M. B. Chavan, *Talanta*, 1988, 35, 357-360.
 33. Group separation of trivalent actinides and lanthanides by tertiary pyridine-type anion-exchange resin embedded in silica beads, T. Suzuki, M. Aida, Y. Ban, Y. Fujii, M. Hara, T. Mitsugashira, *Journal of Radioanalytical and Nuclear Chemistry*, 2003, 255, 581-583.
 34. Solvent extraction with alkyl amines, C. F. Coleman, K. B. Brown, J. G. Moore, D. J. Crouse, *Industrial and Engineering Chemistry*, 1958, 50, 1756-1762.
 35. Transport of uranium(VI) through a supported liquid membrane containing lig 63, K. Akiba, T. Kanno, *Separation Science and Technology*, 1983, 18, 831-841.
 36. Determination of gold by adogen-464 extraction, S. Biswas, H. K. Mondal, S. Basu, *Indian Journal of Chemistry*, 1996, 35A, 804-805.
 37. Uptake of metal ions by extraction chromatography using dimethyl dibutyl tetradecyl-1,3-malonamide (DMDBDMA) as the Stationary Phase, P. K. Mohapatra, S. Sriram, V. K. Manchanda, L. P. Badheka, *Separation Science and Technology*, 2000, 35, 39-55.
 38. N,N,N',N'-Tetraoctyl diglycolamide (TODGA): a promising extractant for actinide-partitioning from high-level waste (HLW), S. A. Ansari, P. N. Pathak, V. K. Manchanda, M. Husain, A. K. Prasad, *Solvent Extraction and Ion Exchange*, 2005, 23, 463-479.
 39. Separation of palladium from high level liquid waste – A review, R. Ruhela, A. K. Singh, B. S. Tomar, R. C. Hubli, *RSC Adv.*, 2014, 4, 24344-24350.
 40. Dipyriddy amide-functionalized polymers prepared by ring-opening-metathesis polymerization (ROMP) for the selective extraction of mercury and palladium, F. Sinner, M. R. Buchmeiser, R. Tessadri, M. Mupa, K. Wurst, G. K. Bonn, *J. Am. Chem. Soc.*, 1998, 120, 2790-2797.
 41. Preconcentration and determination of trace elements with 2,6-diacetylpyridine functionalized amberlite XAD-4 by flow injection and atomic spectroscopy, D. Kara, A. Fisher, S. J. Hill, *Analyst*, 2005, 130, 1518-1523.
 42. Use of ion exchange resins for determination of uranium in ores and solutions, S. Fisher, R. Kunin, *Analytical Chemistry*, 1957, 29, 400-402.

43. Diethylenetriamine-grafted poly(glycidyl methacrylate) adsorbent for effective copper ion adsorption, C. Li, R. Bai, L. Hong, *Journal of Colloid and Interface Science*, 2006, 303, 99-108.
44. Modified activated carbon for the removal of copper, zinc, chromium and cyanide from wastewater, L. Monser, N. Adhoum, *Separation and Purification Technology*, 2002, 26, 137-146.
45. Liquid-liquid extraction of uranium from nitric acid solution using di-n-butylsulfoxide in petroleum ether as extractant, M. H. Khan, S. Shahida, A. Ali, *Radiochim. Acta*, 2008, 96, 35-40.
46. Extraction studies of uranium(VI), plutonium(IV) and americium(III) from nitric acid using the bi-functional carbamoyl methyl sulfoxide ligands, J. S. Gamare, K. V. Chetty, S. K. Mukerjee, S. Kannan, *Anal. Sci.*, 2009, 25, 1167-1170.
47. Studies of extractive removal of silver (I) from nitrate solutions by cyanex 471x, Z. Hubicki, H. Hubicka, *Hydrometallurgy*, 1995, 37, 207-219.
48. Influence of thiocyanate ions on the kinetics and thermodynamics of palladium(II) extraction with dialkyl sulphides, G. Cote, K. M. Ganguly, D. Bauer, *Hydrometallurgy*, 1989, 23, 37-45.
49. Removal of heavy metals from aqueous systems with thiol functionalized superparamagnetic nanoparticles, W. Yantasee, C. L. Warner, T. Sangvanich, R. S. Addleman, T. G. Carter, R. J. Wiacek, G. E. Fryxell, C. Timchalk, M. G. Warner, *Environmental Science & Technology*, 2007, 41, 5114-5119.
50. Preparation of organically functionalized silica gel as adsorbent for copper ion adsorption, W. Hongjie, K. Jin, L. Huijuan, Q. Jiuhi, *Journal of Environmental Sciences*, 2009, 21, 1473-1479.
51. Three modified activated carbons by different ligands for the solid phase extraction of copper and lead, M. Ghaedi, F. Ahmadi, Z. Tavakoli, M. Montazerzohori, A. Khanmohammadi, M. Soylak, *Journal of Hazardous Materials*, 2008, 152, 1248-1255.
52. Extraction and separation of uranium(VI) and protactinium(V) with 1-(4-tolyl)-2-methyl-3-hydroxy-4-pyridone, B. Tamhina, A. Gojmerac, M. J. Herak, *Mikrochim Acta*, 1976, 66, 569-578.

53. Solvent extraction of amino acids into a room temperature ionic liquid with dicyclohexano-18-crown-6, S. V. Smirnova, I. I. Torocheshnikova, A. A. Formanovsky, *Anal Bioanal Chem*, 2004, 378, 1369-1375.
54. Solid phase extractive preconcentration of uranium(VI) onto diarylazobisphenol modified activated carbon, A. M. Starvin, T. P. Rao, *Talanta*, 2004, 63, 225-232.
55. Poly(N-isopropylacrylamide-co-acrylic acid) hydrogels for copper ion adsorption: equilibrium isotherms, kinetic and thermodynamic studies, J. J. Chen, A. L. Ahmad, B. S. Oo, *Journal of Environmental Chemical Engineering*, 2013, 1, 339-348.
56. Removal of heavy metal ions from wastewater by chemically modified plant wastes as adsorbents: a review, W. S. W. Ngah, M. A. K. M. Hanafiah, *Bioresource Technology*, 2008, 99, 3935-3948.
57. Bacterial sorption of heavy metals, M. D. Mullen, D. C. Wolf, F. G. Ferris, T. J. Beveridge, C. A. Flemming, G. W. Bailey, *Appl. Environ. Microbiol.*, 1989, 55, 3143-3149.
58. Biosorption of lead(II), chromium(III) and copper(II) by *R. opacus*: equilibrium and kinetic studies, B. Y. M. Bueno, M. L. Torem, F. Molina, L. M. S. de Mesquita, *Minerals Engineering*, 2008, 21, 65-75.
59. Neutron Absorption Cross Sections for Zirconium-94 and Zirconium-96, R. H. Fulmer, D. P. Stricos, T. F. Ruane, *Nuclear Science and Engineering*, 1971, 46, 314-317.
60. Fundamentals of Radiochemistry, D. D. Sood, A. V. R. Reddy, N. Ramamoorthy, IANCAS, Third Edition, 2007.
61. Copper electrowinning from gold plant waste streams, F. A. Lemos, L. G. S. Sobral, A. J. B. Dutra, *Minerals Engineering*, 2006, 19, 388-398.
62. Agricultural waste material as potential adsorbent for sequestering heavy metal ions from aqueous solutions-a review, D. Sud, G. Mahajan, M. P. Kaur, *Bioresource Technology*, 2008, 99, 6017-6027.
63. Accurate and simple analytic representation of the electron-gas correlation energy, J. P. Perdew, Y. Wang, *Phys. Rev. B:Condens. Matter Mater. Phys.*, 1992, 45, 13244-13249.

64. Generalized gradient approximation made simple, J. P. Perdew, K. Burke, M. Ernzerhof, *Phys. Rev. Lett.*, 1996, 77, 3865-3868.
65. Fully optimized contracted Gaussian basis sets for atoms Li to Kr , A. Schäfer, H. Horn, R. Ahlrichs, *J. Chem. Phys.*, 1992, 97, 2571-2577.
66. Balanced basis sets of split valence, triple zeta valence and quadruple zeta valence quality for H to Rn: Design and assessment of accuracy, F. Weigend, R. Ahlrichs, *Phys. Chem. Chem. Phys.*, 2005, 7, 3297-3305.
67. Energy-adjusted pseudopotentials for the actinides. Parameter sets and test calculations for thorium and thorium monoxide , W. Küchle, M. Dolg, H. Stoll, H. Preuss, *J. Chem. Phys.*, 1994, 100, 7535-7542.
68. A fully direct RI-HF algorithm: Implementation optimized auxiliary basis sets, demonstration of accuracy and efficiency, F. A. Weigend, *Phys. Chem. Chem. Phys.*, 2002, 4, 4285-4291.
69. Efficient use of the correlation basis sets in resolution of the identity MP2 calculations, F. A. Weigend, A. Kohn, C. Hättig, *J. Chem. Phys.*, 2002, 116, 3175-3183.
70. A consistent and accurate ab initio parametrization of density functional dispersion correction (DFT-D) for the 94 elements H-Pu, S. Grimme, J. Antony, S. Ehrlich, H. Krieg, *J. Chem. Phys.*, 2010, 132, 154104.
71. COSMO: a new approach to dielectric screening in solvents with explicit expressions for the screening energy and its gradient , A. Klamt, G. Schüürmann, *J. Chem. Soc. Perkin Trans. 2*, 1993, 5,799-805.
72. Density-functional exchange-energy approximation with correct asymptotic behaviour, A. D. Becke, *Phys. Rev. A: At. Mol. Opt. Phys.*, 1988, 38, 3098-3100.
73. Density-functional approximation for the correlation energy of the inhomogeneous electron gas, J. P. Perdew, *Phys. Rev. B: Condens. Matter Mater. Phys.*, 1986, 33, 8822-8824.
74. Relativistic total energy using regular approximations, E. van Lenthe, E. J. Baerends, J. G. Snijders, *J. Chem. Phys.*, 1994, 101, 9783-9792.
75. The zero-order regular approximation for relativistic effects: The effect of spin-orbit coupling in closed shell molecules, E. van Lenthe, J. G. Snijders, E. J. Baerends, *J. Chem. Phys.*, 1996, 105, 6505-6516.

76. All-electron scalar relativistic basis sets for the actinides, D. A. Pantazis, F. Neese, *J. Chem. Theory Comput.*, 2011, 7, 677-684.
77. Effect of the damping function in dispersion corrected density functional theory, S. Grimme, S. Ehrlich, L. Goerigk, *J. Comput. Chem.*, 2011, 32, 1456-1465.
78. *Atoms in Molecules: A Quantum Theory*, R. F. Bader, Oxford University Press: Oxford, U.K., 1995.
79. *Atoms in Molecules: An Introduction*, P. Popelier, Prentice Hall, NJ, 2000.
80. AIMAll (Version 16.01.09), T. A. Keith, T K Gristmill Software: Overland Park, KS, USA, 2016 (aim.tkgristmill.com).

Synthesis, Characterisation and Experimental Techniques

In this chapter, the synthesis and characterization of functionalised silica gels and the experimental methods adopted for metal ion extraction have been discussed in details. Eight different functionalised silica gels namely, i) single phosphate functional group attached on the silica gel surface through a flexible carbon chain (reported as 'SPFSG'), ii) mono-phosphate functional group attached on the silica gel surface directly (reported as 'MPFSG'), iii) bi-phosphate functionalised silica gel (reported as 'BPFSG'), iv) tri-phosphate functionalised silica gel (reported as 'TPFSG'), v) amine and amido pyridyl phosphate functionalised silica gel (reported as 'AAPPFSG'), vi) 1,8-dihydroxyanthraquinone functionalised silica gel (reported as 'DHA FSG'), vii) amidopyridyl amine functionalised silica gel (APAFSG), viii) butanol functionalised silica gel (BFSG) have been synthesised and characterised for the sorption and separation of uranium, zirconium-hafnium, rare earths, lead, copper, chromium and zinc from aqueous medium. Various tools namely, Fourier Transform Infrared Spectroscopy (FT-IR), Scanning Electron Microscopy (SEM), Energy-Dispersive X-Ray Spectroscopy (EDS), Thermo-Gravimetric Analysis (TGA) and X-Ray Photoelectron Spectroscopy (XPS) etc. that have been used to characterise the ligands, have been discussed in this chapter. Different experimental methods exploited in the metal extraction and separation studies like a) solid phase extraction (SPE), b) liquid-liquid extraction which containing two main sub-categories like i) solvent extraction and ii) membrane separation methods, have been discussed below.

2.1. Synthesis and Characterisation of Functionalised Silica Gels

Alkali treated silica (ASG) has been obtained by the following way. Silica gel has been refluxed with 0.1 mol L^{-1} hydrochloric acid for 3 h to remove iron, if present, and has been made acid free by washing several times with de-ionised water. The conditioned silica gel (25 g) has been treated with 0.1 mol L^{-1} sodium hydroxide for 12 h. It has been then washed with de-ionised water till it has become alkali free. The Alkali treated silica (ASG), thus obtained, has been used in preparing the following functionalised silica gels as described below.

2.1.1. Synthesis & Characterisation of Single Phosphate Functionalised Silica Gel (SPFSG)

2.1.1.1. Synthesis of Single Phosphate Functionalised Silica Gel (SPFSG)

SPFSG has been synthesized as per the reaction scheme shown in Fig.2.1. The ASG (20 g) has been stirred with 1,4-dibromobutane (5 ml) in water (200 ml) for 16 h. It has then been filtered. The brominated silica, thus obtained, has been then stirred with 5 ml of di-(2-ethylhexyl)phosphoric acid shortly named as DEHPA (5 ml) in presence of a base for 18 h. The functionalised silica, thus obtained, has been filtered, washed with ethanol and then dried at $60 \text{ }^{\circ}\text{C}$ for 6 h.

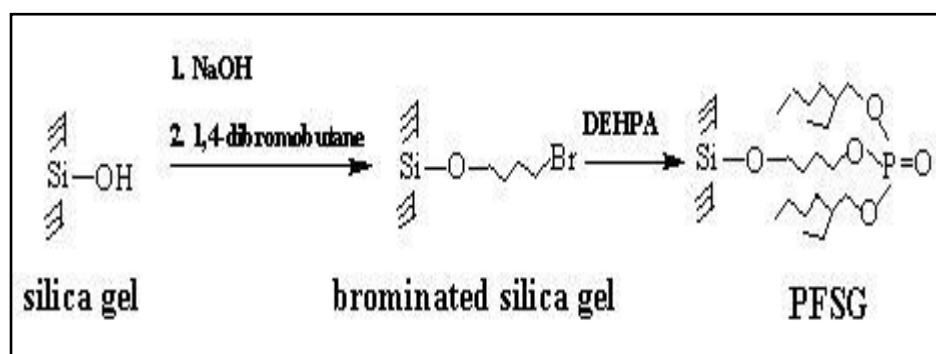


Fig.2.1 Synthesis route of SPFSG

2.1.1.2. Characterisation Studies for SPFSG

2.1.1.2.1. FT-IR Study for SPFSG

IR spectra ($4000\text{--}400 \text{ cm}^{-1}$ using spectrometer-JASCO FTIR-6100) has been recorded for characterisation of the functional groups present in SPFSG (Fig.2.2).

Bands at 958 cm^{-1} and 1208 cm^{-1} in the spectra correspond to P-OR ester (R is alkyl group) stretching frequency, P=O stretching vibration frequencies, respectively. These are the characteristic bands of phosphate group [1]. Bands at 1101 cm^{-1} is attributable to Si-O-Si and Si-O-C stretching vibration frequencies. C-H stretching vibration frequencies are observed at 2930 cm^{-1} . Bands at 635 cm^{-1} , 1465 cm^{-1} and 1620 cm^{-1} are due to Si-O-Si bending vibration, CH_2 bending vibration and H-O-H bending vibrations [2] of adsorbed water molecules on to SPFSG respectively. Therefore, silica gel has been functionalised successfully providing SPFSG as the final product.

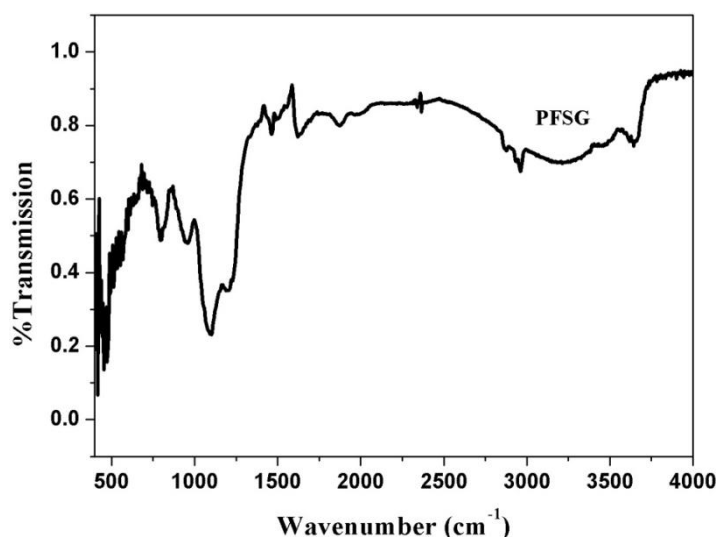


Fig.2.2 FTIR spectra of SPFSG

2.1.1.2.2. SEM and EDS Study for SPFSG

The morphology of the powder has been investigated using Scanning Electron Microscopy (SEM) and chemical composition has been determined through Energy-Dispersive X-Ray Spectroscopy (EDS). SEM image of SPFSG has been shown in Fig.2.3. It shows that the particles of SPFSG are less than $45\mu\text{m}$. EDS spectra of SPFSG, as shown in Fig.2.4, indicates the presence of carbon, phosphorus, oxygen and silicon on the surface of SPFSG. This is attributed to the incorporation of

phosphate group on to the silica gel surface. Additional peak of gold (Au) is due to the application of gold coating over the sample for SEM examination.

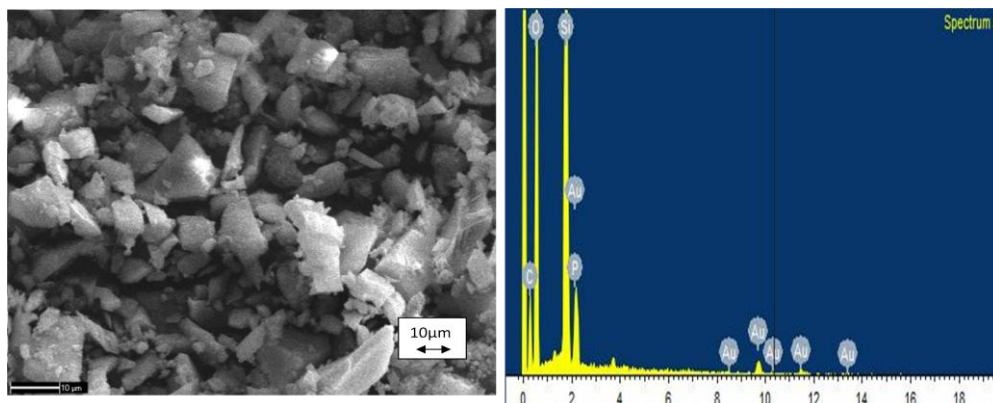


Fig.2.3 SEM spectra of SPFSG

Fig.2.4 EDS spectra of SPFSG
(intensity vs. kinetic energy (keV)
plot)

2.1.1.2.3. TGA Study for SPFSG

TGA scan of SPFSG from 275⁰C to 600⁰C temperature range is shown in Fig.2.5. The weight losses at 362⁰C and 525⁰C are due to the dissociation of phosphate moiety and the decomposition of rest of the organic moiety bonded to the inorganic silica backbone, respectively. Similar results have been reported by Cochez et.al [3].

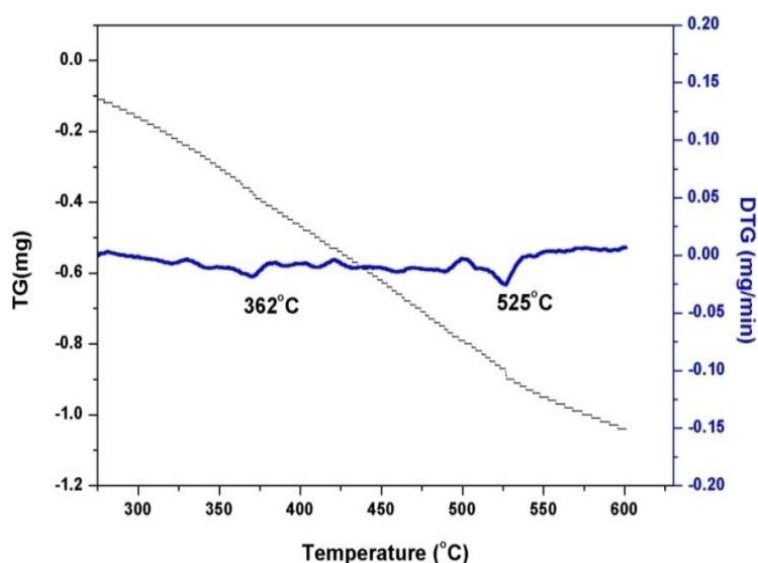
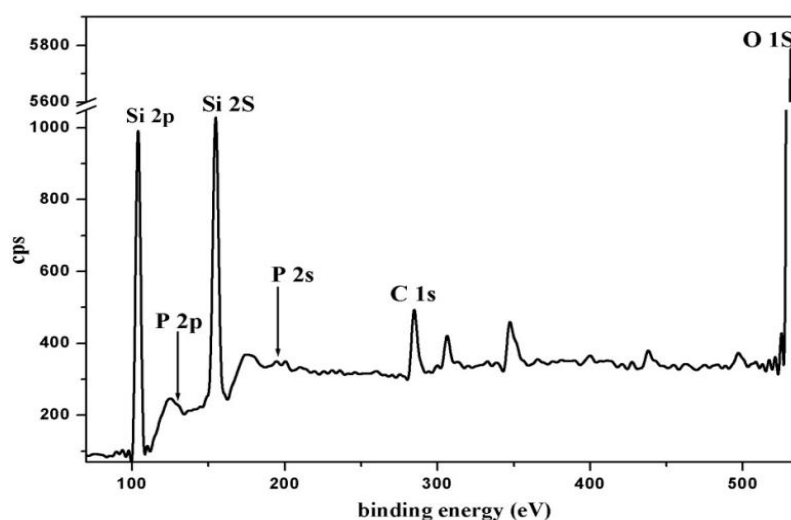


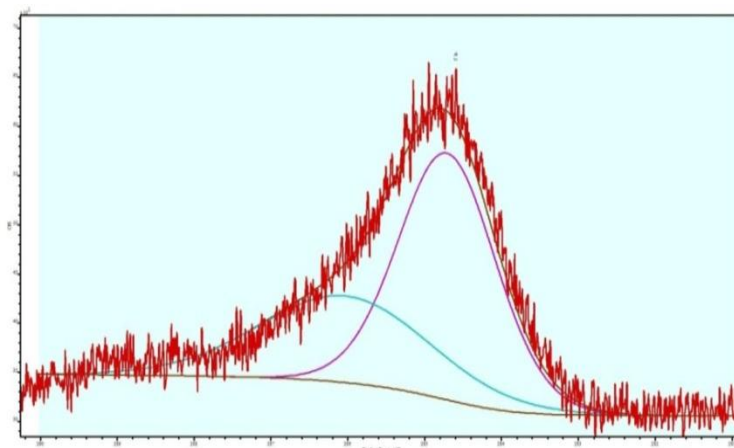
Fig.2.5 TGA spectra of SPFSG

2.1.1.2.4. XPS Study for SPFSG

XPS spectra of SPFSG has been given in Fig.2.6. The peaks in the wide-scan spectra (Fig.2.6a) of SPFSG attribute to Si 2p, P 2p, Si 2s, P 2s, C 1s and O 1s with binding energies at about 104.07, 129.9, 154.8, 192, 284.6 and 531.5 eV respectively. The C 1s spectra (Fig.2.6b) can be curve-fitted into two peak components with binding energies at about 284.71 eV (71%) and 286.04 eV (28.1%) attributable to the C-C/C-H and C-O species respectively [4-6].



(a)



(b)

Fig.2.6 (a) XPS spectra of SPFSG. Peaks at 126.5 eV, 178 eV, 306 eV, 347 eV are due to residual impurities of Cu (3s), Ba (4p), Mg (KLL Auger), CaSO₄ (Ca 2p) respectively which are present in the reagents used in the studies, (b) C1s peak at 284.6 eV in the XPS spectra of SPFSG.

2.1.2. Synthesis & Characterisation of Mono-Phosphate Functionalised Silica Gel (MPFSG)

2.1.2.1. Synthesis of MPFSG

MPFSG has been synthesised as per the reaction scheme shown in Fig.2.7. ASG (25g) has been reacted with diethyl chlorophosphate (15 ml) in ethanol (250 ml) under reflux for 36 hours. The mono-phosphate functionalised silica gel (MPFSG), thus obtained, has been then filtered, washed with ethanol properly to remove all remaining reagent. It has been then dried at 50°C for 11 hours.

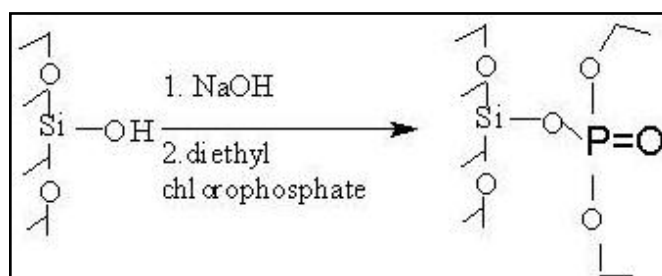


Fig.2.7 Synthesis scheme of MPFSG

2.1.2.2. Characterization studies for MPFSG

2.1.2.2.1 FT-IR Spectra of MPFSG

The FT-IR spectra of MPFSG has been taken (using IR instrument from Bruker, Model TENSOR-27) to characterise it and has been given in Fig.2.8. It shows the presence of similar vibration bands for P=O and P-O-R (R is alkyl group) as shown in case of SPFSG confirming the presence of phosphate group on it.

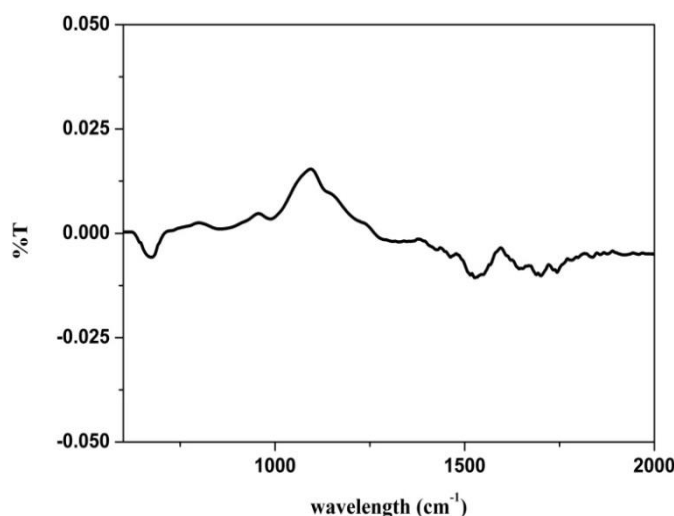


Fig.2.8 FT-IR spectra of MPFSG

2.1.2.2.2 EDS Spectra of MPFSG

EDS spectra of MPFSG (Fig.2.9), shows the presence of carbon, phosphorus, oxygen and silicon on MPFSG sample. This confirms the presence of phosphate group on to the MPFSG surface. Additional peak of gold (Au) in the spectra is due to the application of gold coating over the sample for SEM examination.

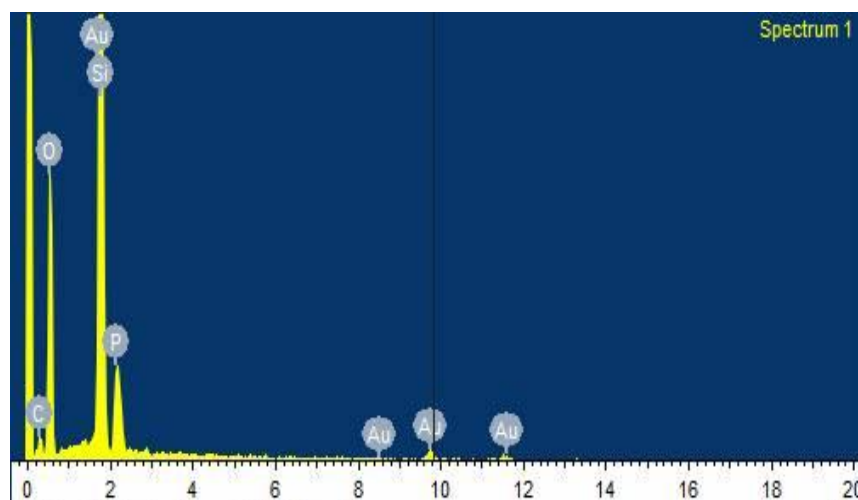


Fig.2.9 EDS spectra of MPFSG (intensity vs. kinetic energy (keV) plot)

2.1.3. Synthesis and Characterisation of Bi-Phosphate Functionalised Silica Gel (BPFSG)

2.1.3.1. Synthesis of BPFSG

ASG (25g) has been reacted with 1,2,3-tribromopropane (5ml) in water (250 ml) under reflux for 18 hours. It has been filtered, washed with de-ionised water and diethylether. The brominated silica gel (BSG-1) thus obtained has been then reacted with 5ml of di-(2-ethylhexyl)phosphoric acid (DEHPA) in presence of a base for 16 hours giving the final product bi-phosphate functionalised silica gel (BPFSG). BPFSG has been filtered, washed with ethanol and dried at 60°C for 10 hours. Synthesis scheme of BPFSG has been given below (Fig.2.10).

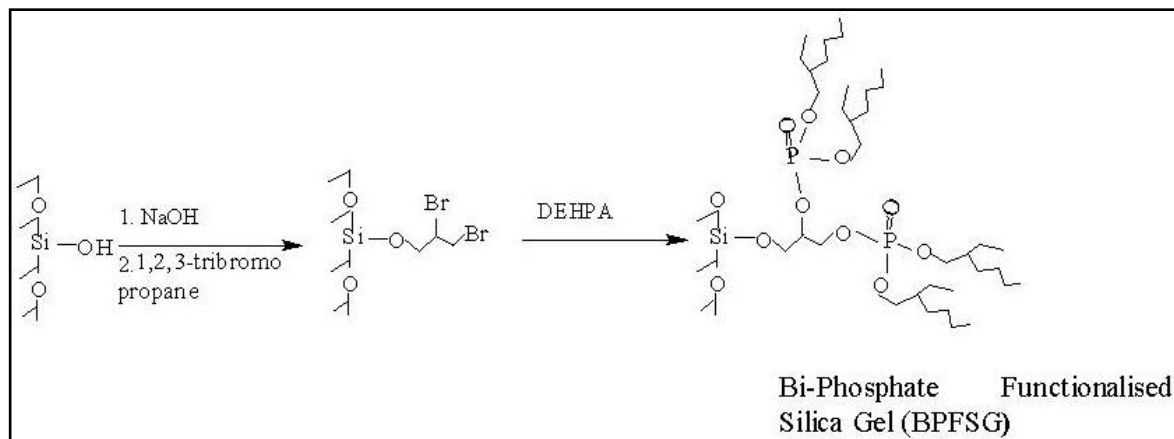


Fig.2.10 Synthesis scheme of BPFSG

2.1.3.2. Characterisation of BPFSG

BPFSG has been characterised by the following techniques.

2.1.3.2.1. FT-IR Study for BPFSG

In the IR spectra, bands at the position of 1208 cm^{-1} corresponds to P=O stretching vibration frequencies. Bands at the position of 635 cm^{-1} , 1465 cm^{-1} and 1620 cm^{-1} correspond to Si-O-Si bending vibration, CH_2 bending vibration and H-O-H bending vibrations of sorbed water molecules on to functionalised silica gel surfaces [1-2]

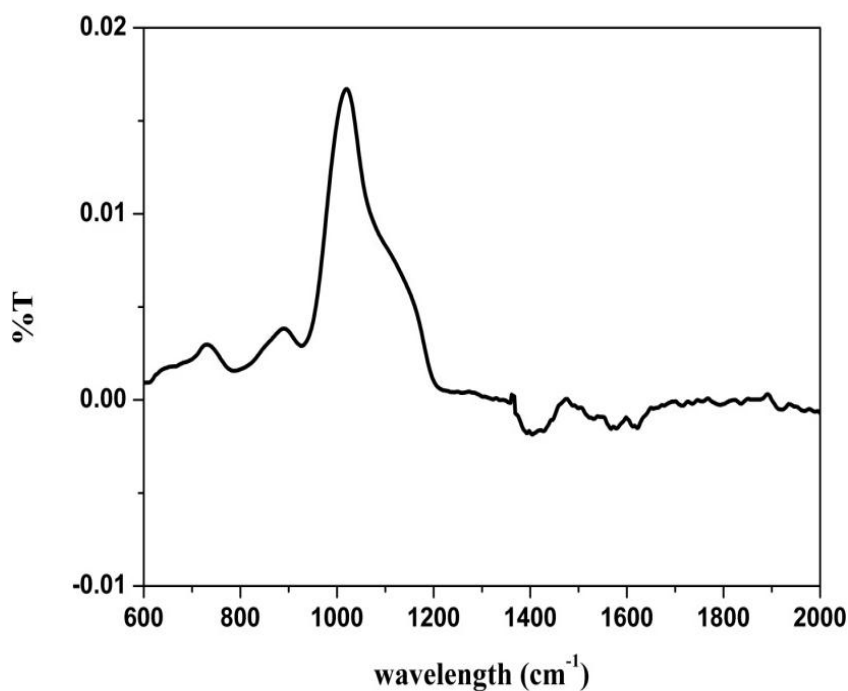


Fig.2.11 FT-IR spectra of BPFSG

2.1.3.2.2. XPS Study for BPFSG

XPS study of BPFSG shows the peaks at the energies of 104.07, 129.9, 154.8, 192, 284.6 and 531.5 eV for Si 2p, P 2p, Si 2s, P 2s, C 1s and O 1s (Fig.2.12) for respectively. This confirms the successful functionalisation of BPFSG.

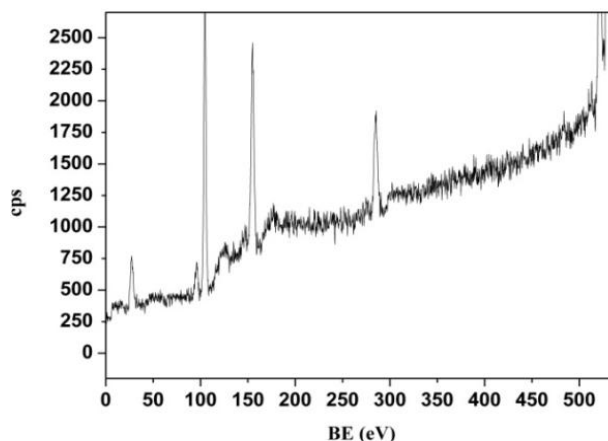


Fig.2.12 XPS study of BPFSG

2.1.4. Synthesis and Characterisation of Tri-Phosphate Functionalised Silica Gel (TPFSG)

2.1.4.1. Synthesis of TPFSG

ASG (25g) has been reacted with 1,1,2,2-tetrabromoethane (5 ml) in water (250 ml) under reflux for 14 hours. It has been filtered, washed with de-ionised water and diethylether. Brominated silica gel has then been reacted with 5ml of di-(2-ethylhexyl) phosphoric acid (DEHPA) in presence of a base for 15 hours. TPFSG, thus obtained, has been filtered, washed with ethanol and dried at 60°C for 10 hours. Synthetic scheme for TPFSG has been depicted in Fig.2.13.

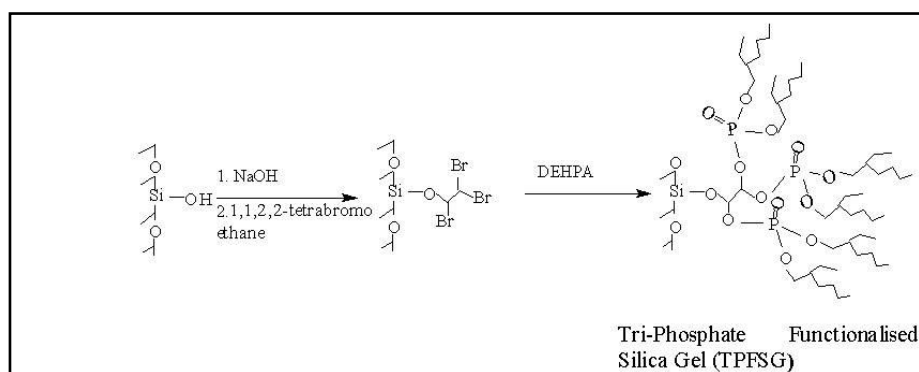


Fig.2.13 Synthesis scheme of TPFSG

2.1.4.2. Characterisation of TPFSG

TPFSG has been characterised by FT-IR, SEM-EDS and XPS spectra as described below.

2.1.4.2.1. FT-IR Spectra of TPFSG

Similar IR peaks like BPFSG have been observed in case of TPFSG (Fig.2.14) which confirms the presence of phosphate group on its surface.

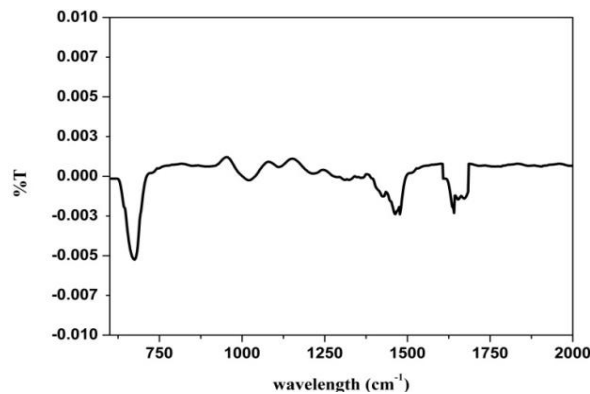


Fig.2.14 FT-IR spectra of TPFSG

2.1.4.2.2. SEM-EDS Study of TPFSG

SEM spectra of TPFSG has been given in Fig.2.15a and the EDS spectra has been given in Fig.2.15b. EDS spectra of TPFSG shows the presence of silicon, phosphorus, carbon and oxygen on its surface which again confirms the successful functionalisation of TPFSG. Additional peak of gold comes due to gold coating during SEM study.

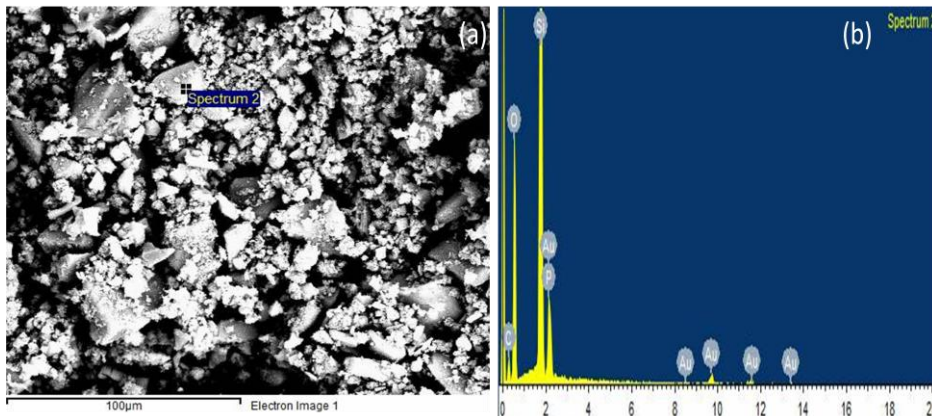


Fig.2.15 (a) SEM spectra of TPFSG, (b) EDS spectra of TPFSG (intensity vs. kinetic energy (keV) plot)

2.1.4.2.3. XPS Study of TPFSG

Peaks of carbon, oxygen, silicon and phosphorus have been observed in the XPS spectra of TPFSG (Fig.2.16) as has been observed in case of BPFSG.

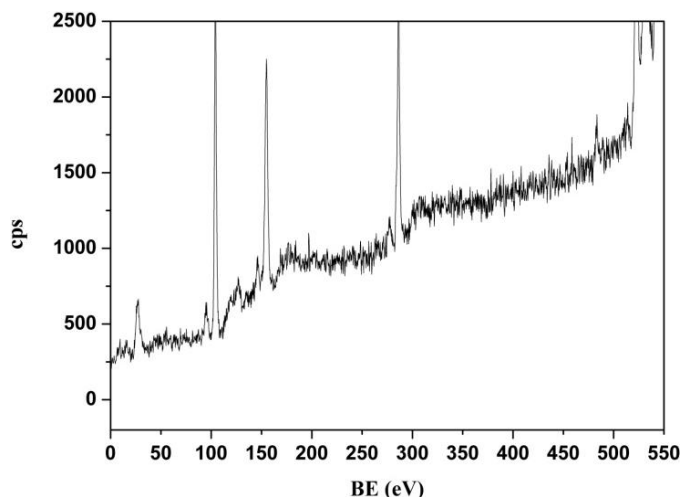


Fig.2.16 XPS spectra of TPFSG

2.1.5. Synthesis and Characterisation of Amine and AmidoPyridyl Phosphate Functionalised Silica Gel (AAPPFSG)

2.1.5.1. Synthesis of AAPPFSG

ASG (25g) has been reacted with 1,4-dibromobutane (5 ml) in water (250 ml) under reflux for 18 hours. It has been filtered and washed with de-ionised water and diethylether. The brominated silica gel (BSG-2), thus obtained, has been reacted with 5ml of ethylenediamine in water (250ml) under reflux for 16 hours. The amine functionalised silica gel (ASG-1) thus obtained has been filtered and washed several times with de-ionised water. ASG-1 has been then reacted again with 1,4-dibromobutane under reflux for 14 hours. The amine functionalised and brominated silica gel (AFBSG), thus obtained, has been filtered and washed properly with de-ionised water. It has been then reacted with tris(aminoethyl)amine in water under reflux for 16 hours. The amine functionalised silica gel (ASG-2) has been filtered, washed with de-ionised water several times to remove residual reagents. ASG-2 has been then reacted with dimethyl-2,6-pyridinedicarboxylate in ethanol under reflux for

18 hours. The amidopyridyl carboxylate functionalised silica gel (APCFSG) has been then filtered, washed with ethanol several times to remove residual reagents. APCFSG has been finally reacted with di-(2-ethylhexyl)phosphoric acid (DEHPA) in water in presence of a base for 18 hours. Amine and amidopyridyl phosphate functionalised silica gel (AAPPFSG) thus obtained is the final product. AAPPFSG has been filtered, washed with de-ionised water and ethanol and then dried at 60°C for 10 hours. The synthetic scheme for AAPPFSG has been given in Fig.2.17.

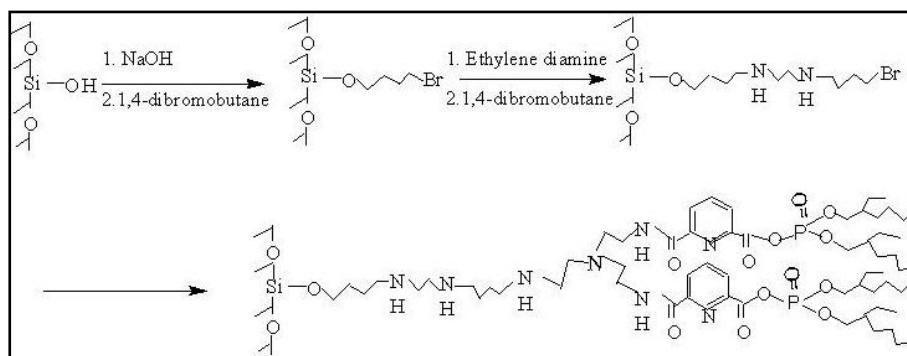


Fig.2.17 Synthesis scheme of AAPPFSG

2.1.5.2. Characterisation of AAPPFSG

2.1.5.2.1. FT-IR Spectra of AAPPFSG

For the characterisation of functionalised silica gels, infra red spectra (4000–400 cm^{-1}) has been recorded for BPFSG, TPFSG and AAPPFSG using diffuse reflectance accessory in a Fourier Transform Infrared Spectroscopy (FT-IR) instrument (Fig.2.18). In the IR spectra for these three functionalised silica gels, vibration frequency at 958 cm^{-1} correspond to P-OR ester (R is alkyl group) bond stretching, at 1101 cm^{-1} correspond to Si-O-Si and Si-O-C bond stretching, at 1208 cm^{-1} correspond to P=O bond stretching and at 2930 cm^{-1} corresponds to C-H bond stretching vibration. Frequencies at 635 cm^{-1} corresponds to Si-O-Si bending vibration, at 1465 cm^{-1} corresponds to CH_2 bending vibration, at 1620 cm^{-1} for H-O-H

bending vibrations for adsorbed water molecules on to the functionalised silica gel surfaces [1-2].

Additional IR bands were observed for AAPPFSG ligand at the following vibrational frequencies. Bands at 1653cm^{-1} , 1687cm^{-1} observed for C=O stretching of amide group [7] and at 1530cm^{-1} for the interaction between amide oxygen atom and the amide nitrogen atom present in the parallel chains [8]; Bands at 1619cm^{-1} assigned to pyridine ring vibration [9]; 1699cm^{-1} , 1734cm^{-1} and 1742cm^{-1} originate due to carbonyl bond vibration of the ester group [10], The broad band at $1780\text{-}1784$, and a weak band at 1855cm^{-1} can be assigned to the symmetric (strong) and asymmetric (weak) C=O stretching vibrations of O=C-O-P=O moiety present in the functional group of AAPPFSG. Nakason et al. observed similar results for the carbonyl groups present in anhydride moiety. [11] Bands at 1797 and 1833cm^{-1} correspond to the cis and trans stereoisomers of O=C=O moiety [12], NH_2 scissoring at 1595cm^{-1} , C-N stretching at 1320cm^{-1} , NH wagging at 932cm^{-1} [13]. These bands characterise the presence of phosphate group on BPFSG, MPFSG and AAPPFSG surfaces.

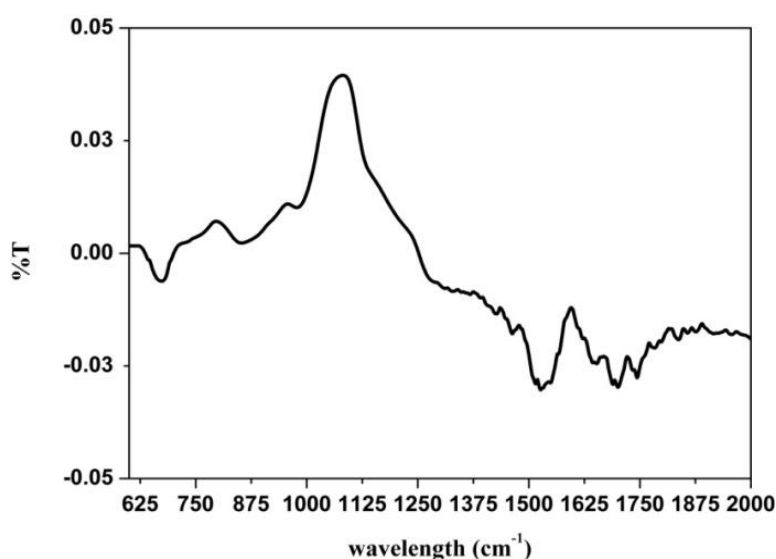


Fig.2.18 IR spectra of AAPPFSG

2.1.5.2.2. SEM-EDS Spectra of AAPPFSG

SEM spectra of AAPPFSG have been given in Fig.2.19a. EDS spectra has been given in Fig.2.19b which shows the presence of silicon, phosphorus, oxygen, nitrogen and carbon on the surface of AAPPFSG which confirms the successful incorporation of functional groups on the surface of AAPPFSG.

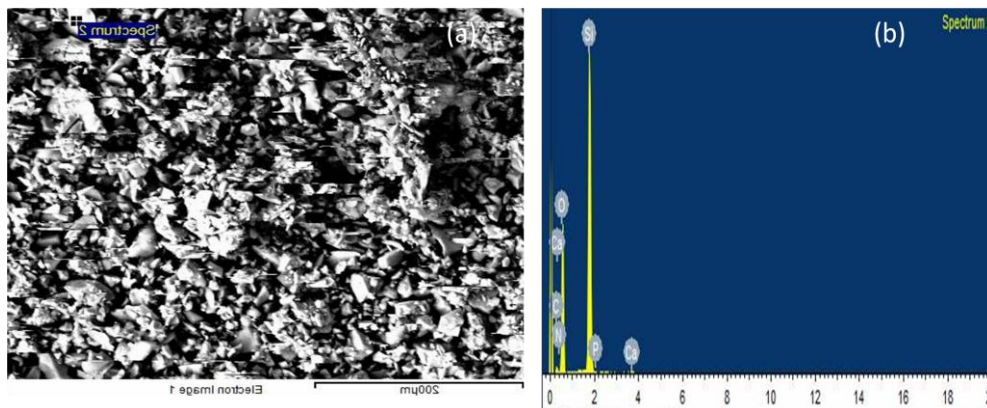


Fig.2.19 (a) SEM spectra of AAPPFSG, (b) EDS spectra of AAPPFSG (intensity vs. kinetic energy (keV) plot)

2.1.5.2.3. XPS Spectra of AAPPFSG

XPS spectra of AAPPFSG (Fig.2.20) shows the peaks of silicon, carbon, nitrogen, oxygen, and phosphorus at binding energies of 104.07eV (for Si 2p), 154.8eV (Si 2s), 284.6eV (for C 1s), 398.3 eV (for N 1s), 531.5 eV (for O 1s), 129.9 eV (for P 2p), 192eV (P 2s). This indicates successful functionalisation of AAPPFSG.

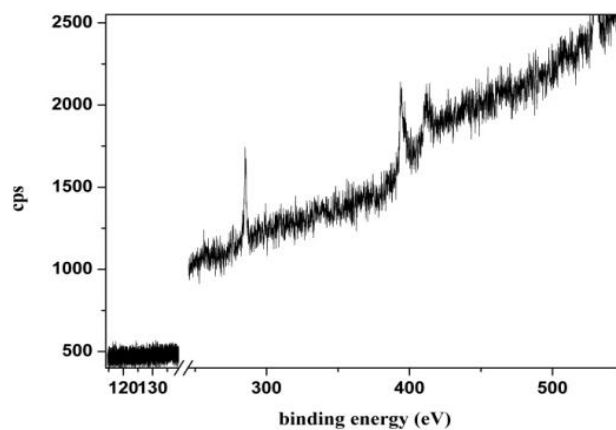


Fig.2.20 XPS of AAPPFSG

2.1.6. Synthesis and Characterisation of 1,8-Dihydroxy Anthraquinone Functionalised Silica Gel (DHAFSG)

2.1.6.1. Synthesis of DHAFSG

25g of alkali treated silica (ASG) has been reacted with 5 ml of 1,1,2,2-tetrabromoethane in water under reflux for 14 hours. It has been filtered, washed with de-ionised water and diethylether to remove the remaining reagents completely. The brominated silica has been then reacted with 7 ml of tris(aminoethyl)amine in water under reflux for 8 hours. It has been filtered, washed with water to remove all the amines present in it. The amine functionalised silica has then been reacted with 1,8-dihydroxy anthraquinone (10g) in anhydrous diethyl ether for 18 hours under reflux. The final product, DHAFSG, thus obtained, has been filtered, washed with di-ethyl ether and ethanol to remove any trace of reagent present in it. It has been dried at 60⁰C for ~8 hours. Synthetic scheme of DHAFSG has been given in Fig.2.21.

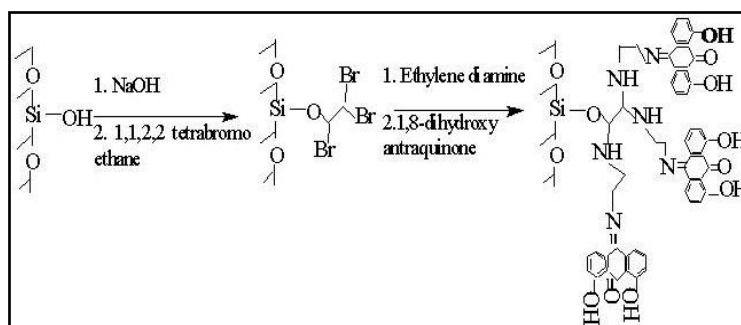


Fig.2.21 Synthesis scheme of DHAFSG

2.1.6.2. Characterisation of DHAFSG

2.1.6.2.1. FT-IR Spectra of DHAFSG

IR spectra of DHAFSG have been given in Fig.2.22. In the IR spectra, peak at 691 cm⁻¹ for Si-O bond of silica [14], 1275 cm⁻¹ corresponds to phenolic group [15]; at 1462cm⁻¹ for CH₂ bending and also C-H stretching [14], 1568 cm⁻¹ for C-C bond vibration in benzene ring [15], at 1638 cm⁻¹ for C=N vibration [16], at 1690 cm⁻¹ corresponds to vibrations of phenyl ketone [17].

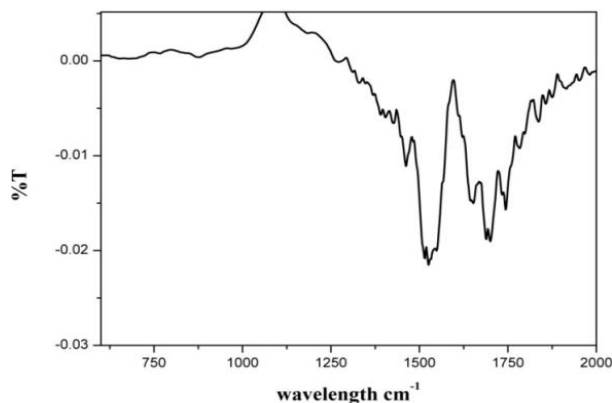


Fig.2.22 FT-IR spectra of DHAFSG

2.1.6.2.2. SEM-EDS Study of DHAFSG

SEM spectra of DHAFSG has been given in Fig.2.23a and the EDS spectra has been given in Fig.2.23b. From the EDS spectra it is observed that silicon, oxygen, carbon and nitrogen are present on the surface of DHAFSG. This confirms the successful incorporation of functional group on the surface of DHAFSG. Additional peak of gold has come from the gold coating on the sample during SEM study.

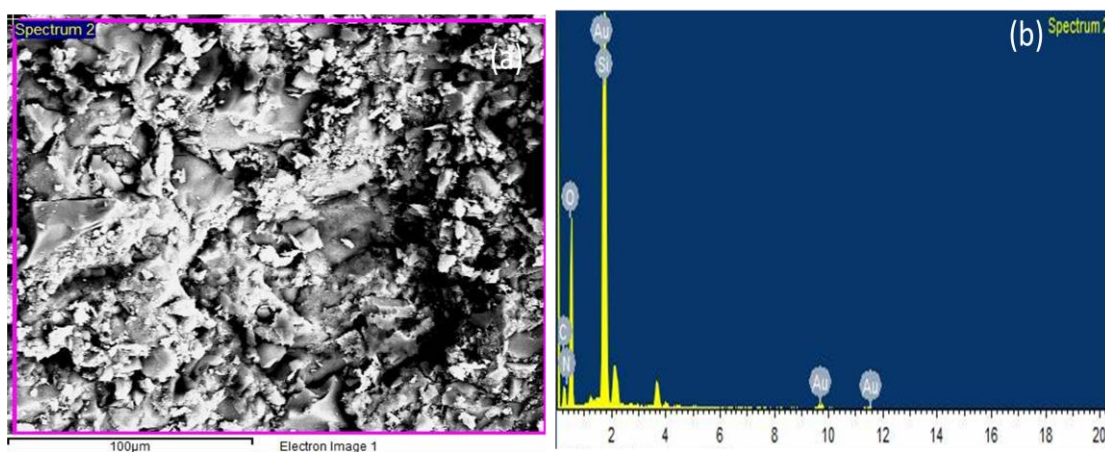


Fig.2.23 (a) SEM spectra of DHAFSG, (b) EDS spectra of DHAFSG ((intensity vs. kinetic energy (keV) plot))

2.1.7. Synthesis and Characterisation of AmidoPyridylAmine Functionalised Silica Gel (APAFSG)

2.1.7.1. Synthesis of APAFSG

ASG (20g) has been then reacted with 1,4-dibromobutane (5ml) in water (250ml) under reflux for 20 hours. It has been filtered and washed with de-ionised

water and diethylether. The brominated silica gel (BSG), thus obtained, has been reacted with 5ml of tris(aminoethyl)amine in water (250ml) under reflux for 18 hours. The amine functionalised silica gel (ASG-1) thus obtained has been filtered and washed several times with de-ionised water. ASG-1 has been then reacted again with dimethyl-2,6-pyridinedicarboxylate in ethanol under reflux for 16 hours. The amidopyridyl carboxylate functionalised silica gel (APCFSG) thus obtained, has been filtered, washed with ethanol several times to remove residual reagents. APCFSG has been again reacted with tris(aminoethyl)amine (5ml) for another 18 hours. The amidopyridyl amine functionalised silica gel (APAFSG) thus obtained is the final product. APAFSG has been filtered, washed with de-ionised water and ethanol and then dried at 60°C for 10 hours. Synthesis scheme of APAFSG has been given in Fig.2.24.

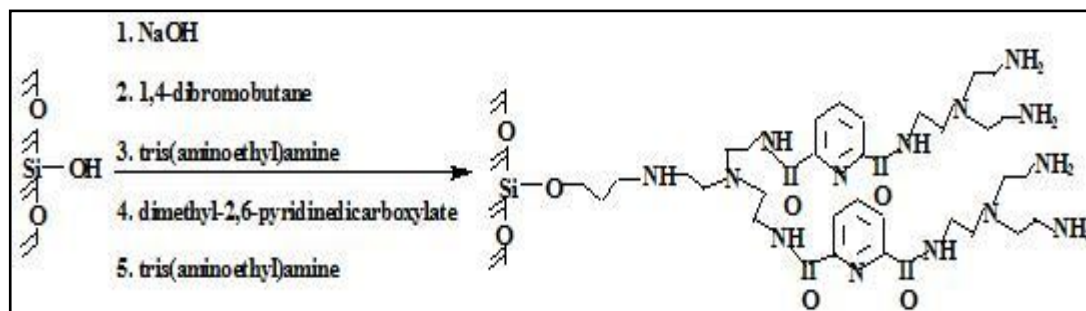


Fig.2.24 Synthesis scheme of APAFSG

2.1.7.2. Characterisation of APAFSG

APAFSG has been characterised by FT-IR (using spectrometer-JASCO FTIR-6100) (Fig.2.25). The peaks at 1530 cm^{-1} , 1653 cm^{-1} and 1687 cm^{-1} come due to amide group [7-8], 1101 cm^{-1} is due to Si-O-Si vibration [2], at 1619 cm^{-1} for pyridine group [9] and at 1595 cm^{-1} , 1314 cm^{-1} , 932 cm^{-1} for amine group [13]. Bands at 1367 cm^{-1} due to gauche conformation of alkanes [18] and at 1492 cm^{-1} due to hydrogen bonding between the carbonyl oxygen of amide group and hydrogen of amine [19]. Band at 1427 cm^{-1} is due to CH₂ scissoring of the alkanes [20].

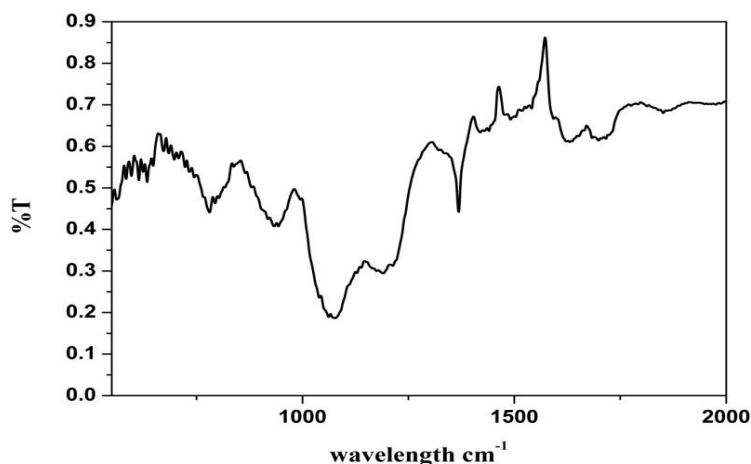


Fig.2.25 FT-IR spectra of APAFSG

2.1.8. Synthesis and Characterisation of Butanol Functionalised Silica Gel (BFSG)

2.1.8.1. Synthesis of BFSG

BFSG has been obtained by the following way. ASG (25g) has been with 1,4-dibromobutane (10ml) in water for 20 hours. It has been washed with water and diethyl ether properly to remove the reagents completely. It has been dried at 45⁰C to remove ether completely and then reacted with 0.1M sodium hydroxide for 10 hours. The final product BFSG thus obtained, has been washed with water and ethanol to remove all the reagents completely from BFSG. It has been dried at 60⁰C for 8 hours and has been used for further studies. Synthetic scheme for BFSG has been given in Fig.2.26.

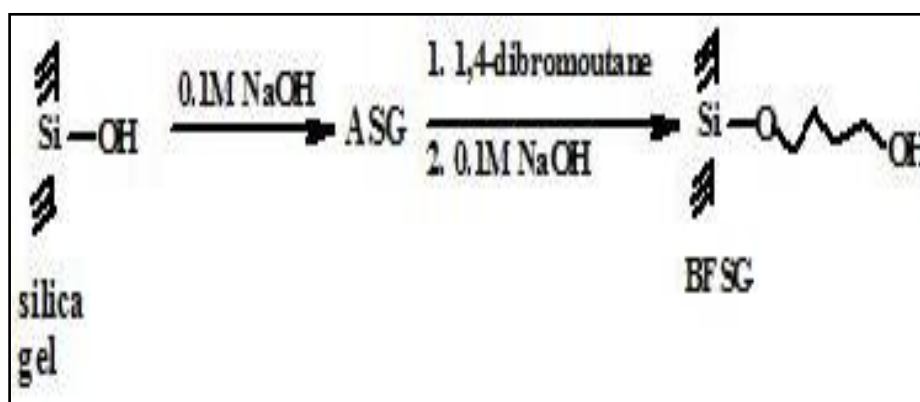


Fig.2.26 Synthesis of BFSG

2.1.8.2. Characterisation of BFSG

BFSG has been characterised by EDS spectra which has been given below (Fig.2.27). It shows the presence of silicon, carbon and oxygen on its surface confirming successful incorporation of butanol group on its surface. Additional peaks of Mg, Ca may be due to their uptake by BFSG from water used in the synthesis process.

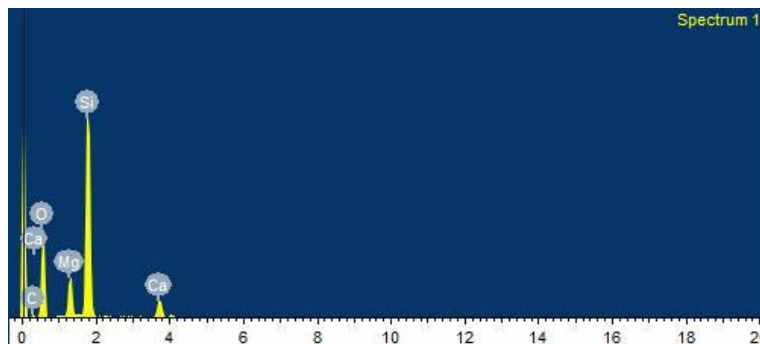


Fig.2.27 EDS spectra of BFSG

2.2. Experiments and Analysis

2.2.1. Reagents and Solution Preparations

2.2.1.1. Reagents

U_3O_8 powder used in the studies has been obtained from our institution. Standard solutions (used for Inductively Coupled Plasma i.e. ICP analysis) for uranium, iron, calcium, aluminium, magnesium, rare earths, zirconium, hafnium, copper, lead, zinc, chromium, mercury and silicon procured from Merck are all analytical reagent grade standards. Silica gel powder (procured from Thomas Baker), nitric acid (procured from Thomas Baker), sodium hydroxide (procured from Polyfarm), magnesium oxide (procured from Merck), ferric chloride (procured from Merck), calcium nitrate (procured from Chemco fine chemicals, Mumbai), hydrochloric acid (procured from S-D-Fine chemicals), sodium carbonate (procured from Polypharm), lead chloride (procured from Sigma Aldrich), zinc sulphate (procured from Merck), copper sulphate (procured from polypharm), potassium dichromate (procured from S-D-Fine chemicals) have been used in the studies. All the reagents used in the studies are of analytical reagent grade.

2.2.1.2. Preparation of Solutions and Analysis

Measured quantity of U_3O_8 has been dissolved in nitric acid and used as the stock solution. Uranium feed solutions have been prepared from this stock solution by proper dilutions and pH adjustment. Adjustment of pH has been done using sodium hydroxide or, sodium carbonate as mentioned in the respective experiments. Stock solution containing calcium, magnesium, iron, aluminium and uranium has been prepared by dissolving measured quantities of calcium nitrate, magnesium oxide and ferric chloride, U_3O_8 in nitric acid. Lead chloride, zinc sulphate, copper sulphate, potassium dichromate have been dissolved in nitric acid and pH adjusted to pH 5 using sodium hydroxide.

Simulated silicide fuel scraps dissolver solution, abbreviated as 'SSFSDS', (results using it has been described in chapter 3) has been prepared as per the reported composition by Rodrigues et. al. [21]. It has been prepared by mixing measured volumes of U_3O_8 stock solution and standard solutions (ICP standards) of aluminium and silicon altogether.

For extraction of Pd from aqueous hydrochloric acid solution (as described in chapter 6), stock solution of 10-2 M Pd(II) has been prepared in 3.0 M HCl by dissolving appropriate amount of $PdCl_2$ in hydrochloric acid. Aliquots have been taken from this stock solution and properly adjusted for Pd(II) and hydrochloric acid concentration, and have been used for different experiments. Simulated spent catalyst dissolver solution (SSCD) has been prepared using metal salts in concentrated HCl. Further, the stock solution has been diluted to appropriate concentration of metal ions and acid for liquid-liquid extraction. The concentrations of the metal ions present SSCD solution are given in Table 2.1.

Table 2.1 Simulated spent catalyst dissolver (SSCD) solution

Serial No	Element	Concentration (mg/l)
1	Pd (II)	88.1
2	Cr (VI)	81.8
3	Fe (III)	1002.4
4	Mn (II)	528.6
5	Ni (II)	1138.2
6	Pt (II)	85.8

Solutions of Pd(II) in nitric acid medium have been prepared in the similar way as in the hydrochloric acid medium as described above.

Quantitative determination of all the elements i.e. aluminium, magnesium, calcium, iron, uranium, rare earths, zirconium, hafnium, mercury, copper, lead, zinc, chromium have been performed using Inductively Coupled Plasma Atomic Emission Spectrometry (ICP-AES) technique.

^{241}Am used for the experiments described in chapter 5, has been purified before use [23]. ^{152}Eu has been obtained from Board of Radiation and Isotope Technology (BRIT), Mumbai, India; ^{140}La , ^{147}Nd and ^{177}Lu have been prepared by the neutron activation of Nd_2O_3 powder in research reactor with thermal neutron flux of 1×10^{13} n/cm²/s. Concentrations of radiotracers like ^{241}Am , ^{152}Eu and ^{147}Nd have been estimated by gamma ray spectrometry method using HPGe detector.

A high purity germanium detector coupled to a 4096 channel analyzer has been used to detect the activity of the radionuclides during HLW experiment as described in chapter 6. Energies used for the various radionuclides are as follows: ^{106}Ru -621keV, ^{137}Cs -662keV, ^{144}Ce -133keV, ^{241}Am -59keV, ^{152}Eu -121.8keV and ^{85}Sr -514keV. Spectro-photometry using the chromogenic reagent 2-(5-bromo-2-pyridylazo)-5-diethylaminophenol (Br-PADAP), has been used to analyze uranium. TTA extraction followed by radiometry has been used to analyze plutonium.

Solutions of Pb(II), Cu(II), Zn(II) and Cr(VI) metal ions as used for experiments described in chapter 7, have been obtained by dissolving lead nitrate, copper sulphate, zinc chloride and potassium dichromate in water respectively. The concentrations of metal ions in these solutions have been measured by ICP-AES.

2.2.2. Solid Phase Extraction (SPE) Method: Sorption Experiments

SPE method has been broadly described in chapter 1, section 1.2. All the sorption experiments under this section have been carried out in batch mode. A measured quantity of functionalised silica gel has been contacted with a measured feed volume of known concentration of metal ion at room temperature i.e. 303K (if not mentioned otherwise) during the sorption studies.

2.2.2.1. Sorption Equilibration

Sorption studies where the aqueous solution having known metal concentration has been equilibrated with a definite amount of functionalised silica gel, can be monitored by two parameters namely, the distribution coefficient (D) and equilibrium sorption capacity (Q_e , mg g⁻¹). The distribution coefficient (D) and the equilibrium sorption capacity (Q_e , mg g⁻¹) have been calculated with the following formulae:

$$D = \frac{C_0 - C_e}{C_e} \times \frac{V}{m} \quad (2.1)$$

$$Q_e = (C_0 - C_e) \times \frac{V}{m} \quad (2.2)$$

Where, C_0 and C_e are the metal ion concentration (mg ml⁻¹) at $t=0$ and at equilibrium in the solution, V is the total volume of solution (ml); and m is the mass of adsorbent (g).

2.2.2.2. Sorption Extraction

Percentage of metal extraction by sorption method can be given as

$$\% \text{ Extraction} = \frac{(\text{metal ion sorbed in mg})}{(\text{metal ion in feed in mg})} \times 100 \quad (2.3)$$

2.2.2.3. pH Variation of Feed Solution

A fixed quantity of functionalised silica gel has been equilibrated with a fixed volume of aqueous solution of known metal ion concentration with different pH. The raffinate solution has been analysed for the metal ion concentration and the percentage extraction has been calculated using equation (2.3).

2.2.2.4. Sorption Kinetics Studies

All the metal ion sorption kinetics has been investigated by two kinetic models, namely, pseudo-first and pseudo-second-order models [23].

2.2.2.4.1. Pseudo 1st-Order Kinetic Model

The pseudo-first-order kinetic equation can be written as

$$\frac{dq_t}{dt} = k_f(q_e - q_t) \quad (2.4)$$

where q_t (mg g^{-1}) is the amount of metal ion sorbed at time t (min), q_e (mg g^{-1}) is the sorption capacity at equilibrium, and k_f (min^{-1}) is the rate constant for pseudo-first-order model.

Integrating and applying the initial conditions $q_t = 0$ at $t = 0$ and $q_t = q_t$ at $t = t$, the equation becomes

$$\log(q_e - q_t) = \log q_e - \frac{k_f t}{2.303} \quad (2.5)$$

2.2.2.4.2. Pseudo 2nd-Order Kinetic Model

The pseudo-second order kinetic model can be given by following equation

$$\frac{dq_t}{dt} = k_s(q_e - q_t)^2 \quad (2.6)$$

where k_s is the rate constant of pseudo-second-order model (in $\text{mg g}^{-1} \text{min}^{-1}$). By definite integration of equation (2.6) with boundary conditions $q_t = 0$ when $t = 0$ and $q_t = q_t$ at $t = t$, the following equation is obtained:

$$\frac{t}{q_t} = \frac{1}{k_s q_e^2} + \left(\frac{1}{q_e}\right) t \quad (2.7)$$

2.2.2.5. Sorption Isotherm Studies

The equilibrium sorption of metal ion onto functionalised silica gels has been analyzed using Langmuir and Freundlich isotherms [24-25].

2.2.2.5.1. Langmuir Isotherm Model

Langmuir model is the theoretical model for monolayer sorption onto a surface with finite number of identical sites [24]. The linearization form of Langmuir equation can be given as below

$$\frac{C_e}{q_e} = \frac{\alpha_L C_e}{K_L} + \frac{1}{K_L} \quad (2.8)$$

K_L and α_L are the equilibrium constants of Langmuir equation. Plotting C_e/q_e against C_e yields a straight line with slope, α_L/K_L , and intercept $1/K_L$. The ratio α_L/K_L indicates the theoretical monolayer saturation capacity, Q_0 .

2.2.2.5.2. Freundlich Isotherm Model

Freundlich isotherm is applicable to sorption on heterogeneous surface as well as multilayer sorption [25]. The model can be presented by equation

$$\log q_e = \log K_F + \frac{1}{n} \log C_e \quad (2.9)$$

By plotting $\log q_e$ versus $\log C_e$, constant K_F and exponent $1/n$ can be calculated.

2.2.2.6. Determination of Loading Capacity

Loading capacity (mg g^{-1}) has been determined by equilibrating a measured quantity of functionalised silica gel with the feed solution containing known

concentration of metal ions repeatedly. The raffinate solution has been analysed for the metal ion. This process has been repeated until a significant amount of metal ion remains unadsorbed in the raffinate solution. The loading capacity has been calculated using the following equation

$$\text{Loading Capacity}(\text{mgg}^{-1}) = \frac{\text{total loaded metal (mg)}}{\text{sorbent quantity (g)}} \quad (2.10)$$

2.2.2.7. Thermodynamic Studies

Thermodynamic studies were carried out by equilibrating a measured quantity of functionalised silica gel with a measured volume of feed solution with a known concentration of metal ions at a particular temperature. The metal ion concentration in the raffinate solution has been measured and the extraction coefficient 'D' of the metal ion as well as the extraction coefficient 'Q_e' have been calculated using equations (2.1) and (2.2) respectively. The sorption equation can be given as



where, 'M' is the metal ion with 'n' positive charges, 'X' is the anion with 'm' negative charges and 'L' is the ligand for complexation; x, y and z are the stoichiometries of metal, anion and ligand required for the complexation reaction respectively. Charge of the complex species is (nx-my) which is zero for the neutral complex. 'aq' stands for the aqueous phase and 's' stands for the solid phase in case of SPE method.

The equilibrium constant after sorption can be given as

$$K_{\text{eq.}} = \frac{[\text{L}_z\text{M}_x\text{A}_y]_{\text{s}}^{(nx-my)}}{[\text{M}^{n+}]_{\text{aq.}}^x \cdot [\text{A}^{m-}]_{\text{aq.}}^y \cdot [\text{L}]_{\text{s}}^z} \quad (2.12)$$

where, $[\text{L}_y\text{MX}_{(n-m+1)}]_{\text{s}}$ is the concentration of metal ion on the solid phase (in the form of complex) after equilibration, $[\text{M}^{n+}]_{\text{aq.}}$ and $[\text{X}^{m-}]_{\text{aq.}}$ are the concentration of metal ion and concentration of anion in the aqueous phase after equilibration.

Incorporating the expression for distribution coefficient 'D' from equation 2.1, taking logarithm on both sides and rearranging we get,

$$\ln D = \ln K + y \ln[A^{m-}] + z \ln[L] \quad (2.13)$$

where, $K = K_{eq} \cdot \frac{m}{V}$

From thermodynamics we get,

$$\ln K_{eq.} = -\frac{\Delta H_0}{RT} + \frac{\Delta S_0}{R} \quad (2.14)$$

Incorporating the expression for $K_{eq.}$ in equation 2.14 we get,

$$\ln D = -\frac{\Delta H_0}{RT} + \frac{\Delta S_0}{R} + \ln \frac{m}{V} + y \ln[A^{m-}] + z \ln[L] \quad (2.15)$$

Keeping all the parameters constant from the plot of $\ln D$ vs. $1/T$ we will get the enthalpy of reaction ' ΔH_0 ' and from the intercept, the entropy of reaction ' ΔS_0 '.

2.2.2.8. Effect of other Metal Ions on Sorption

Effect of other metal ions has been studied by equilibrating the aqueous solution containing all the metal ions of known concentration with measured quantity of functionalised silica gel. The raffinate solution obtained after equilibration has been analysed for all the metal ions. The percentage extraction for all the metal ions has been calculated by using equation (2.3).

2.2.2.9. Desorption and Re-usability

Desorption studies have been carried out in batch mode. All the desorption studies have been carried out in two steps: i) functionalised silica gel has been equilibrated with a fixed volume of aqueous solution with known metal ion concentration, ii) the metal-loaded functionalised silica gel (as obtained after step one) has been then equilibrated with the eluent solution. The desorption percentage of metal ion has then been calculated by measuring the metal ion concentration in the eluent solution by using the following equation (2.16).

$$\% \text{ Desorption} = \frac{(\text{metal ion desorbed})}{(\text{metal ion sorbed})} \times 100 \quad (2.16)$$

Re-usability studies for the functionalised silica gels have been carried out by performing the loading and de-loading experiments repeatedly. The aqueous samples have been analysed each time for the metal values loaded and de-loaded. Percentage of extraction by sorption and percentage of de-sorption have been calculated using equation (2.3) and (2.16) respectively.

2.2.2.10. Column Studies

Column studies for the metal ions have been carried out by loading the column of known bed volume with the metal ion solution at a fixed flow rate of the loading solution. Elution of the loaded metals has been carried out with the suitable eluent solution at a fixed flow rate. Samples have been collected at a volume multiples of bed volume and have been analysed for the metal ions. Elution experiments have been carried out until the complete elution of all the metal ions. Percentage of elution has been calculated using equation 2.16.

2.2.3. Liquid-Liquid Extraction Studies

2.2.3.1. Solvent Extraction Studies

Solvent extraction method has already been elaborated in chapter 1, section 1.1. For solvent extraction system, the uptake of metal ion in the organic extractant solution is expressed in terms of distribution ratio (D_M) and percentage of extraction (% E) of metal ion. Selectivity for a metal ion is presented in terms of separation factor (β). These terms are defined as

$$\text{Distribution Ratio } (D_M) = [M]_{\text{org.}} / [M]_{\text{raff.}} \quad (2.17)$$

$$\% \text{ Extraction } (\% E) = D_M / (D_M + 1) \quad (2.18)$$

Equation 2.18 is valid for equal vol. of org. and aq. phases

$$\text{Separation factor } (\beta) = D_M / D_{\text{impurity}} \quad (2.19)$$

2.2.3.2. Supported Liquid Membrane (SLM) Studies

Supported liquid membrane method has been elaborated in chapter 1, section 1.2. The transport equations through the membrane can be given by

$$J = P_f \cdot C_f \quad (2.20)$$

where, P_f is the feed side permeability coefficient, C_f is the concentration of the metal ion at the feed side. Flux is also expressed as

$$J = -(1/Q) (dV_f C_f) / dt \quad (2.21)$$

where V_f is the feed volume, Q is the exposed area of the membrane.

$$Q = A \cdot \varepsilon \quad (2.22)$$

where, A is the geometrical area of the membrane and ε is the porosity of the membrane. Combining two transport equations (2.20) and (2.21) and integrating we get,

$$\ln\left\{ \frac{V_{f,0} C_{f,0}}{V_{f,t} C_{f,t}} \right\} = QPt / V_f \quad (2.23)$$

where $V_{f,0}$, $C_{f,0}$, $V_{f,t}$ and $C_{f,t}$ represent the volume and concentration of the feed solution at the beginning of the transport study and after time 't' respectively. If the volume of the feed solution does not change significantly, the above equation can be written as

$$\ln(C_{f,t} / C_{f,0}) = - (Q/V_f) Pt \quad (2.24)$$

Percentage transport of the ions through the membrane is given by

$$\%T = 100 \times (C_{f,0} - C_{f,t}) / C_{f,0} \quad (2.25)$$

Permeability and percentage transport are calculated from equations (2.24) and (2.25) respectively.

References

1. Protein conformation changes induced by a novel organophosphate-containing water-soluble derivative of a C60 fullerene nanoparticle, X. Zhang, C. Shu, L. Xie, C.

- Wang, Y. Zhang, J. Xiang, L. Li, Y. Tang, J. Phys. Chem. C, 2007, 111, 14327-14333.
2. Fourier transform infrared spectroscopic characterization of Kaolinite from Assam and Meghalaya, northeastern India, Bhaskar J. Saikia¹, Gopalakrishnarao Parthasarathy, J. Mod. Phys., 2010, 1, 206-210.
 3. Thermal degradation of methyl methacrylate polymers functionalized by phosphorus-containing molecules I. TGA/FT-IR experiments on polymers with the monomeric formula $\text{CH}_2\text{C}(\text{CH}_3)\text{C}(\text{O})\text{OCHRP}(\text{O})(\text{OC}_2\text{H}_5)_2$ ($\text{R}=\text{H}, (\text{CH}_2)_4\text{CH}_3, \text{C}_6\text{H}_5\text{Br}, \text{C}_{10}\text{H}_7$), M. Cochez, M. Ferriol, J. V. Weber, P. Chaudron, N. Oget, J. L. Mieloszynski, Polymer Degradation and Stability, 2000, 70, 455-462.
 4. Formation of stable Si-O-C submonolayers on hydrogenterminated silicon (111) under low-temperature conditions, Y. L. Khung, S. H. Ngalim, A. Scaccabarozzil, D. Narducci, J. Nanotechnol, 2015, 6, 19-26.
 5. X-ray photoelectron spectroscopy of graphitic carbon nanomaterials doped with heteroatoms, T. Susi, T. Pichler, P. Ayala, J. Nanotechnol., 2015, 6, 177-192.
 6. Handbook of X-Ray Photoelectron Spectroscopy, C. D. Wanger, W. M. Riggs, L. E. Davis, J. F. Moulder, G. E. Muilenberg.
 7. Vibrational assignments of trans-N-methylacetamide and some of its deuterated isotopomers from band decomposition of IR, visible, and resonance Raman spectra, X. G. Chen, R. S. Stenner, S. A. Asher, N. G. Mirkin, S. Krimm, J. Phys. Chem., 1995, 99, 3074-3083.
 8. The infrared spectra of polypeptides in various conformations: amide I and II bands, T. Miyazawa, E. R. Blout, J. Am. Chem. Soc., 1961, 83, 712-719.
 9. Structure and activity of fluorinated alumina. 1. Determination of the number of protonic sites by an infrared study of adsorbed pyridines, R. A. Matulewicz, F. P. J. M. Kerkhof, J. A. Moulijn, H. J. Reitsma, Journal of Colloid and Interface Science, 1980, 77, 110-119.
 10. Components of the carbonyl stretching band in the infrared spectra of hydrated 1,2-diacylglycerolipid bilayers: a re-evaluation, R. N. A. H. Lewis, R. N. McElhaney, W. Pohle, H. H. Mantsch, Biophysical Journal, 1994, 67, 2367-2375.
 11. Material characterisation the grafting of maleic anhydride onto natural rubber, C. Nakason, A. Kaesaman, P. Supasanthitikul, Polymer Testing, 2004, 23, 35-41.

12. Infrared spectrum and structure of intermediates in the reaction of OH with CO, D. E. Milligan, M. E. Jacox, *The Journal of Chemical Physics*, 1971, 54, 927-942.
13. Nanoscale assembly of amine-functionalised colloidal iron oxide, K. C. Barick, M. Aslam, P. V. Prasad, V. P. Dravid, D. Bahadur, *Journal of Magnetism and magnetic materials*, 2009, 321, 1529-1532.
14. Fourier transform infrared spectroscopic characterization of kaolinite from Assam and Meghalaya, Northeastern India Bhaskar J. Saikia¹, Gopalakrishnarao Parthasarathy, *J. Mod. Phys.*, 2010, 1, 206-210.
15. An in situ ATR-FTIR study: the surface coordination of salicylic acid on aluminum and iron (III) oxides, M. V. Blber', W. Stumm, *Environ. Sci. Technol.*, 1994, 28, 763-768.
16. Nonlinear optical properties, spectroscopic studies and structure of 2-hydroxy-3-methoxy-N-(2-chloro-benzyl)-benzaldehyde-imine, H. Ünver, A. Karakas, A. Elmali, *Journal of Molecular Structure*, 2004, 702, 49-54.
17. Three novel cyclic amides from *Clausena lansium*, Y. M. He, C. Y. Yong, H. Liang, *Phytochemistry*, 1988, 27, 2, 445-450.
18. Fourier transform infrared spectrometric determination of alkyl chain conformation on chemically bonded reversed phase liquid chromatography packings, L. C. Sander, J. B. Callis, and L. R. Field, *Anal. Chem.*, 1983, 55, 1068-1075.
19. Stability and structural features of DNA intercalation with ethidium bromide, acridine orange and methylene blue, S. Nafisi, A. A. Saboury, N. Keramat, J. F. Neault, H. A. T. Riahi, *Journal of Molecular Structure*, 2007, 827, 35-43.
20. Effects of short-time vibratory ball milling on the shape of FT-IR spectra of wood and cellulose, M. Schwanninger, J.C. Rodrigues, H. Pereira, B. Hinterstoisser, *Vibrational Spectroscopy*, 2004, 36, 23-40.
21. Reprocessing RERTR silicide fuels, G. C. Rodrigues, A. P. Gouge, DP-1657, 1983, United States.
22. Ethyl-bis-triazinylpyridine (Et-BTP) for the separation of americium(III) from trivalent lanthanides using solvent extraction and supported liquid membrane methods, A. Bhattacharyya, P. K. Mohapatra, A. Roy, T. Gadly, S. K. Ghosh, V. K. Manchanda, *Hydrometallurgy*, 2009, 99, 18-24.

23. Modeling of sorption kinetics: the pseudo-second order equation and the sorbate intraparticle diffusivity, W. Plazinski, J. Dziuba, W. Rudzinski, *Adsorption*, 2013, 19, 1055-1064.
24. The adsorption of gases on plane surfaces of glass, mica and platinum, I. Langmuir, *J. Am. Chem. Soc.*, 1918, 40, 1361-1403.
25. Over the adsorption in solution, H. M. F. Freundlich, *Z. Phys. Chem.*, 1906, 57, 385-471.

Selective Separation of Uranium with Phosphate Functionalised Silica Gels

3.1 Introduction

Global demand for electricity is increasing to manifest the modern technology to assist human civilisation. About 11% of global electricity production is contributed by nuclear energy [1]. On the other hand, the global warming and increasing environmental pollution generated from other resources of power generation is a big worry now-a-days. Nuclear industry produces electricity with very low environmental pollution which are managed in a controlled way, compared to fossil fuels or, gaseous fuels [2].

Uranium is the most important element in nuclear industry as it is used in fuel as fissile element for nuclear power production [3-5]. Uranium is used in the form of metal alloy, oxide, carbide, nitride in the nuclear fuel rod or, pellet [6-7]. Uranium also has its natural radioactivity which damages kidney and it also accumulates in bone [8-9]. As per the instruction of World Health Organisation (WHO) instruction, concentration of uranium in the drinking water should be below $15\mu\text{g L}^{-1}$ [10]. But uranium is found more in aqueous streams near the mining area [11], nuclear industry waste-water [12], and areas where phosphate fertilizer is used [13]. On the other hand, the average concentration of uranium is as low as 3mg kg^{-1} on the earth's crust [14-15]. Therefore, recovery of uranium from all resources is advantageous for our society to meet its growing demand as well as its harmless discharge to the environment.

Different methods have been tried for the recovery of uranium from aqueous solution e.g., precipitation [16], solvent extraction [17], electrolysis [18], electrodeposition [18-20], ion exchange [21-22], and liquid membranes [23]. Solid phase extracton (SPE) method, where the metal ions in the aqueous medium get sorbed on to solid sorbent, is used when the metal ion concentration in the aqueous solution is low (in few mg/L). SPE has some advantages namely, i) simple operation, ii) low cost and iii) safe handling while processing hazardous samples [24-29].

Different types of solid sorbents have been developed worldwide for exploring SPE method e.g., functionalised inorganic substances [30-43], polymeric resins [44-46], carbon based sorbents [46-53], bio-sorbent [54-55] etc. for metal ion sorption. Some sorbents also have limitations due to their low mechanical stability and swelling when used in aqueous medium [56]. Silica gel has some advantages over these problem e.g., i) it does not swell or shrink like the polymeric resins and ii) has good thermal stability, iii) high surface area and iv) large pore size giving appropriate accessibility of metal ions to the complexing groups present in the sorbent [57-58]. Choice of sorbent for SPE method depends upon its selectivity, re-usability and cost-effectiveness. Many of the solid sorbents have limitations due to i) slow kinetics [59] and ii) irreversible sorption [60] of metal ions. Chelating sorbents are being developed for their high sorption capacity and high selectivity. Chelating sorbents are prepared by two methods: i) impregnating the solid substance with the chelating group and ii) chemically bonding or, grafting of the chelating group on the solid substance [61-64]. Impregnation method is not very adoptable due to leaching of chelating group from the sorbent. Chemical reaction for grafting the functional group on the solid sorbent is the most adoptable technique to prepare chelating sorbents. A number of silica gel sorbents modified with chelating ligands containing ligands with oxygen, nitrogen,

phosphonate, phosphate and phosphoryl donors have been reported for extraction and preconcentration of uranium from aqueous solutions [65-70]. However, the need for better sorbent with respect to sorption capacity, selectivity and reusability still persists.

In this aspect, this work is dedicated to mono and multiple phosphate functionalised ligand grafted on the surface of silica gel for the selective sorption of uranium ions from aqueous medium. This work consists of evaluation of sorption of uranium from aqueous nitric acid medium using single-phosphate functionalised silica gel (SPFSG), bi-phosphate functionalised silica gel (BPFSG), tri-phosphate functionalised silica gel (TPFSG), amine and amido pyridyl phosphate functionalised silica gel (AAPPFSG). Experimental and theoretical studies have been carried out for exploring the sorption behaviour of uranium from aqueous nitric acid medium.

3. 2 Results and Discussion

All the sorption experiments with PFSG sorbent have been carried out in uranyl nitrate medium at pH1 adjusted by sodium hydroxide solution as uranium hydrolyses above pH3.5 in uranyl nitrate-sodium hydroxide medium [71]. Studies of uranium sorption on BPFSG, TPFSG and AAPPFSG have been carried out at pH 4.5 in uranyl nitrate-sodium carbonate medium where uranyl carbonate complexes remain in aqueous solution at this pH [71].

3.2.1 Kinetics Studies

Fig.3.1 shows the sorption of uranium on SPFSG, BPFSG, TPFSG and AAPPFSG as a function of time. It is observed that kinetic is very fast and sorption equilibrium is attained in less than fifteen minutes in all the cases. The kinetic data have been fitted in the pseudo-first order and pseudo-second order kinetic models

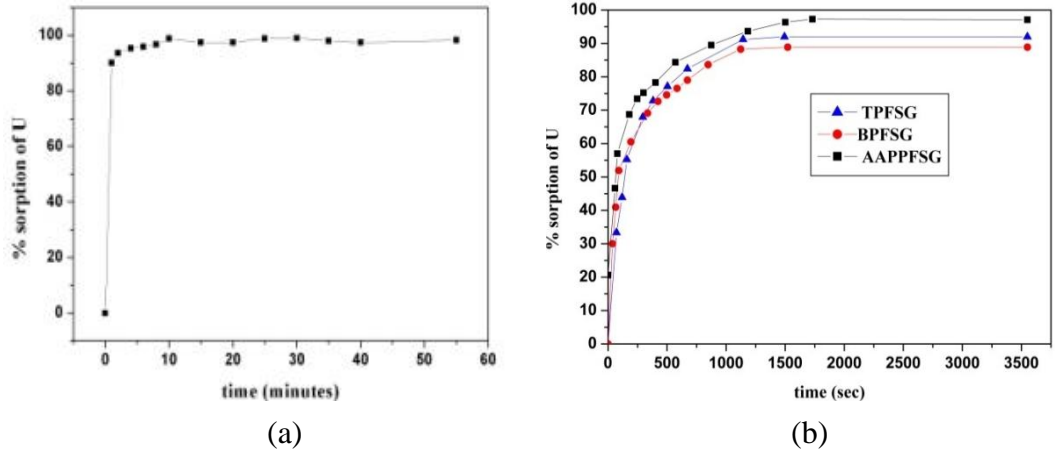


Fig.3.1 Sorption kinetics for uranium: % sorption of uranium vs. time using (a) SPFSG, (b) BPFSG, TPFSG and AAPPFSG.

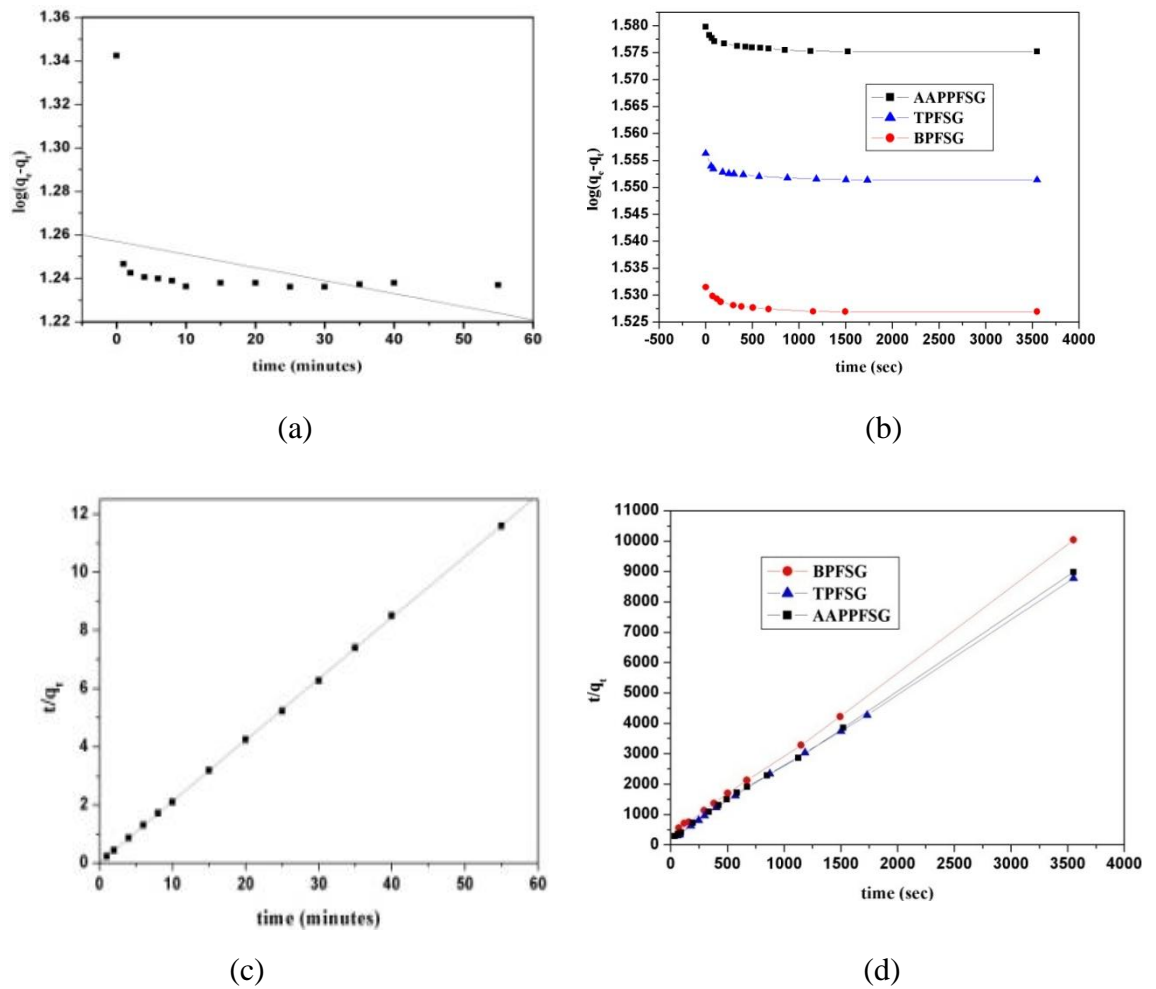


Fig.3.2 Pseudo first order kinetic plots using (a) SPFSG, (b) BPFSG, TPFSG and AAPPFSG; pseudo second order kinetic plots using (c) SPFSG, (d) BPFSG, TPFSG and AAPPFSG for uranium sorption.

have been given in Fig.3.2. It has been observed that (Fig.3.2), for the pseudo-second order kinetic plot i.e., q_t/t against t plot, the data points are determined to be very close to linearity with correlation coefficient closed to one. This infers that the sorption of uranium onto SPFSG, BPFSG, TPFSG and AAPPFSG can be explained well with the pseudo second order kinetic model. This further implies that the rate controlling step for the sorption reactions is the complexation of uranium with the functional groups present on the functionalised silica gels.

3.2.2 Effect of pH of Feed Solution on Uranium Sorption

To obtain the effect of pH on uranium sorption on to functionalised silica gels, sorption studies have been carried out with variation of pH of the feed solution as given in Fig.3.3. In case of SPFSG (Fig.3.3a), under the experimental condition of high sorbent dose i.e. 2 gL^{-1} SPFSG and low initial uranium concentration i.e. 50 mgL^{-1} , a very high sorption of uranium is observed all over the pH range (pH 1-6) due to the availability of large number of binding sites. It is observed that sorption decreases very slowly at higher pH. At low pH, there is a competition between H_3O^+ ion and uranyl ion for getting sorbed on to PFSG surface. But the uranium atom in the uranyl ion has a very high affinity for binding with oxygen atom due to its high ionic potential which leads to a strong chelation of uranyl ion with the $\text{P}=\text{O}$ oxygen atom. As the pH increases, formation of $[\text{UO}_2(\text{OH})]^+$ species increases due to the hydrolysis of uranyl ion as obvious from the speciation diagram [71]. At pH 5-6, more than 55% $[\text{UO}_2(\text{OH})]^+$ species is present in the solution. The affinity of uranium for oxygen atom is somewhat met by the oxygen atom present in hydroxyl ion in the $[\text{UO}_2(\text{OH})]^+$ species. Therefore, the uranium atom present in $[\text{UO}_2(\text{OH})]^+$ species has a less binding tendency with the $\text{P}=\text{O}$ oxygen atom compared to that uranium atom present in bare uranyl ion. This decreases the binding of uranium at higher pH. However, the

competition with H_3O^+ ion decreases at higher pH due to its less availability. Therefore, a very small decreasing trend of sorption of uranium onto PFSG is observed at higher pH.

In case of sorption of uranium on to BPFSG and TPFSG (Fig.3.3b), it is observed that sorption of uranium is maximum in the pH range 4.5-5.5 where uranium is present as neutral UO_2CO_3 species[71]. But in case of AAPPFSG (Fig.3.3b), considerable decrease in sorption is observed at pH greater than 4.5. These observations are deduced from three factors i) surface charge of the sorbents, ii) species present in the solution, iii) bulkiness of the sorbent. At lower pH, surface of the sorbent is positively charged due to protonation of the functional groups present on the sorbent causing less of uranium chelation on the sorbent. Sorption of uranium increases in the pH range 3-5 because the functional groups present in the sorbent gets de-protonated and chelates strongly with the neutral uranyl carbonate. Also, at higher pH i.e. $\text{pH} > 4.5$, bulky uranium species e.g. $\text{UO}_2(\text{CO}_3)_2^{2-}$ and $\text{UO}_2(\text{CO}_3)_3^{4-}$ are formed due to strong complexation of carbonates with the uranyl ion. The

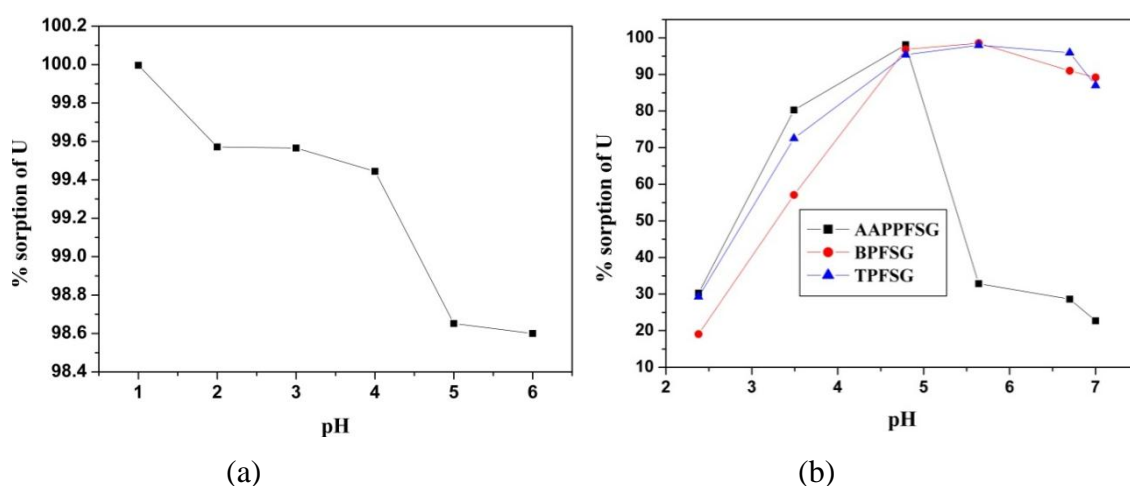


Fig.3.3 Effect of feed pH on sorption of uranium on (a) SPFG, (b) BPFSG, TPFSG and AAPPFSG.

decrease in sorption of these bulky uranium species is prominently observed in case of AAPPFSG. Because of the bulkiness around the binding sites in case of AAPPFSG, steric hindrance is created to the approaching big uranyl carbonate species to the binding sites which affects greatly the sorption of uranium on to AAPPFSG above pH 4.5.

3.2.3 Sorption Isotherm Studies

Sorption isotherm studies give the information about concentration of uranium present in the aqueous solution and on the sorbent at equilibrium. The isotherm plot (Fig.3.4) showed that uptake of uranium on the sorbent increases as the uranium concentration in the feed solution increases. Isotherm data have been fitted in both Langmuir and the Freundlich models to analyse the nature of sorption of uranium by the sorbents. Fig.3.5 shows the plot of C_e/q_e against C_e and Fig.3.6 shows the plot of $\log C_e$ against $\log q_e$ for Langmuir and Freundlich model respectively. It is found (Fig.3.5) that under the experimental conditions Langmuir model fits well with the experimental data. Loading capacities of SPFSG, BPFSG, TPFSG and AAPPFSG for uranium has been given in Table 3.1. (found to be 25mg/g, 34mg/g, 36mg/g and 38mg/g).

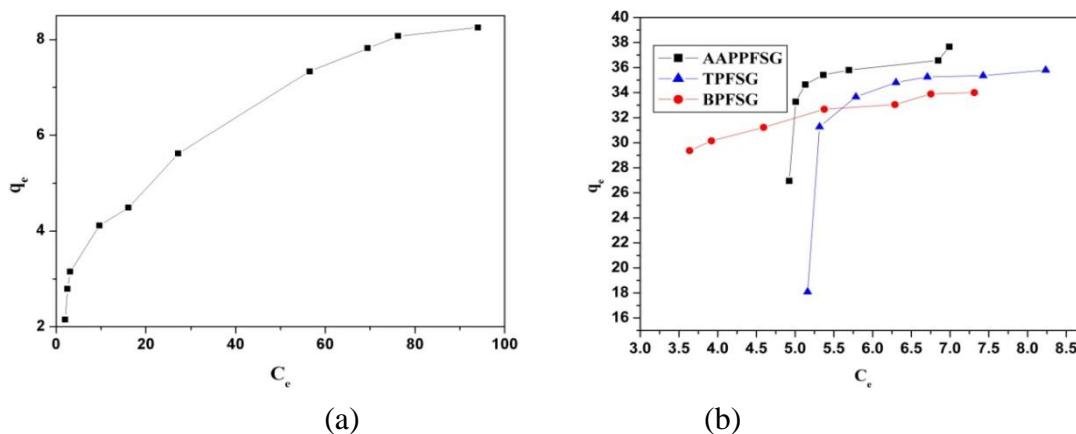


Fig.3.4 Isotherms for uranium sorption on to (a) SPFSG, (b) BPFSG, TPFSG and AAPPFSG

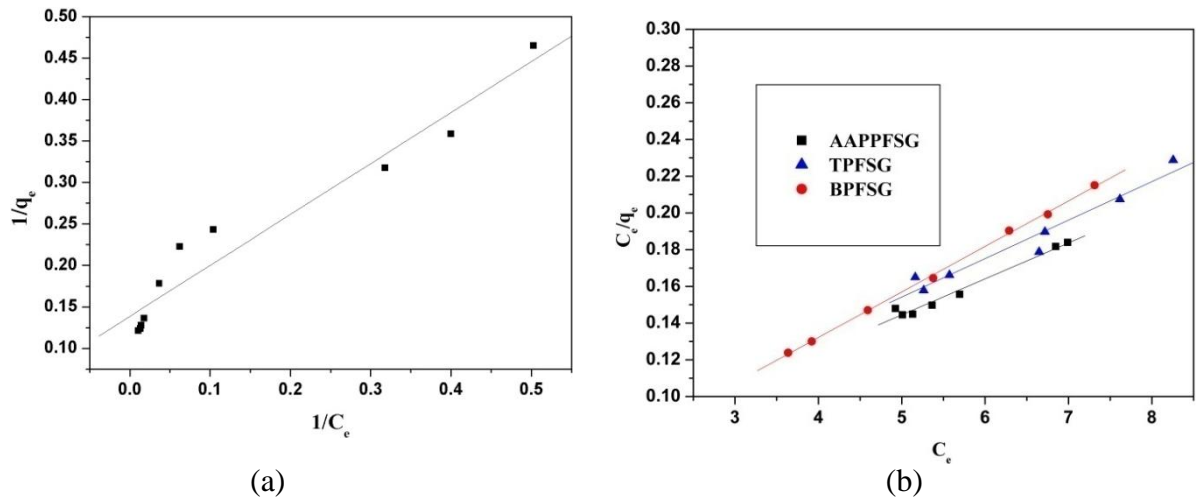


Fig.3.5 Sorption behaviour of uranium: Langmuir plot for (a) SPFG, (b) BPFSG, TPFSG, and AAPPFG

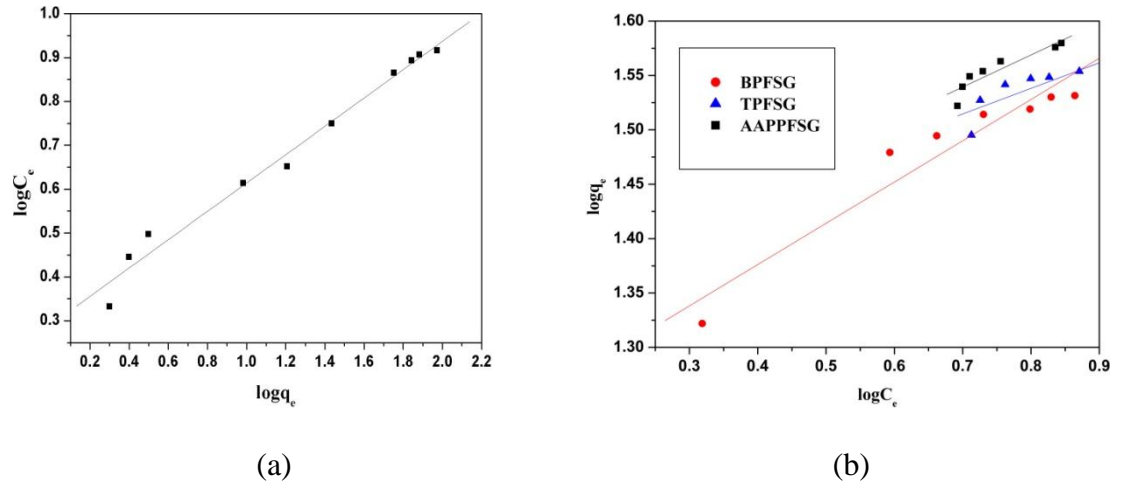


Fig.3.6 Sorption behaviour of uranium: Langmuir plot for (a) SPFG, (b) BPFSG, TPFSG, and AAPPFG

3.2.4 Effect of other Metal Ions on Uranium Sorption

For practical usage of functionalised silica gels, SPFG has been tested for its selectivity towards uranium over other metal ions. For this study, 0.5g of SPFG has been equilibrated with previously prepared feed solution at pH1 as mentioned before containing multi-elements like aluminium, magnesium, calcium, iron and uranium; concentration of each metal ion in the solution is 200 mgL^{-1} . Percentage extraction of each metal ion has been plotted in Fig.3.7. It is obvious that sorption of uranium is very high on to SPFG with almost negligible sorption of other elements (Fig.3.7)

from a feed solution at pH 1 made in nitric acid medium. This provides the selectivity of SPFSG towards uranium over other metal ions and shows its usefulness for practical applications.

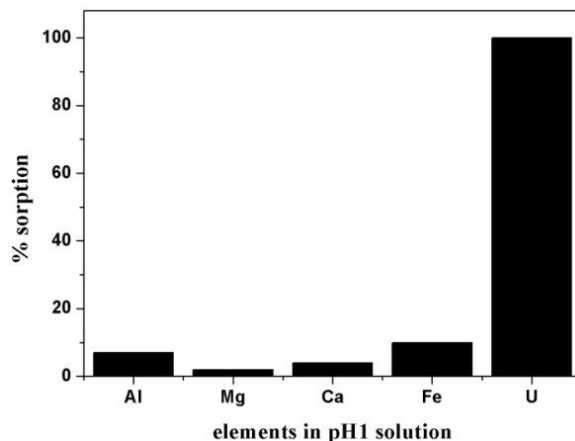


Fig.3.7 Effect of metal ions on sorption of uranium

3.2.5 Desorption Studies and Reusability of Sorbents

Functionalised silica gels e.g., SPFSG, has shown a good sorption ability and a desirable selectivity for uranium over a range of competing metal ions. From the application point of view, studies on the desorption behaviour and reusability of functionalised silica gels is mandatory. All the desorption experiments reported below have been carried out from loaded SPFSG. It is clear that as the pH of the eluent increases, release percents of uranium decreases (Fig.3.8). There is no remarkable release of uranium from loaded SPFSG when the pH value is above 0.5. Percentage release of uranium decreases from 70% to 20% when the pH of the eluent is increased from pH 0 to pH 0.5. This is due to the fact that the protonation of the phosphate moiety present in SPFSG and subsequent dissociation of uranyl–phosphate complex takes place easily at lower pH. This leads to the facile recovery of loaded SPFSG at low pH of the eluent (pH 0 in case of SPFSG). The re-usability of SPFSG has been found to be almost unchanged after 4 cycles of usage (Fig.3.9) indicating its feasible repeated use.

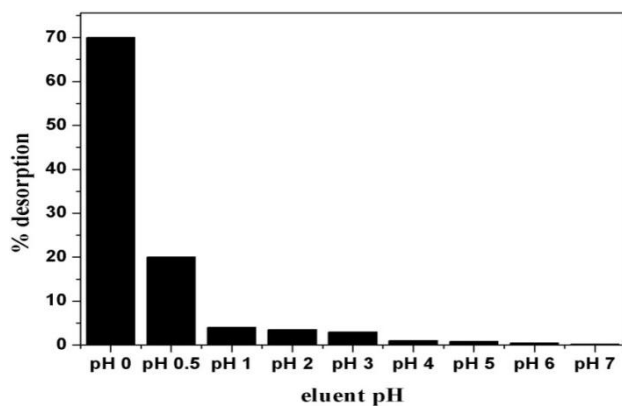


Fig.3.8 Desorption of uranium vs. eluent pH

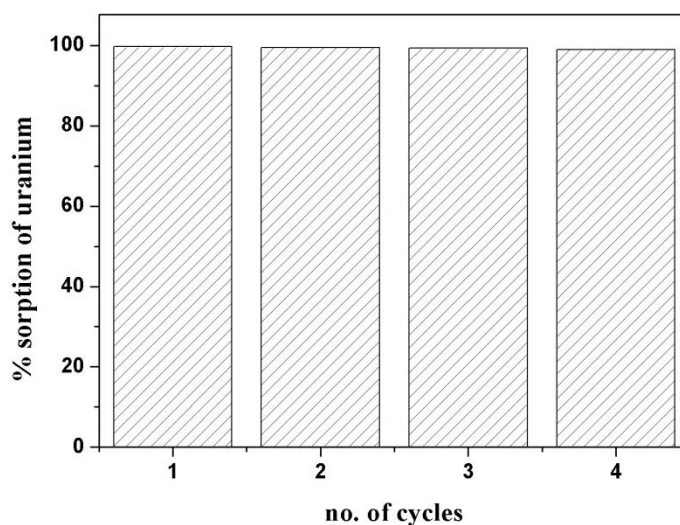


Fig.3.9 Reusability test for SPFSG sorbent: % sorption of uranium vs. number. of cycles

3.2.6 Separation and Recovery of Uranium from SSFSDS

SPFSG has been tested for the recovery of uranium from SSFSDS. SSFSDS has been prepared as described before. It contains uranium, silicon and aluminium and the concentration of these elements has been analysed by ICP-AES. For the sorption study, 3g of SPFSG has been equilibrated with 3 ml of SSFSDS. It shows that uranium is sorbed preferentially over other metals present in SSFSDS; thus separating uranium from other elements present in SSFSDS (Table 3.1). For back extraction of uranium, loaded SPFSG has been equilibrated with nitric acid solutions (pH=0). Studies show that four stages of back extraction recovers >99% uranium from the

loaded SPFSG. Therefore, SPFSG can be used for separation and recovery of uranium from SSFSDS.

Table 3.1 Sorption behaviour of elements present in SSFSDS on to SPFSG

Elements	Elements in feed (g/L)	Elements in raff (g/L)	%Sorption
Uranium	19.7	0.02	99.88
Silicon	0.1	0.08	20.1
Aluminium	32.4	30.2	6.8

3.2.7 Quantum Chemical Studies on the Binding Ability of Uranyl Ion with the Ligand

The optimized structure of uranyl nitrate bound to SPFSG has been shown in Fig.3.10. The two weakly bound water molecules of solvated uranyl nitrate have been displaced with SPFSG ligand forming a 2:1 (ligand:metal) complex. Upon complexation of uranyl ion with SPFSG ligand which contains the phosphate binding site, the U=O and P=O bond lengths become slightly lengthened which are reflected elongated in their vibrational frequencies. The computed asymmetric vibrational frequencies (ν_{asym}) of U=O in the product is in line with the experimental estimates from FT-IR spectroscopy. Particularly, the computed red shifting in the asymmetric stretching is well reproduced by our calculations. From the FT-IR spectra it is obtained that the P=O bond vibration has shifted from 1208 cm^{-1} to 1128 cm^{-1} due to co-ordination with UO_2^{2+} ion. This shift of P=O vibration frequency with respect to pure PFSG is about 80 cm^{-1} . The computed asymmetric vibrational frequencies (ν_{asym}) of bare and coordinated P=O is again reproduced within a difference of 35 cm^{-1} . These variations in the structures lead to favourable binding affinities whose

magnitude is $3.8 \text{ kcal mol}^{-1}$. Thus, our computation predictions correlate nicely with the experimental data.

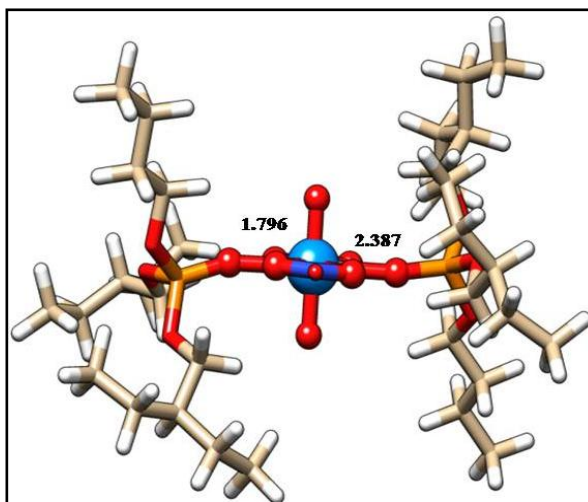


Fig.3.10 Optimized structure of uranyl bound to SPFG

3.3. Conclusions

SPFG has been used for the sorption studies of uranium from nitric acid-sodium hydroxide medium; BPFSG, TPFSG and AAPPFG have been used for the sorption studies of uranium from nitric acid-sodium carbonate medium. Sorption behaviours of uranium have been investigated by batch techniques in all the experiments. Sorption experiments have proved that SPFG, BPFSG, TPFSG and AAPPFG can be used to separate uranium from nitric acid medium with high sorption capacity. Sorption of uranium has been found to be very fast, with the equilibrium being attained within ten minutes. Computational prediction matches well with the experimental results. SPFG has shown a desirable selectivity for uranium over the competing metal ions. Desorption of uranium from loaded SPFG is easy and thus has shown an excellent reusability of SPFG. SPFG has also shown its potential application in recovery of uranium from SSFSDS.

References

1. Carbon emission and mitigation cost comparisons between fossil fuel, nuclear and renewable energy resources for electricity generation, R. E. H. Sims, H. H. Rogner, K. Gregory, *Energy Policy*, 2003, 31, 1315-1326.
2. Opportunities and challenges for a sustainable energy future, S. Chu, A. Majumdar, *Nature*, 2012, 488, 294-303.
3. Assessment of Homogeneous Thorium/Uranium Fuel for Pressurized Water Reactors, A. Galperin, E. Shwageraus, M. Todosow, *Nuclear Technology*, 2002, 138, 111-122.
4. Development of very-high-density low-enriched-uranium fuels, J. L. Snelgrove, G. L. Hofman, M. K. Meyer, C. L. Trybus, T. C. Wiencek, *Nuclear Engineering and Design*, 1997, 178, 119-126.
5. Fuels for research and test reactors, status review, D. Stahl, ANL-83-5, 1982, DE83 014267.
6. Stoichiometric Effects on Performance of High-Temperature Gas-Cooled Reactor Fuels from the U-C-O System, F. J. Homan, T. B. Lindemer, E. L. Long Jr., T. N. Tieg, R. L. Beatty, *Nuclear Technology*, 1977, 35, 428-441.
7. Fabrication and testing of uranium nitride fuel for space power reactors, R. B. Matthews, K. M. Chidester, C. W. Hoth, R. E. Mason, R. L. Petty, *Journal of Nuclear Materials*, 1988, 151, 334-344.
8. Chronic Ingestion of Uranium in Drinking Water: A Study of Kidney Bioeffects in Humans, M. L. Zamora, B. L. Tracy, J. M. Zielinski, D. P. Meyerhof, M. A. Moss, *Toxicological Sciences*, 1998, 43, 68-77.
9. Bone as a possible target of chemical toxicity of natural uranium in drinking water, P. Kurttio, H. Komulainen, A. Leino, L. Salonen, A. Auvinen, H. Saha, *Environ. Health Perspect.*, 2005, 113, 68-72.
10. Impact of organic matter and speciation on the behaviour of uranium in submerged ultrafiltration, A. J. C. Semião, H. M. A. Rossiter, A. I. Schäfer, *Journal of Membrane Science*, 2010, 348, 174-180.
11. The significance of groundwater-stream interactions and fluctuating stream chemistry on waterborne uranium contamination of streams - a case study from a gold mining site in South Africa, F. Winde, I. J. van der Walt, *J. Hydrol.*, 2004, 287, 178-196.

12. Improved performance of a biomaterial-based cation exchanger for the adsorption of uranium (VI) from water and nuclear industry wastewater, T. S. Anirudhan, P. G. Radhakrishnan, *Journal of Environmental Radioactivity*, 2009, 100, 250-257.
13. Fertilizer-Derived Uranium and its Threat to Human Health, E. Schnug, B. G. Lottermoser, *Environ. Sci. Technol.*, 2013, 47, 2433-2434.
14. Adsorption of uranium (VI) from aqueous solution onto cross-linked chitosan, G. Wang, J. Liu, X. Wang, Z. Xie, N. Deng, *J. Hazard. Mater.*, 2009, 168, 1053-1058.
15. Selective removal of dissolved uranium in drinking water by nanofiltration, A. F. Reguillon, G. Lebuzzit, D. Murat, I. Foos, C. Mansour, M. Drave, *Water Res.*, 2008, 42, 1160-1166.
16. Uranium co-precipitation with iron oxide minerals, M. C. Duff, J. U. Coughlin, D. B. Hunter, *Geochimica et Cosmochimica Acta*, 2002, 66, 3533-354.
17. A study of uranium solvent extraction equilibria with Alamine 336 in kerosene, N. A. Yakubu, A. W. L. Dudeney, *Hydrometallurgy*, 1987, 18, 93-104.
18. Separation and Recovery of Uranium Metal from Spent Light Water Reactor Fuel Via Electrolytic Reduction and Electrorefining, S. D. Herrmann, S. X. Li, *Nuclear Technology*, 2010, 171, 247-265.
19. Uranium electrodeposition for alpha spectrometric source preparation, O. A. Dumitru, R. C. Begy, D. C. Nita, L. D. Bobos, C. Cosma, *Journal of Radioanalytical and Nuclear Chemistry*, 2013, 298, 1335-1339.
20. Extraction of uranium (VI) by 1.1 M tri-n-butylphosphate/ionic liquid and the feasibility of recovery by direct electrodeposition from organic phase, P. Giridhar, K. A. Venkatesan, S. Subramaniam, T. G. Srinivasan, P. R. V. Rao, *Journal of Alloys and Compounds*, 2008, 448, 104-108.
21. Resin-in-pulp method for uranium recovery from leached pulp of low grade uranium ore, K. Mirjalili, M. Roshani, *Hydrometallurgy*, 2007, 85, 103-109.
22. Recovery of uranium from carbonate solutions using strongly basic anion exchanger 4: column operation and quantitative analysis, Y. Song, Y. Wang, L. Wang, C. Song, Z. Z. Yang, A. Zhao, *React Funct Polym*, 1999, 39, 245-252.
23. Uphill transport of uranium across a liquid membrane, H. Matsuoka, M. Aizawa, S. Suzuki, *Journal of Membrane Science*, 1980, 7, 11-19.

24. Selective adsorption of uranium(VI) onto prismatic sulfides from aqueous solution, F. H. Wang, Q. Liu, R. M. Li, Z. H. Li, *Colloids Surf. A*, 2016, 490, 215-221.
25. Removal of uranium (VI) from aqueous solution by amidoxime functionalized super paramagnetic polymer microspheres prepared by a controlled radical polymerization in the presence of DPE, D. Z. Yuan, L. Chen, X. Xiong, *Chem. Eng. J.*, 2016, 285, 358-367.
26. Uranium (VI) sorption by multiwalled carbonnanotubes from aqueous solution, I. I. Fasfous, J. N. Dawoud, *Appl. Surf. Sci.*, 2012, 259, 433-440.
27. Facile preparation of oxine functionalized magnetic Fe₃O₄ particles for enhanced uranium (VI) adsorption, L. C. Tan, J. Wang, Q. Liu, *Colloids Surf. A*, 2015, 466, 85-91.
28. Adsorption of uranium (VI) from sulphate solutions using amberlite IRA-402 resin: equilibrium, kinetics and thermodynamics study, M. Solgy, M. Taghizadeh, D. Ghoddocynejad, *Ann. Nucl. Energy*, 2015, 75, 132-138.
29. Enhanced adsorption of uranium (VI) using a three-dimensional layered double hydroxide/graphene hybrid material, L. C. Tan, Y. L. Wang, Q. Liu, J. Wang, *Chem. Eng. J.*, 2015, 259, 752-760.
30. Sorption and desorption of uranyl ions by silica gel: pH, particle size and porosity effects, P. Michard, E. Guibal, T. Vincent, P. Le Cloirec, *Micropor Mater*, 1996, 5, 309-324.
31. Tris(2-aminoethyl) amine functionalized silica gel for solid-phase extraction and preconcentration of Cr(III), Cd(II) and Pb(II) from waters, X. Huang, X. Chang, Q. He, Y. Cui, Y. Zhai, N. Jiang, *J. Hazard. Mater.*, 2008, 157, 154-160.
32. Phosphonate and carboxylic acid co-functionalized MoS₂ sheets for efficient sorption of uranium and europium: Multiple groups for broad-spectrum adsorption, S. Yang, M. Hua, L. Shen, X. Han, M. Xu, L. Kuang, D. Hua, *J. Hazard. Mater.*, 2018, 354, 191-197.
33. Synthesis of FC-supported Fe through a carbothermal process for immobilizing uranium, L. Kong, H. Zhang, K. Shih, M. Su, Z. Diao, J. Long, L. Hou, G. Song, D. Chen, *J. Hazard. Mater.*, 2018, 357, 168-174.

34. Efficient extraction of uranium from aqueous solution using an amino-functionalized magnetic titanate nanotubes, J. Zhu, Q. Liu, Z. Li, J. Liu, H. Zhang, R. Li, J. Wang, *J. Hazard. Mater.*, 2018, 353, 9-17.
35. Uranium sorption on bentonite modified by octadecyltrimethylammonium bromide, M. Majdan, S. Pikus, A. Gajowiak, D. Sternik, E. Zięba, *J. Hazard. Mater.*, 2010, 184, 662-670.
36. Investigation of strontium and uranium sorption onto zirconium-antimony oxide/polyacrylonitrile (Zr-Sb oxide/PAN) composite using experimental design, P. Cakir, S. Inan, Y. Altas, *J. Hazard. Mater.*, 2014, 271, 108-119.
37. Sorption of uranium(VI) from aqueous solutions by akaganeite, S. D. Yusan, S. Akyil, *J. Hazard. Mater.*, 2008, 160, 388-395.
38. Sorption of uranium (VI) on homoionic sodium smectite experimental study and surface complexation modelling, S. Korichi, A. Bensmaili, *J. Hazard. Mater.*, 2009, 169, 780-793.
39. Magnetic graphene based nanocomposite for uranium scavenging, H. H. E. Maghrabi, S. M. Abdelmaged, A. A. Nada, F. Zahran, S. A. E. Wahab, D. Yahea, G. M. Hussein, M. S. Atrees, *J. Hazard. Mater., Part B*, 2017, 322, 370-379.
40. Chlorite alteration in aqueous solutions and uranium removal by altered chlorite, E. Kim, H. Ahn, H. Y. Jo, J. H. Ryu, Y. K. Koh, *J. Hazard. Mater.*, 2017, 327, 161-170.
41. Hierarchically structured layered-double-hydroxides derived by ZIF-67 for uranium recovery from simulated seawater, R. Li, R. Che, Q. Liu, S. Su, Z. Li, H. Zhang, J. Liu, L. Liu, J. Wang, *J. Hazard. Mater.*, 2017, 338, 167-176.
42. Efficient removal of uranium from aqueous solution by zero-valent iron nanoparticle and its graphene composite, Z. J. Li, L. Wang, L. Y. Yuan, C. L. Xiao, L. Mei, L. R. Zheng, J. Zhang, J. H. Yang, Y. L. Zhao, Z. T. Zhu, Z. F. Chai, W. Q. Shi, *J. Hazard. Mater.*, 2015, 290, 26-33.
43. Simultaneous reduction and adsorption for immobilization of uranium from aqueous solution by nano-flake Fe-SC, L. Kong, Y. Zhu, M. Wang, Z. Li, Z. Tan, R. Xu, H. Tang, X. Chang, Y. Xiong, D. Chen, *J. Hazard. Mater.*, 2016, 320, 435-441.
44. Uranium (VI) recovery from aqueous medium using novel floating macroporous alginate-agarose-magnetite cryobeads, A. Tripathi, J. S. Melo, S. F. D'Souza, *J. Hazard. Mater.*, 2013, 246-247, 87-95.

45. Adsorption of uranium (VI) from aqueous solution onto cross-linked chitosan, G. Wang, J. Liu, X. Wang, Z. Xie, N. Deng, *J. Hazard. Mater.*, 2009, 168, 1053-1058.
46. Kinetic, equilibrium and thermodynamic studies on sorption of uranium and thorium from aqueous solutions by a selective impregnated resin containing carminic acid, A. R. Sani, A. H. Bandegharaei, S. H. Hosseini, K. Kharghani, H. Zarei, A. Rastegar, *J. Hazard. Mater.*, 2015, 286, 152-163.
47. Solid phase extraction of uranium (VI) onto benzoylthiourea-anchored activated carbon, Y. Zhao, C. Liu, M. Feng, Z. Chen, S. Li, G. Tian, L. Wang, J. Huang, S. Li, *J. Hazard. Mater.*, 2010, 176, 119-124.
48. The removal of uranium(VI) from aqueous solutions onto activated carbon: Kinetic and thermodynamic investigations, A. Mellah, S. Chegrouche, M. Barkat, *Journal of Colloid and Interface Science*, 2006, 296, 434-441.
49. Sorption of uranium(VI) using oxime-grafted ordered mesoporous carbon CMK-5, G. Tian, J. Geng, Y. Jin, C. Wang, S. Li, Z. Chen, H. Wang, Y. Zhao, S. Li, *J. Hazard. Mater.*, 2011, 190, 442-450.
50. Uranium(VI) adsorption on graphene oxide nanosheets from aqueous solutions, Z. Li, F. Chen, L. Yuan, Y. Liu, Y. Zhao, Z. Chai, W. Shi, *Chemical Engineering Journal*, 2012, 210, 539-546.
51. "Stereoscopic" 2D super-microporous phosphazene-based covalent organic framework: Design, synthesis and selective sorption towards uranium at high acidic condition, S. Zhang, X. Zhao, B. Li, C. Bai, Y. Li, L. Wang, R. Wen, M. Zhang, L. Ma, S. Li, *J. Hazard. Mater.*, 314, 2016, 95-104.
52. A catechol-like phenolic ligand-functionalized hydrothermal carbon: One-pot synthesis, characterization and sorption behavior toward uranium, B. Li, L. Ma, Y. Tian, X. Yang, J. Li, C. Bai, X. Yang, S. Zhang, S. Li, Y. Jin, *J. Hazard. Mater.*, 271, 2014, 41-49.
53. Solid phase extraction of uranium (VI) onto benzoylthiourea-anchored activated carbon, Y. Zhao, C. Liu, M. Feng, Z. Chen, S. Li, G. Tian, L. Wang, J. Huang, S. Li, *J. Hazard. Mater.*, 2010, 176, 119-124.
54. Biosorption of uranium and thorium, M. Tsezos, B. Volesky, *Biotechnology and Bioengineering*, 1981, 23, 583-604.

55. Biosorption of uranium (VI) from aqueous solution using calcium alginate beads, C. Gok, S. Aytas, J. Hazard. Mater., 2009, 168, 369-375.
56. Polymer Cookery. 2. Influence of Polymerization Pressure and Polymer Swelling on the Performance of Molecularly Imprinted Polymers, S. A. Piletsky, A. Guerreiro, E. V. Piletska, I. Chianella, K. Karim, A. P. F. Turner, Macromolecules, 2004, 37, 5018-5022.
57. Adsorption of uranium (VI) on silica mesoporous material SBA-15 with short channels, X. H. Wang, G. R. Zhu, C. J. Gao, CIESC J., 2013, 64, 2480-2487.
58. Phosphoryl functionalized mesoporous silica for uranium adsorption, X. Guo, Y. Feng, L. Ma, D. Gao, J. Jing, J. Yu, H. Sun, H. Gong, Y. Zhang, Applied Surface Science, 2017, 402, 53-60.
59. Kinetics of sorption and desorption of copper(II) and lead (II) on activated carbon, W. Andrzej, M. K. Thomas, Water Environment Research, 1993, 65, 238-244.
60. Conditioning-Annealing Studies of Natural Organic Matter Solids Linking Irreversible Sorption to Irreversible Structural Expansion, M. Sander, Y. Lu, J. J. Pignatello, Environ. Sci. Technol., 2006, 40, 170-178.
61. Grafting of Ion-Imprinted Polymers on the Surface of Silica Gel Particles through Covalently Surface-Bound Initiators: A Selective Sorbent for Uranyl Ion, M. Shamsipur, J. Fasihi, K. Ashtari, Anal. Chem., 2007, 79, 7116-7123.
62. Trialkylamine Impregnated Macroporous Polymeric Sorbent for the Effective Removal of Chromium from Industrial Wastewater, N. Rajesh, A. S. Krishna Kumar, S. Kalidhasan, Vidya Rajesh, J. Chem. Eng. Data, 2011, 56, 2295-2304.
63. Metal anion sorption on chitosan and derivative materials: a strategy for polymer modification and optimum use, P. Chassary, T. Vincent, E. Guibal, Reactive and Functional Polymers, 2004, 60, 137-149.
64. Extraction of metal ions using chemically modified silica gel: a PIXE analysis, P.K. Jal, R. K. Dutta, M. Sudershan, A. Saha, S. N. Bhattacharyya, S. N. Chintalapudi, B. K. Mishra, Talanta, 2001, 55, 233-240.
65. Use of benzoylthiourea immobilized on silica gel for separation and preconcentration of uranium (VI), M. Merdivan, S. Seyhan, C. Gok, Microchim. Acta, 2006, 154, 109-114.

66. Determination of trace metals in seawater by on-line column preconcentration inductively coupled plasma mass spectrometry, S. Hirata, Y. Ishida, M. Aihara, K. Honda, O. Shikino, *Anal. Chim. Acta*, 2001, 438, 205-214.
67. Extraction of uranyl ions from aqueous solutions using silica-gel-bound macrocycles for alpha contaminated waste water treatment, F. Barbette, F. Rascalou, H. Chollet, J. L. Babouhot, F. Denat, R. Guilard, *Anal. Chim. Acta*, 2004, 502, 179-187.
68. Silica with immobilized phosphinic acid-derivative for uranium extraction, T. M. Budnyak, A. V. Strizhak, A. G. Płaska, D. Sternik, I. V. Komarov, D. Kołodyńska, M. Majdan, V. A. Tertykh, *J. Hazard. Mater.*, 2016, 314, 326-340.
69. Facile functionalized of SBA-15 via a biomimetic coating and its application in efficient removal of uranium ions from aqueous solution, J. K. Gao, L. A. Hou, G. H. Zhang, P. Gu, *J. Hazard. Mater.*, 2015, 286, 325-333.
70. Solid phase extraction using silica gel modified with murexide for preconcentration of uranium (VI) ions from water samples, S. Sadeghi, E. Sheikhzadeh, *J. Hazard. Mater.*, 2009, 163, 861-868.
71. Uranium (VI) speciation diagrams in the $\text{UO}_2^{2+}/\text{CO}_3^{2-}/\text{H}_2\text{O}$ system at 25°C, A. Krestou, D. Panias, *The European Journal of Mineral Processing and Environmental Protection*, 4, 2004, 113-129.

Effect of Amido Pyridyl Functional Group in Phosphate Functionalised Silica Gels on the Enhanced Separation of Zirconium from Hafnium

4.1. Introduction

Zirconium and hafnium have completely different nuclear properties in respect of their thermal neutron absorption cross sections and therefore, are used frequently in two different applications in nuclear industry namely, as cladding material and as control rod material respectively [1-2]. Due to very high thermal neutron absorption cross section of hafnium, it decreases the neutron flux inside nuclear reactor. Therefore, zirconium should not contain more than 100 ppm of hafnium along with it for its application as cladding material. Moreover, zirconium and hafnium have similar chemical properties due to their similar atomic radii (1.45 Å and 1.44 Å, respectively) and similar valence electron configurations ($4d^25s^2$ and $5d^26s^2$, respectively) [3-4] and hence, they coexist in nature [5]. Therefore, separation of zirconium from hafnium is necessary mainly for their nuclear applications and also for their individual applications as compounds and alloys.

Separation of zirconium from hafnium are carried out by conventional and established methods such as fractional crystallization, precipitation, solvent extraction, molten salt distillation, selective reduction, extractive distillation etc. [6-7]. Over these techniques, solid phase extraction (SPE), where the metal ions present in the aqueous medium are sorbed onto surface of solid extractants by ion exchange or, complex formation, has some advantages like it is a simple process, high process efficiency and low cost of operation [8]. Titanium dioxide [9-14], manganese dioxide [15], graphene oxide [16-18], activated carbon [19-26], carbon nanotube [27-

31,32,33], polymeric resin [8], [34-35], ion exchange resin [36-37] are the commonly used structural materials for SPE.

Silica gel as a solid support has some advantages over other solid-phase support materials due to its unique properties like i) its high mechanical stability in aqueous medium, ii) good thermal stability and iii) suitable accessibility of metal ions to bind with the ligand incorporated on the silica gel surface due to appropriate pore size of silica gel [38-40]. Therefore, development of new chemically modified mesoporous and nanoporous silica based materials have now drawn attraction of researchers worldwide [41-49].

Different ligands like methyl isobutyl ketone (MIBK), tributyl phosphate (TBP), cyanex923, cyanex925, di(2-ethylhexyl)phosphoric acid (D2EHPA) are the commonly used for the separation of zirconium from hafnium using solvent extraction method [50-54]. Moreover, MIBK and TBP solvents have also been tried for industrial separation of zirconium and hafnium. But, there are some disadvantages for their large scale applications e.g., in case of MIBK solvent system, i) high solvent loss, ii) atmospheric pollution, iii) poor working environment produced due to the waste stream which contains high concentrations of organic by-products with low flash point, iv) high vapour pressure and v) high solubility in the aqueous phase [8], [55-56]. Similarly, for TBP solvent the disadvantages due to i) high aqueous solubility, ii) high rate of corrosion the equipments being handled, iii) emulsion formation in continuous production facility [57] create problem in large scale operation. SPE method can solve many of these problems.

The solid phase extractants reported so far for the separation of zirconium from hafnium consist of amine group, thiol group, sulphonic acid group, dihydroxy phosphine oxide group, crown ether group etc as the functional groups [58-60]. To the

best of authors' knowledge, there is no report found on phosphate group immobilised on silica gel surface for the separation of zirconium from hafnium from aqueous medium. In this work, phosphate ligands has been fixed on solid silica gel material which will perform like TBP attached to a solid support and will work as a solid sorbent in SPE method. In this context, three functionalised silica gels have been synthesised namely, mono-phosphate functionalised silica gel (MPFSG), bi-phosphate functionalised silica gel (BPFSG), amine and amido pyridyl phosphate functionalised silica gel (AAPPFSG) and they have been tested for the separation of zirconium from hafnium in nitric acid medium.

4.2. Results and Discussion

Synthesis and characterisation of mono-phosphate functionalised silica gel (MPFSG), bi-phosphate functionalised silica gel (BPFSG), amine and amido pyridyl phosphate functionalised silica gel (AAPPFSG) have been discussed in details in chapter 2. In this chapter, the evaluation of these sorbents for the separation of zirconium from hafnium from nitric acid medium have been discussed.

4.2.1. Effect of pH of Feed Solution on Zr and Hf Sorption

Sorption of zirconium and hafnium changes with pH of the feed solution. Sorption variation for zirconium and hafnium has been given in Fig.4.1. This variation in sorption is due to two reasons: the surface charge of the functionalised silica gel and the different speciation of the metal ions at different pH of the feed solutions. A moderate sorption is observed up to about pH 1.2 (Fig.4.1) due to the competition between the protons present in the solution and the metal ions and most of the binding sites present on the surface of the functionalised silica gel are protonated. Below pH 1.6, the medium is acidic enough for the surface of the sorbent to be protonated and the hydrolysed species of zirconium and hafnium (i.e. $Zr(OH)^{3+}$

and $\text{Hf}(\text{OH})^{3+}$) are also less preferably sorbed on the binding sites compared to the protons present in the solution due to the less ionic potentials of these species. For these reasons, a net decrease in sorption for zirconium and hafnium is observed in the pH range 1.2-1.6. As the pH of the solution increases more (above pH 1.6), the number of protons present in the solution decreases and the sorption increases slowly (Fig.4.1) for both the metal ions due to large number of available binding sites.

As it is observed from Fig.4.1, separation of zirconium from hafnium vary throughout the observed pH range. Separation is more below pH 1.2 for all these functionalised silica gels.

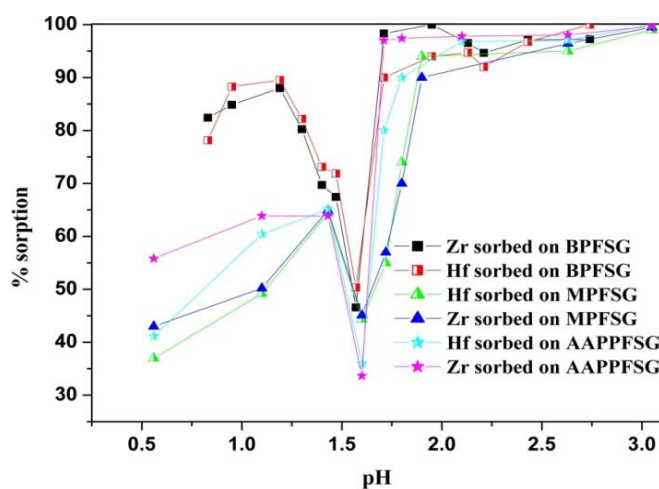


Fig.4.1 Effect of pH of feed solution on sorption of zirconium and hafnium

4.2.2. Kinetics Studies

Sorption of zirconium and hafnium on MPFSG, BPFSG and AAPPFSG have been studied as a function of time (Fig.4.2). It has been observed that kinetic is fast in all these cases as the sorption equilibrium are attained within 10 minutes with the sorbent dose of 1.2 gL^{-1} . Among these three functionalised silica gels, sorption equilibration time increases in the order of $\text{MPFSG} < \text{BPFSG} < \text{AAPPFSG}$. This is due to the accessibility of the functional groups to the approaching metal ions which plays the major role here. In case of MPFSG, the phosphate functional groups which are directly attached to the silica gel surface, are easily accessible to the metal ions. In

case of BPFSG, there are two phosphate groups attached to the silica gel surface through a flexible carbon chain which poses small steric hindrance compared to MPFSG. In case of AAPPFSG bulkiness is present around the functional groups which pose high steric hindrance to the approaching metal ions making the kinetics slower than BPFSG. The data of the kinetics studies have been fitted in the pseudo first order and pseudo second order kinetic models. The data points in $\log(q_e - q_t)$ vs. time plot corresponding to the pseudo-first order kinetic model (Fig.4.3a), deviate much from linearity compared to the pseudo-second order kinetic plot i.e. q_t/t vs. t plot (Fig.4.3b).

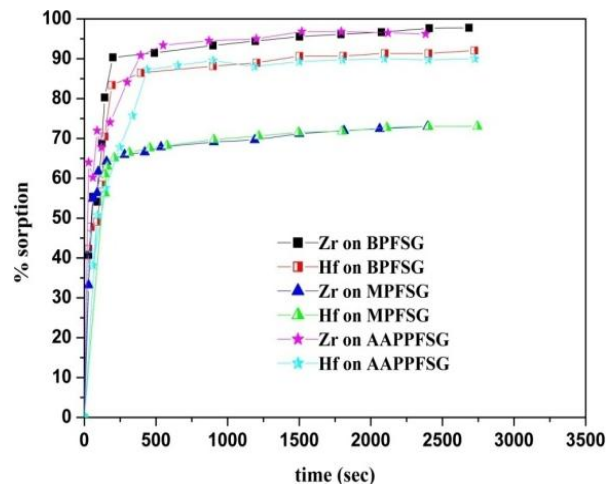


Fig.4.2 Sorption kinetics for zirconium and hafnium: % sorption vs. time (sec)

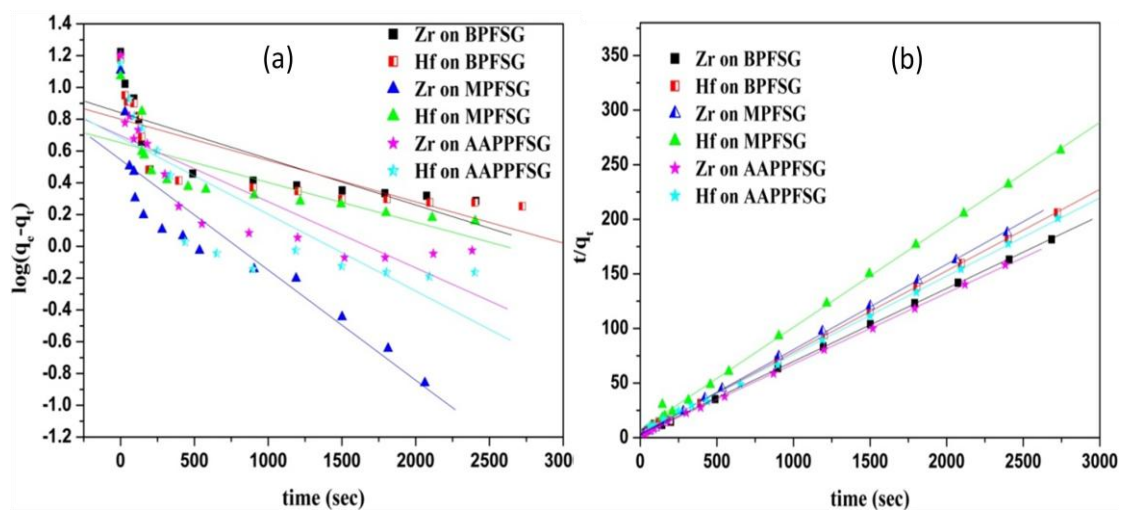


Fig.4.3 (a) Pseudo first order and (b) pseudo second order kinetic plots for zirconium and hafnium sorption

This indicates sorption of zirconium and hafnium on the functionalised silica gels i.e., MPFSG, BPFSG and AAPPFSG follow pseudo-second order kinetic model which signifies that the rate determining step for the sorption of zirconium and hafnium is the complexation reaction of the metal ions with the functional groups.

4.2.3. Sorption Isotherm Studies

Sorption isotherm studies for zirconium and hafnium using MPFSG, BPFSG and AAPPFSG have been carried out separately with variation of feed concentrations of zirconium and hafnium (concentration range: 25-200 mg L⁻¹ at pH 1.8). It is observed that the sorption of zirconium and hafnium increase with the increase in their feed concentration (Fig.4.4) in all these cases. Zirconium shows a slightly higher equilibrium sorption capacity (q_e) over hafnium. Equilibrium sorption capacity (q_e) for zirconium and hafnium on the functionalised silica gels decreases in the order BPFSG \approx AAPPFSG > MPFSG as obvious from Fig.4.4. There are two phosphate groups as the binding sites which are chemically bound to a flexible carbon chain in case of BPFSG which gives a moderate sorption of zirconium and hafnium. Whereas, sorption does not increase very high in case of AAPPFSG though there are multiple

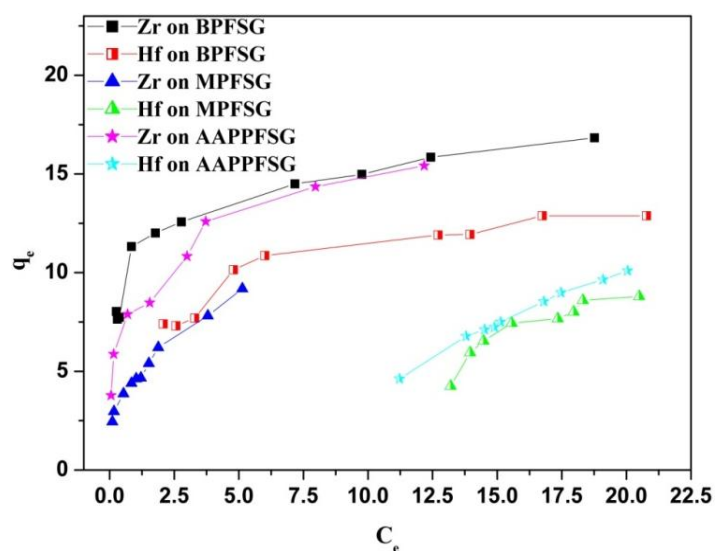


Fig.4.4 Isotherm plot for zirconium and hafnium sorption

number of functional groups present in it. This is due to the bulkiness around the binding site which poses steric hindrance to the metal ion species approaching to the binding sites. Least sorption compared to BPFSG and AAPPFSG is observed in case of MPFSG due to the presence of single phosphate group as the binding site.

Further, the sorption equilibrium data has been fitted to Langmuir as well as Freundlich isotherm model.

Both the Langmuir and the Freundlich isotherm models have been used to fit the sorption isotherm data (Fig.4.5). Fig.4.5 shows the plot of $1/q_e$ vs. $1/C_e$ (Fig.4.5a) plot and $\log q_e$ vs. $\log C_e$ (Fig.4.5b) plot for Langmuir and Freundlich model respectively. It is found that under the experimental conditions Freundlich model fits well with the experimental data. This suggests that the surface of the functionalised silica gels are heterogeneous in nature where sorption of zirconium and hafnium takes place.

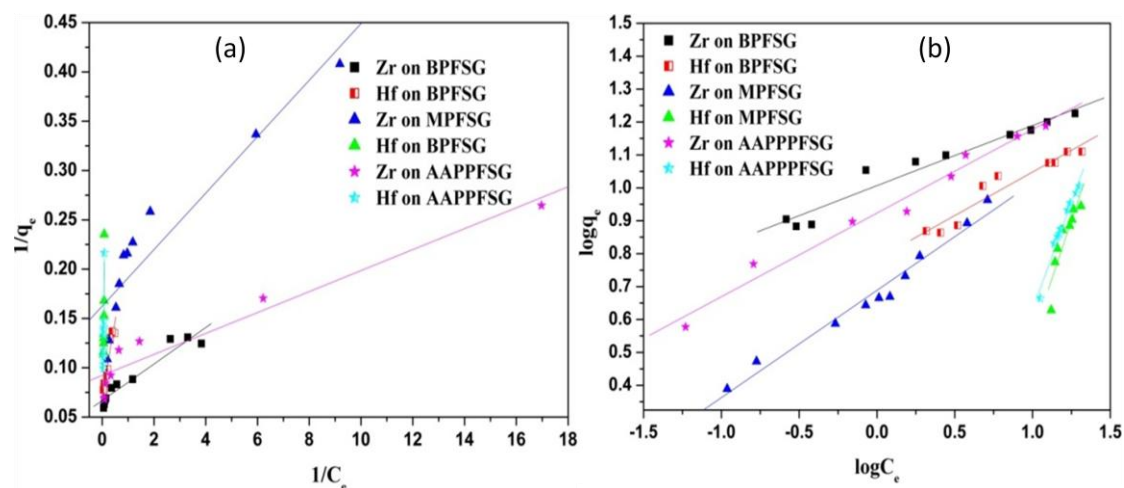


Fig.4.5 (a) Langmuir isotherm model, (b) Freundlich isotherm model for sorption of zirconium and hafnium

4.2.4. Loading Capacities (mg/g) of Zirconium and Hafnium on to Loaded Functionalised Silica Gels

Loading capacities of zirconium and hafnium have been tabulated below (Table 4.1).

Table 4.1 Loading capacities of zirconium and hafnium

Ligand	Loading capacity of Zr (mg g^{-1})	Loading capacity of Hf (mg g^{-1})
MPFSG	12.3	11.8
BPFSG	16.7	15
AAPPFSG	16	14.2

4.2.5. Desorption Studies for Zirconium and Hafnium from Loaded Functionalised Silica Gels

All the functionalised silica gels have shown desirable selectivity for zirconium over hafnium for their sorption from nitric acid medium. Studies on their desorption behaviour is essential for their usage in different applications. It is observed from pH variation study (Fig.4.1) that separation of zirconium and hafnium is possible below pH1 at nitric acid medium. Desorption studies for zirconium and hafnium have been carried out in batch mode using eluents of variable pH. The metal loaded functionalised silica has been equilibrated with the eluents as described in chapter 2. Fig.4.6 gives the desorption behaviour of zirconium and hafnium. It is observed that pH 0.65 is the pH of the eluent which gives maximum desorption of zirconium and hafnium.

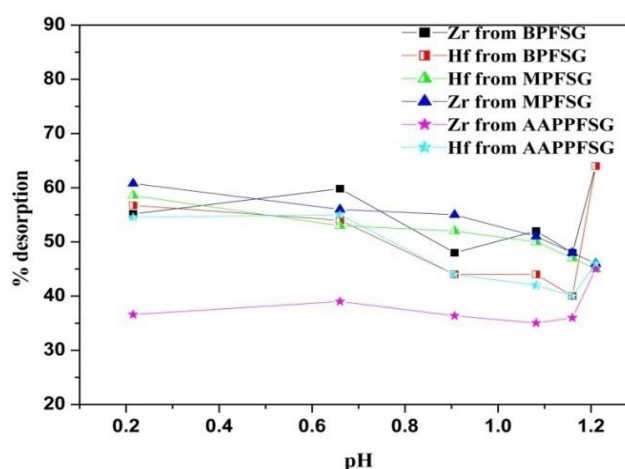


Fig.4.6 Desorption studies for zirconium and hafnium

4.2.6. Column Studies

Column studies for the separation of zirconium and hafnium have been carried out as described in chapter 2. Eluent pH has been maintained at 0.65 for all the elution studies. Fig.4.7 gives the column separation behaviour of zirconium and hafnium using MPFSG, BPFSG and AAPPFSG sorbents. It has been observed that separation of zirconium and hafnium increases as the number of phosphate groups as the binding sites increases and therefore, separation decreases in the order AAPPFSG > BPFSG > MPFSG.

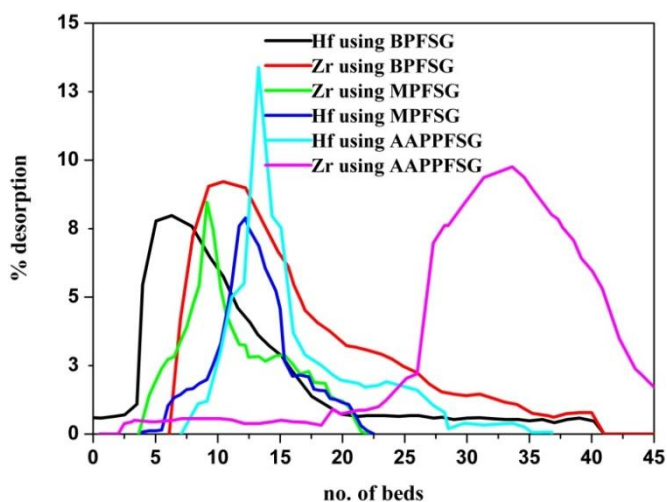


Fig. 4.7 Column studies for zirconium and hafnium separation

4.2.7. Quantum Chemical Studies on the Sorption Behaviour of Zr and Hf with Phosphate Functionalised Silica Gel

Computational studies have been carried out to understand the sorption behaviour of Zr and Hf with MPFSG, BPFSG and AAPPFSG ligands and the corresponding optimised structure are presented in Fig.4.8. For the geometry optimisation, one hydroxyl ion and four water molecules have been considered into calculation as shown in the figure below. The optimised bond lengths of the oxygen atoms present in P=O of phosphate group, hydroxyl ion and the surrounding water molecules with zirconium and hafnium; the effective charges on zirconium and hafnium and the binding energies of the complexes have been tabulated in Table 4.2.

Table 4.2 Geometrical parameter, binding energies and charge of the metal ions complexed with MPFSG, BPFSG and AAPPFSG with zirconium and hafnium

	MPFSG		BPFSG		AAPPFSG	
	Zr	Hf	Zr	Hf	Zr	Hf
P-O-M (phosphate) length (Å)	2.00	2.01	2.00	2.00	2.10	2.10
M-O (hydroxyl) length (Å)	1.87	1.88	1.88	1.88	1.89	1.90
M-O (water) length (Å)	2.23- 2.27	2.24- 2.28	2.23- 2.27	2.24- 2.27	2.21- 2.35	2.21- 2.35
M (charge)	1.101	1.205	1.073	1.189	0.861	0.963
Binding energy (kcal/mol)	-79.48	-79.35	-94.18	-93.9	-160.89	-161.59

(M stands for zirconium and hafnium)

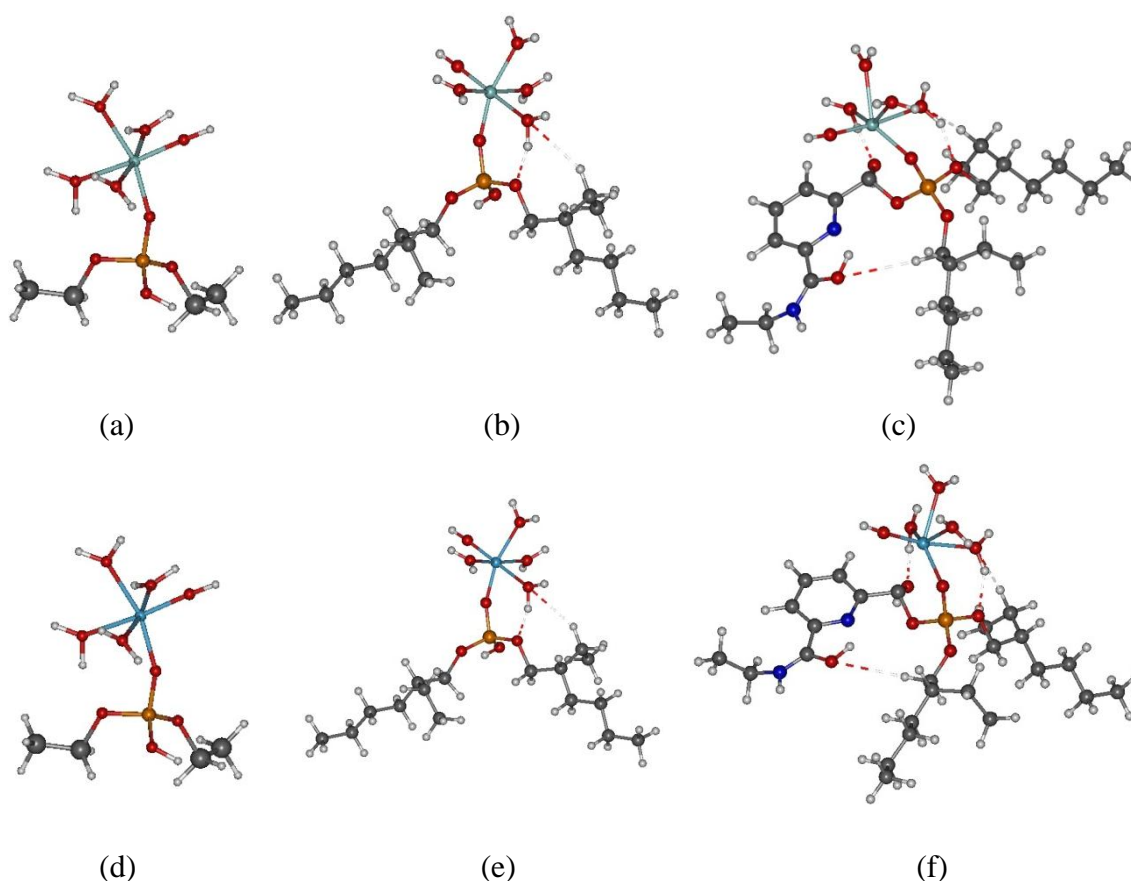


Fig.4.8 Optimised geometries of zirconium with (a) MPFSG, (b) BPFSG and (c) AAPPFSG; and of hafnium with (d) MPFSG, (e) BPFSG and (f) AAPPFSG

From Table 4.2, it is very clear that interaction of metal ions with the AAPPFSG is almost two times more than that of MPFSG and BPFSG. The results are very close in agreement with the experimental observation. In all cases, binding energy of Zr and Hf is found to be very close to each other.

4.3 Conclusions

Sorption and the desorption studies of zirconium and hafnium have been performed by batch mode. Optimised conditions from the batch mode of experiments then have been applied to manifest the column studies for the separation of zirconium from hafnium. Sorption kinetics is fast for both zirconium and hafnium where sorption equilibrium is reached within ten minutes using MPFSG, BPFSG and AAPPFSG sorbents. It has been observed that as the number of binding sites on the sorbent increase, the sorption of zirconium and hafnium on the sorbent increase. Therefore, sorption of both zirconium and hafnium increases in the order MPFSG < BPFSG < AAPPFSG. This trend of sorption is also supported by the computed binding energies which have been obtained from the theoretical computations performed to look into the binding of these ligands with zirconium and hafnium.

These functionalised silica gels have been tested for the separation of zirconium from hafnium. It is observed that as the number of binding sites increases, selectivity of ligands towards zirconium increases. Therefore, AAPPFSG sorbent which has the maximum number of binding sites gives a better separation of zirconium from hafnium under the experimental conditions compared to BPFSG and MPFSG sorbents.

References

1. Zirconium and hafnium metallurgy, B. K. Xiong, W. G. Wen, X. M. Yang, H. Y. Li, F. C. Luo, W. Zhang, J. M. Guo, Metallurgical Industry Press, Beijing, 2006.

2. Zirconium and hafnium separation without waste generation, A. B. V. Da Silva, and P. A. Distin, *CIM Bull*, 1998, 91, 221-224.
3. Nuclear-grade zirconium prepared by combining combustion synthesis with molten-salt electrorefining technique, H. Li, H. Nersisyan, K. Park, S. Park, J. Kim, J. Lee, *J. Nucl. Mater.*, 2011, 413, 107-113.
4. Pyrochemical separation of zirconium and hafnium tetrachlorides using fused salt extractive distillation process, D. Sathiyamoorthy, S. M. Shetty, D. K. Bose, C. K. Gupta, *High Temp. Mater. Process.*, 1999, 18, 213-226.
5. Zirconium and hafnium separation, Part 1. liquid/liquid extraction in hydrochloric acid aqueous solution with aliquat 336, L. Poriel, A. F. Re'guillon, S. P. Rostaing, M. Lemaire, *Separation Science and Technology*, 2006, 41, 1927-1940.
6. Chemical modification of silica surface by immobilization of functional groups for extractive concentration of metal ions, P. K. Jal, S. Patel, B. K. Mishra, *Talanta*, 2004, 62, 1005-1028.
7. Production of nuclear grade zirconium: A review, L. Xu, Y. Xia, A. van Sandwijk, Q. Xu, Y. Yang, *Journal of Nuclear Materials*, 2015, 466, 21-28.
8. Equilibrium and kinetic data of adsorption and separation for zirconium and hafnium onto MIBK extraction resin, X. Zhi-gao, W. Yan-ke, Z. Jian-dong, Z. Li, W. Li-jun, *Trans. Nonferrous Met. Soc. China*, 2010, 20, 1527-1533.
9. Adsorption mechanism of arsenic on nanocrystalline titanium dioxide, M. Pena, X. Meng, G. P. Korfiatis, C. Jing, *Environ. Sci. Technol.*, 2006, 40, 1257-1262.
10. Enhanced bioaccumulation of cadmium in carp in the presence of titanium dioxide nanoparticles, X. Zhang, H. Sun, Z. Zhang, Q. Niu, Y. Chen, J. C. Crittenden, *Chemosphere*, 2007, 67, 160-166.
11. Uranium sorption on various forms of titanium dioxide - influence of surface area, surface charge, and impurities, M. J. Comarmond, T. E. Payne, J. J. Harrison, S. Thiruvoth, H. K. Wong, R. D. Aughterson, G. R. Lumpkin, K. Muller, H. Foerstendorf, *Environ. Sci. Technol.*, 2011, 45, 5536-5542.
12. Adsorption of As(V) and As(III) by nanocrystalline titaniumdioxide, M. E. Pena, G. P. Korfiatis, M. Patel, L. Lippincott, X. Meng, *Water Research*, 2005, 39, 2327-2337.

13. Adsorption of arsenate and arsenite on titanium dioxide suspensions, P. K. Dutta, A. K. Ray, V. K. Sharma, F. J. Millero, *Journal of Colloid and Interface Science*, 2004, 278, 270-275.
14. Nanometer titanium dioxide immobilized on silica gel as sorbent for preconcentration of metal ions prior to their determination by inductively coupled plasma atomic emission spectrometry, Y. Liu, P. Liang, L. Guo, *Talanta*, 2005, 68, 25-30.
15. Studies on the adsorption of traces of zirconium on manganese dioxide from acid solutions, S. M. Hasany, E. U. Haq, S. B. Butt, *Separation Science and Technology*, 1986, 21, 1125-1139.
16. Adsorption of divalent metal ions from aqueous solutions using graphene oxide, R. Sitko, E. Turek, B. Zawisza, E. Malicka, E. Talik, J. Heimann, A. Gagor, B. Feist, R. Wrzalik, *Dalton Trans.*, 2013, 42, 5682.
17. Reduced graphene oxide–metal/metal oxide composites: facile synthesis and application in water purification, T. S. Sreeprasad, S. M. Maliyekkal, K. P. Lisha, T. Pradeep, *Journal of Hazardous Materials*, 2011, 186, 921-931.
18. Fabrication of highly porous biodegradable monoliths strengthened by graphene oxide and their adsorption of metal ions, N. Zhang, H. Qiu, Y. Si, W. Wang, J. Gao, *Carbon*, 2011, 49, 827-837.
19. Adsorption of copper, nickel and lead ions from synthetic semiconductor industrial wastewater by palm shell activated carbon, Y. B. Onundi, A. A. Mamun, M. F. A. Khatib, Y. M. Ahmed, *Int. J. Environ. Sci. Tech.*, 2010, 7, 751-758.
20. Removal of copper (II) and lead (II) ions from aqueous solutions by adsorption on activated carbon from a new precursor hazelnut husks, M. Imamoglu, O. Tekir, *Desalination*, 2008, 228, 108-113.
21. Adsorption of nickel (II) from aqueous solution onto activated carbon prepared from coirpith, K. Kadirvelu, K. Thamaraiselvi, C. Namasivayam, *Separation and Purification Technology*, 2001, 24, 497-505.
22. Adsorption of Cu(II), Cd(II), Zn(II), Mn(II) and Fe(III) ions by tannic acid immobilised activated carbon, A. Ucer, A. Uyanik, S.F. Aygun, *Separation and Purification Technology*, 2006, 47, 113-118.

23. Determination of trace metal ions by AAS in natural water samples after preconcentration of pyrocatechol violet complexes on an activated carbon column, I. Narin, M. Soylak, L. Elci, M. Dogan, *Talanta*, 2000, 52, 1041-1046.
24. Heavy metals removal by adsorption onto peanut husks carbon: characterization, kinetic study and modeling, S. Ricordel, S. Taha, I. Cisse, G. Dorange, *Separation and Purification Technology*, 2001, 24, 389-401.
25. Multi-element preconcentration of heavy metal ions from aqueous solution by APDC impregnated activated carbon, P. Daorattanachai, F. Unob, A. Imyim, *Talanta*, 2005, 67, 59-64.
26. Review of modifications of activated carbon for enhancing contaminant uptakes from aqueous solutions, C. Y. Yin, M. K. Aroua, W. M. Ashri, W. Daud, *Separation and Purification Technology*, 2007, 52, 403-415.
27. Sorption of $^{243}\text{Am}(\text{III})$ to multiwall carbon nanotubes, X. Wang, C. Chen, W. Hu, A. Ding, D. Xu, X. Zhou, *Environ. Sci. Technol.*, 2005, 39, 2856-2860.
28. Comparative study of heavy metal ions sorption onto activated carbon, carbon nanotubes, and carbon-encapsulated magnetic nanoparticles, K. Pyrzynska, M. Bystrzejewski, *Colloids and Surfaces A: Physicochem. Eng. Aspects*, 2010, 362, 102-109.
29. Adsorption of Ni(II) from aqueous solution using oxidized multiwall carbon nanotubes, C. Chen, X. Wang, *Ind. Eng. Chem. Res.*, 2006, 45, 9144-9149.
30. Adsorption of heavy metal ions with carbon nanotubes, A. Stafiej, K. Pyrzynska, *Separation and Purification Technology*, 2007, 58, 49-52.
31. Removal of lead(II) from aqueous solution by adsorption onto manganese oxide-coated carbon nanotubes, S. G. Wang, W. X. Gong, X. W. Liu, Y. W. Yao, B. Y. Gao, Q. Y. Yue, *Separation and Purification Technology*, 2007, 58, 17-23.
32. Functionalized carbon nanotube (CNT) membrane: progress and challenges, M. Sianipar, K. Khoiruddin, F. Iskandar, I. G. Wenten, *RSC Adv.*, 2017, 7, 51175-51198.
33. Surface functionalization of carbon nanotubes: fabrication and applications, S. Mallakpour, S. Soltanian, *RSC Adv.*, 2016, 6, 109916-109935.
34. Solid/liquid extraction of zirconium and hafnium in hydrochloric acid aqueous solution with anion exchange resins kinetic study and equilibrium analyses, A. F. Re'guillon, K. Fiaty, P. Laurent, L. Poriel, S. P. Rostaing, M. Lemaire, *Ind. Eng. Chem. Res.*, 2007, 46, 1286-1291.

35. Separation and preconcentration of zirconium and/or hafnium using alizarine red S immobilized on natural or polymeric support, M. M. Hassanien, Separation Science and Technology, 2005, 40, 1621-1634.
36. Distribution of zirconium and hafnium between cation-exchange resin and acid solutions. The column separation with nitric acid-citric acid mixture, J. T. Benedict, W. C. Schumb, C. D. Coryell, J. Am. Ceram. Soc., 1954, 76, 2036-2040.
37. Anion exchange of complex ions of hafnium and zirconium in HCl-HF mixtures, E. H. Huffman, R. C. Lilly, J. Am. Ceram. Soc., 1951, 73, 2902-2905.
38. Solid phase extraction using silica gel modified with murexide for preconcentration of uranium (VI) ions from water samples, S. Sadeghi, E. Sheikhzadeh, Journal of Hazardous Materials, 2009, 163, 861-868.
39. Mesoporous silica SBA-15 functionalized with phosphonate derivatives for uranium uptake, Y. L. Wang, L. Zhu, B. L. Guo, S. W. Chen, W. S. Wu, NewJ.Chem., 2014, 38, 3853.
40. Assessment of phosphate functionalised silica gel (PFSG) for separation and recovery of uranium from simulated silicide fuel scraps dissolver solution (SSFSDS), A. Das, M. Sundararajan, B. Paul, S. M. Chopade, A. K. Singh, V. Kain, Colloids and Surfaces A, 2017, 530, 124-133.
41. Mesoporous organosilica adsorbents: nanoengineered materials for removal of organic and inorganic pollutants, A. Walcarius, L. Mercier, J. Mater. Chem., 2010, 20, 4478-4511.
42. Synthesis of mesoporous silica nanoparticles, S. H. Wu, C. Y. Mou, H. P. Lin, Chem. Soc. Rev., 2013, 42, 3862-3875.
43. A silica/PVA adhesive hybrid material with high transparency, thermostability and mechanical strength, H. Pingan, J. Mengjun, Z. Yanyan, H. Ling, RSC Adv., 2017, 7, 2450-2459.
44. Improvement of mechanical performance of solution styrene butadiene rubber by controlling the concentration and the size of *in situ* derived sol-gel silica particles, V. S. Raman, A. Das, K. W. Stöckelhuber, S. B. Eshwaran, J. Chanda, M. Malanin, U. Reuter, A. Leuteritz, R. Boldt, S. Wießner, G. Heinrich, RSC Adv., 2016, 6, 33643-33655.

45. Silica supported ceria nanoparticles: a hybrid nanostructure to increase stability and surface reactivity of nano-crystalline ceria, P. Munusamy, S. Sanghavi, T. Varga, T. Suntharampillai, *RSC Adv.*, 2014, 4, 8421-8430.
46. *N*-Phenylaminomethyl hybrid silica, a better alternative to achieve reinforced PU nanocomposites, Q. Zhang, X. Huang, Z. Meng, X. Jia, K. Xi, *RSC Adv.*, 2014, 4, 18146-18156.
47. Natural rubber materials: volume 2: composites and nanocomposites, S. Thomas, C. H. Chan, L. Pothen, J. Joy, H. Maria, 2013, Chapter 7, 205-219, <http://dx.doi.org/10.1039/9781849737654-00205>.
48. Super-tough double-network hydrogels reinforced by covalently compositing with silica-nanoparticles, Q. Wang, R. Hou, Y. Cheng, J. Fu, *Soft Matter*, 2012, 8, 6048-6056.
49. Preparation of a mixed-mode silica-based sorbent by click reaction and its application in the determination of primary aromatic amines in environmental water samples, Y. Zhu, W. Zhang, L. Li, C. Wu, J. Xing, *Anal. Methods*, 2014, 6, 2102-2111.
50. Method for separating hafnium from zirconium, J. A. Sommers, J. G. Perrine, 2002, US Patents No. 6737030.
51. Determination of optimum process conditions for the extraction and separation, M. Taghizadeh, R. Ghasemzadeh, S. N. Ashrafizadeh, K. Saberyan, M. G. Maragheh, 2008.
52. Extraction and recovery of zirconium from zircon using Cyanex 923, B. Gupta, P. Malik, N. Mudhar, *Solvent. Extr. Ion. Exch.*, 2005, 23, 345-357.
53. Extraction and separation of Zr (IV) and Hf (IV) from nitrate medium by some CYANEX extractants, A. A. Nayl, Y. A. E. Nadi, J. A. Daoud, *Sep. Sci. Technol.*, 2009, 44, 2956-2970.
54. Separation of Hf (IV)-Zr (IV) in H₂SO₄ solutions using solvent extraction with D₂EHPA or Cyanex 272 at different reagent and metal ion concentrations, M. S. Lee, R. Banda, S. H. Min, *Hydrometallurgy*, 2015, 152, 84-90.
55. Solvent extraction for the separation of Zr and Hf from aqueous solutions, R. Banda, S. L. Man, *Sep. Purif. Rev.*, 2015, 44, 243-249.
56. Zirconium-hafnium production in a zero liquid discharge process, T. S. Snyder, E. D. Lee, 1992, US Patents No. 5112493.

57. Solvent extraction of zirconium with tributyl phosphate, A. E. Levitt, H. Freund, J. Am. Ceram. Soc., 2002, 78, 1545-1549.
58. Preparation and properties of nano-silica modified negative acrylate photoresist, C. K. Lee, T. M. Don, W. C. Lai, C. C. Chen, D. J. Lin, L. P. Cheng, Thin Solid Films, 2008, 23, 8399-8407.
59. A chelating resin containing 1-(2-thiazolylazo)-naphthol as the functional group: synthesis and sorption behavior for trace metal ion, W. Lee, S. Lee, C. Lee, Y. Kim, Microchem. J., 2001, 70, 195-203.
60. Preparation of silica gel bound crown ether and its extraction performance towards zirconium and hafnium, W. Qin, S. Xu, G. Xu, Q. Xie, C. Wang, Z. Xu, Chemical Engineering Journal, 2013, 225, 528-534.

Separation of Actinides from Rare Earth Metals by Dihydroxy Anthraquinone and Ethyl-Bis-Triazinylpyridine Based Ligands

5.1 Introduction

Uranium has its use in nuclear industry as a fissile element [1]. Uranium is used in natural or enriched ^{235}U in nuclear reactors as an elemental alloy or oxide, carbide etc. forms [2]. Specifications for nuclear grade uranium is that it should contain < 10 ppm of rare earths in it [3] due to very high neutron absorption cross section of rare earths causing deficit in required neutron flux inside reactors. Therefore, separation of rare earths from uranium is mandatory from spent fuel as well as other resources for nuclear grade uranium production. On the other hand, rare earths have wide applications in various fields. Therefore, rare earths separated from radioactive elements have no issues for its use in public domain.

Rare earths are used in various domains in our life such as electric traction drives in hybrids, plug-In, electric vehicles, as permanent magnets, in wind and hydro power generation, in handheld wire-less devices and computer disc drives, in cordless power tools, in medical imaging-MRI, in X-ray imaging, in flat screen display, in catalytic converters and other emission reduction technologies, in fiber optics, in Ni metal hydride batteries for energy storage, in capacitors with high energy density etc. [4]. The global scenario for the production of rare earths is given below [5].

Rare earths are present as trivalent lanthanide ions i.e. Ln^{3+} (Ln represents the lanthanides) forming complexes with water or nitrate ion in nitric acid medium. Rare earth cations are very hard acid cations [6] and therefore, binds strongly with hard donor ligands i.e. containing oxygen, nitrogen atoms at the binding sites namely,

Table 5.1 Country wise production of rare earths

Country	Mine production (metric ton)	Reserves (metric ton)
United States	–	13,000,000
Australia	–	1,600,000
Brazil	550	48,000
China	130,000	55,000,000
Commonwealth of Independent States	–	19,000,000
India	2700	3,100,000
Malaysia	350	30,000
Other countries	–	22,000,000
World total	133,600	113,778,000

D₂EHPA (di-2-ethylhexyl phosphoric acid), PC88A (i.e. 2-ethylhexyl 2-ethylhexyl phosphonic acid monoethyl hexyl ester), versatic 10 (i.e. neodecanoic acid), TBP (i.e. tributyl phosphate), alamine 336, LIX 84, LIX 621 [7-8] etc. Uranium (VI) also has a very high ionic potential and therefore binds strongly with hard donor oxygen atoms like TBP, D₂EHPA, TOPO (trioctyl phosphine oxide), di-2-ethylhexyldithiophosphoric acid (DEHDTPA), di-(2-ethylhexyl) sulfoxide (DEHSO). The thio-organophosphorous extractants like bis(2,4,4-trimethylpentyl) phosphinic acid (cyanex 272) and trioctylphosphine oxide (cyanex 923) are also the oxygen donor ligands used for the extraction of uranyl ion [9]. Separation of uranium and rare earths takes place at the particular feed acidity where their extraction differs greatly from each other [10-13].

In this regard, 1,8-dihydroxy anthraquinone functionalised silica gel (DHAFSG) has been synthesised, characterised and used for the separation of uranium and rare earths from nitric acid medium. Synthesis and characterisation of 1,8-dihydroxy anthraquinone functionalised silica gel (DHAFSG) have been

discussed in chapter 2. In this chapter, the experimental and theoretical studies have been discussed for the complexation behaviour of DHAFSG with rare earths and uranium and experiments on the separation of rare earths and uranium have been discussed also. Moreover, a nitrogen based ligand namely, ethyl-bis-triazinylpyridine (Et-BTP) has also been tried for the separation of trivalent lanthanides and actinides using solvent extraction and membrane technologies which have been described in this chapter. Complexes of DHAFSG with rare earths and uranium have also been focused at molecular level.

5.2. Results & Discussion

5.2.1. Sorption Studies of Rare Earths and Uranium using 1,8-Dihydroxy Anthraquinone Functionalised Silica Gel (DHAFSG) by Solid Phase Extraction (SPE) Technique

Sorption studies of rare earths on DHAFSG from nitric acid medium have been carried out in batch mode. Studies for the sorption variation with pH of feed solution, kinetic studies, isotherm studies for rare earths have been discussed below.

5.2.1.1. pH Variation of Feed Solution

For the variation of sorption with pH of the feed solution, europium (Eu), samarium (Sm), ytterbium (Yb), yttrium (Y), dysprosium (Dy) and erbium (Er) have

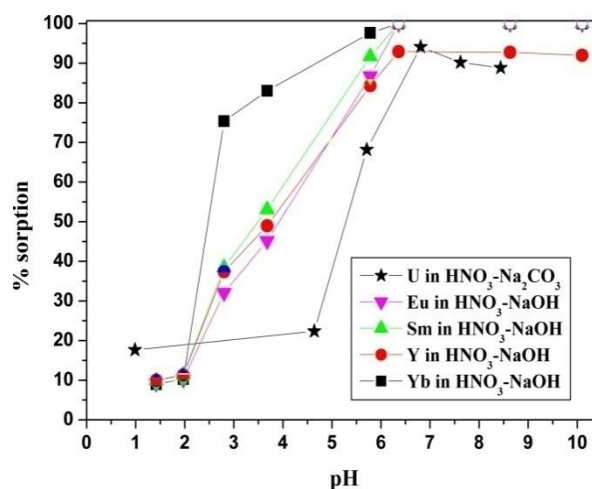


Fig.5.1 Sorption of rare earths and uranium on DHAFSG

been taken for the studies. It has been observed that sorption of rare earths increase as the pH of feed solution increases and becomes constant after pH 6. Maximum sorption of rare earths took place at about pH 6. Most of the rare earths hydrolyse at higher pH (i.e., pH>7) [14] increasing the percentage sorption.

5.2.1.2. Sorption Kinetics Studies

Sorption kinetics for rare earths with DHAFSG has been studied at pH 6 where maximum sorption has been observed. Eu, Sm, Y, Yb and U have been taken for kinetics. Sorption kinetics is fast for all the elements under observation and sorption equilibrium is achieved within five minutes with a sorbent dose of 2gL^{-1} in all the cases. (Fig 5.2) For analysis of the nature of sorption kinetics, data have been fitted with pseudo first order and pseudo second order kinetic models as described in chapter 2. Kinetics data deviates largely from linearity from the pseudo first order kinetic model but fits well with the pseudo second order kinetic model as is obvious from Fig. 5.3.

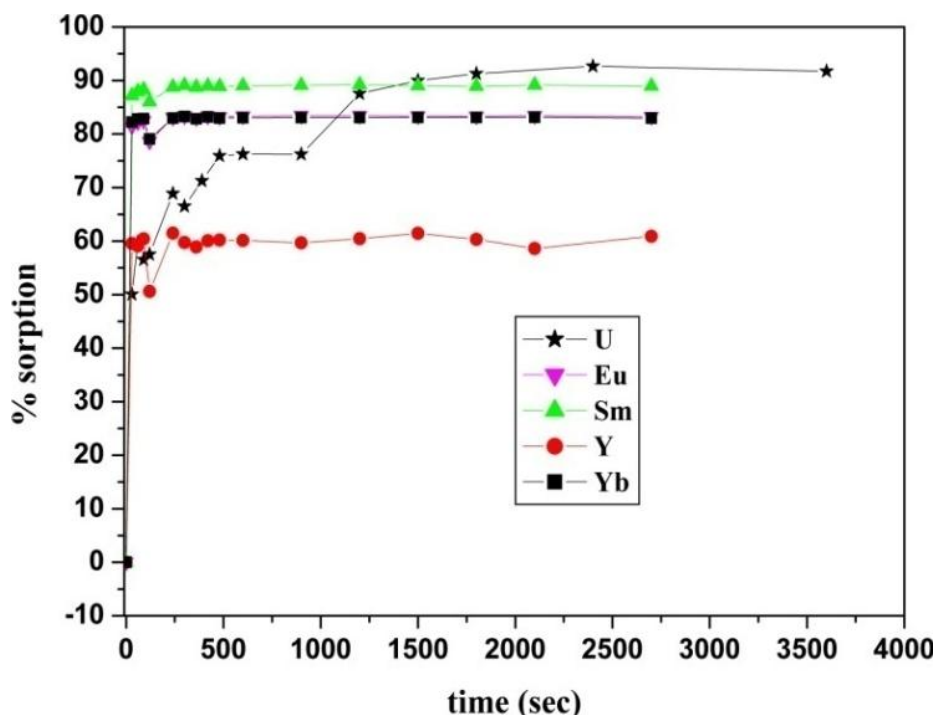


Fig.5.2 Sorption kinetics of rare earths and uranium on DHAFSG

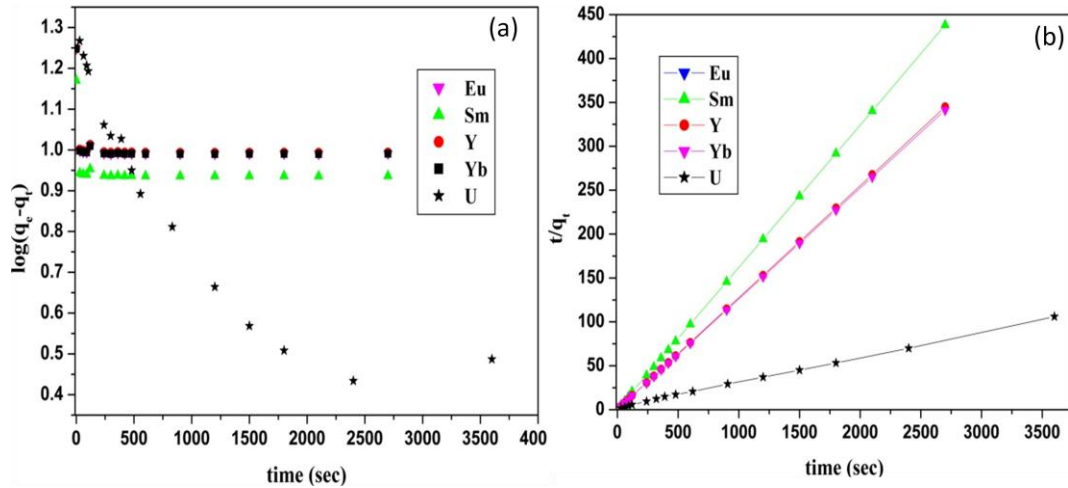


Fig.5.3 Kinetic models fitting (a) pseudo first order and (b) pseudo second order kinetic model

5.2.1.3. Sorption Isotherm Studies

Sorption isotherm studies for Eu, Sm, Y, Yb and U have been carried out separately on DHAFSG (Fig.5.4) with variation of feed concentrations (concentration range was 25-200 mg L⁻¹ at pH 6). In all these cases, sorption of rare earths increases with the increase in their feed concentration (Fig.5.4). To find out the nature of sorption of rare earths on DHAFSG, sorption isotherm data have been fitted in Langmuir and Freundlich isotherm models (discussed in chapter 2).

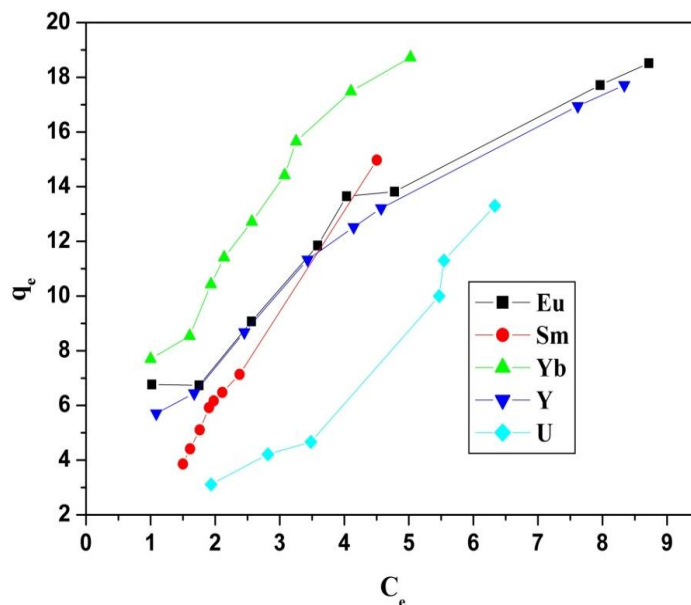


Fig.5.4 Isotherm studies of rare earths and uranium on DHAFSG

It is clear from Fig.5.5 that sorption data deviates from linearity with Langmuir model but are close to linearity in case of Freundlich model. DHAFSG has heterogeneous binding sites on its surface on which sorption of rare earths take place.

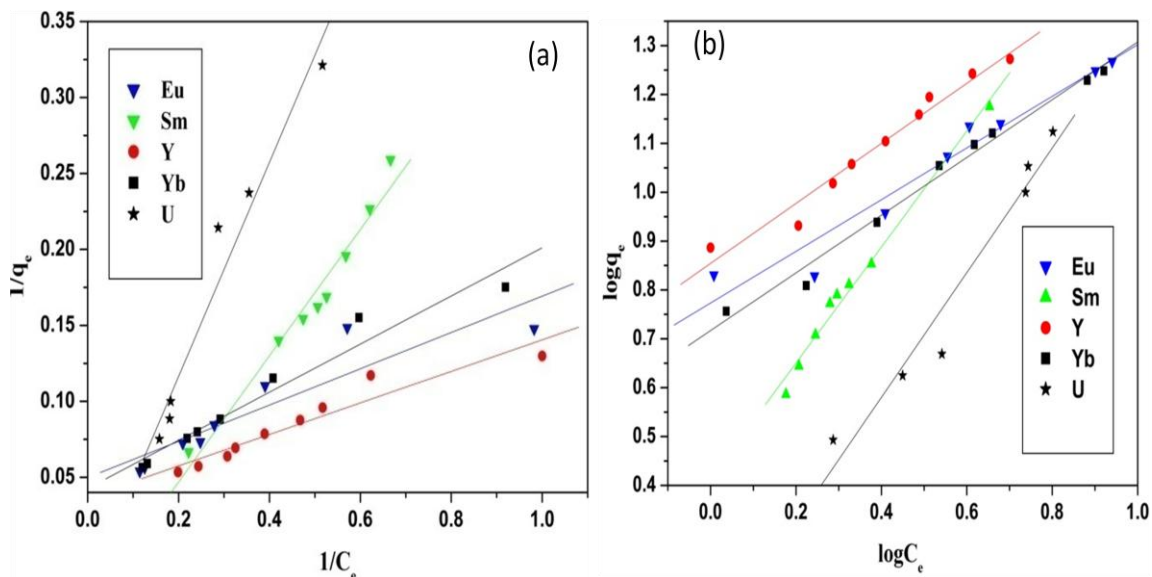


Fig.5.5 Isotherm data for rare earths and uranium sorption on DHAFSG: (a) Langmuir plot, (b) Freundlich plot

5.2.1.4. Studies for Loading Capacities of Rare Earths and Uranium on DHAFSG

Loading capacities of Eu, Sm, Y and Yb have been determined separately by equilibrating a fixed quantity of DHAFSG with excess volume of rare earth feed solution with known concentrations of individual rare earths at pH 6 as described in chapter 2. Loading capacities have been given in Table 5.2.

Table 5.2 Loading capacities of rare earths and uranium on DHAFSG

Elements	Loading Capacities (mg/g)
Eu	23
Sm	20
Yb	24
Y	21
U	15

5.2.1.5. Separation of Rare Earths and Uranium from Loaded DHAFSG

It has been observed that separation of rare earth elements from uranium is not very high at different pH of the feed solution (Fig.5.1), therefore, their separation has been tried with different chemical reagents. For the separation studies in batch mode, a fixed measured quantity of DHAFSG has been loaded with a measured volume of feed solution with known concentration of U, Eu, Sm, Y and Yb at pH 6 each time before the elution studies. The loaded DHAFSG has been then treated with different eluents (of fixed volume) for the de-sorption separation studies and the eluent solutions have been analysed for the metal ions. Aqueous solutions of sodium carbonate, hydrochloric acid, oxalic acid, ethylenediamine tetraacetic acid (EDTA) etc. have been tried as the eluents for the de-sorption studies. It has been observed that 0.01M sodium carbonate solution selectively elutes out all the loaded uranium; after that 0.02M hydrochloric acid is used to complex out the rare earth elements. This two step process completely separates uranium from the rare earth elements. Whereas, oxalic acid make the complexes with both rare earth elements as well as uranium. 0.01M oxalic acid elutes 95% of the loaded rare earth elements along with 5% loaded uranium. 0.01M EDTA (pH >5) elutes 90% loaded rare earth elements along with 70% loaded uranium.

5.2.1.6. Theoretical Studies on the Complexation Behaviour of Rare Earths and Uranium with DHAFSG

For carrying out the theoretical studies, Eu(III) and uranyl ion have been considered as the representatives of rare earth elements and actinides respectively. In all these cases, DHAFSG ligand has been considered to be deprotonated at only one site of the phenolic–OH group present in the anthraquinone ring. DHAFSG binds with the metal ion through the oxygen atom of deprotonated phenolic –OH group and also through the oxygen atom of benzo-ketone present in the anthraquinone ring. But the oxygen

atom of benzo-ketone present in the anthraquinone ring gets protonated after the optimisation of geometry of mere DHAFSG ligand (Fig.5.6). For Eu(III), geometries have been optimised considering two cases like i) two hydroxyl ions along with four water molecules (Fig.5.7a) and also for ii) one hydroxyl ion along with five water molecules (Fig.5.7b) present in the co-ordination sphere of Eu(III). In case of uranyl ion, two water molecules have been considered in its co-ordination sphere (Fig.5.7c). The bond lengths from the optimised geometries have been provided in Table 5.3.

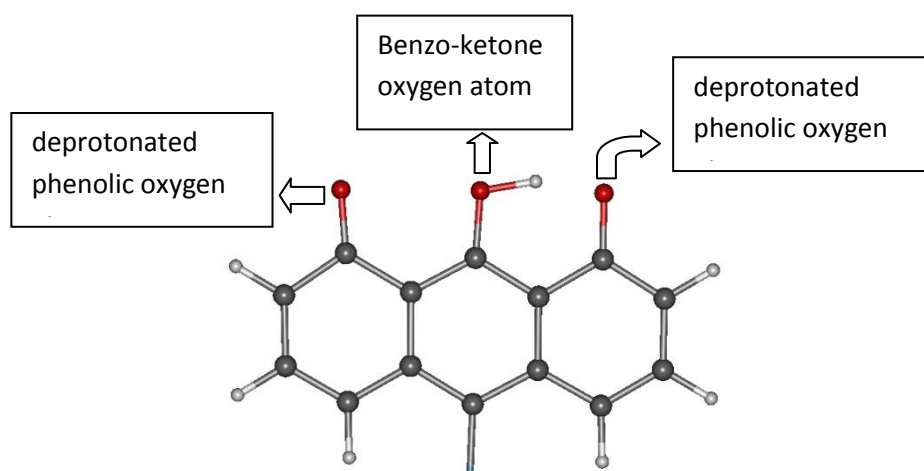


Fig.5.6 Binding sites from anthraquinone ring of DHAFSG

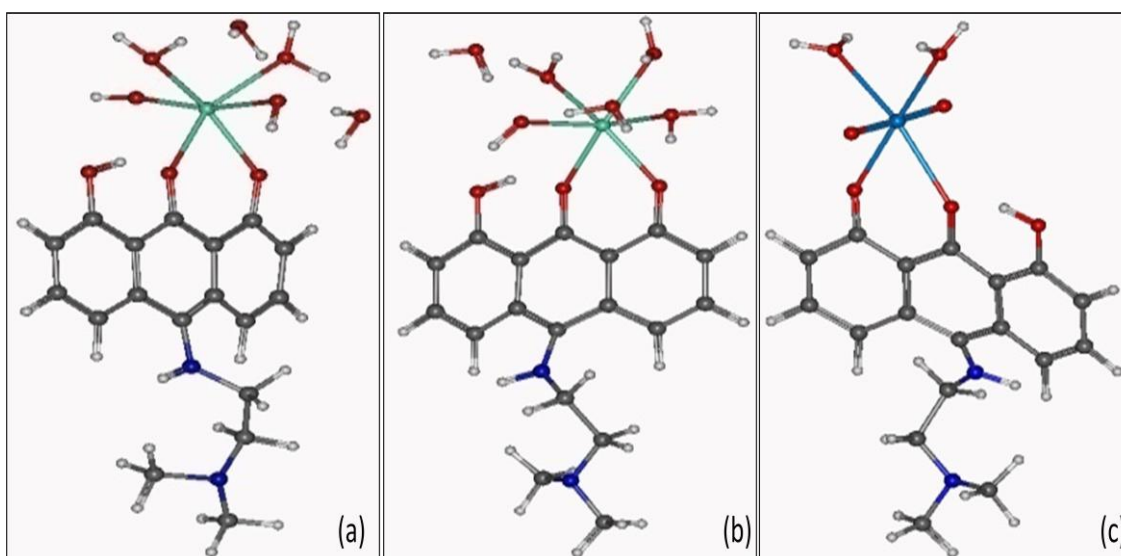


Fig.5.7 DHAFSG complexes with (a) Eu(OH)₂.4H₂O, (b) Eu(OH).5H₂O and (c) UO₂.2H₂O

Table 5.3 Optimised bond lengths of Eu(III) and U(VI) complexes with DHAFSG

	Eu(OH) ₂ .4H ₂ O (Å)	Eu(OH).5H ₂ O (Å)	UO ₂ .2H ₂ O (Å)
M-O (phenolic oxygen)	2.30	2.25	2.50
M-O (benzo-ketone oxygen)	2.35	2.32	2.72
M-O (hydroxyl)	2.09	2.33	----
	2.40		
M-O (water)	2.41	2.41	2.74
	2.44	2.51	2.73
	---	2.57	---

5.2.2. Separation Studies of Rare Earths and Actinides using Ethyl-Bis-Triazinyl Pyridine (Et-BTP) by Solvent Extraction Technique

Ligands with hard donor atom like ‘oxygen’ has a preference for rare earths as is the case of DHAFSG as described above under the experimental conditions. Ligands with ‘nitrogen’ donor atom like has also preference for rare earths over actinides as is reported by Zhao et. al. for 2,6-bis(5,6-dihexyl-1,2,4-triazin-3-yl) pyridine (isohexyl-BTP) as extractant in ionic liquid medium [15]. But the extraction behaviour by bis-triazinylpyridine (BTP) ligands changes remarkably in the presence of diluents [16]. On the other hand, BTP derivatives like phenyl substituted BTP has been found to be most insoluble BTP in organic phase whereas, methyl substituted BTP derivative has significant solubility in the aqueous phase. Therefore, Et-BTP has been chosen for the studies due to its favourable extraction behaviour.

Synthesis and characterisation of Et-BTP ligand has been discussed by Bhattacharyya et. al. [17]. The extraction behaviour of rare earth and actinide using ethyl-bis-triazinylpyridine (Et-BTP) has been described below by solvent extraction technique. For these studies, europium (III) i.e. Eu³⁺ and americium (III) i.e. Am³⁺

have been considered as the representatives of the lanthanide and actinide elements respectively. Solvent extraction studies have optimised the extraction parameters like organic diluent used with Et-BTP, feed and strip conditions.

5.2.2.1. Choice of Appropriate Diluents for Et-BTP Solvent

Several organic diluents have been tried to solubilise the reagent (Et-BTP) and the extracted complex in the organic phase to improve extraction and subsequent separation efficiencies of rare earths and actinides. Poor solubility of the Et-BTP and poor extractibility has been observed when n-decanol, benzyl alcohol, 1-octanol, hexone and tert-butyl-benzene have been tried as diluents (Table 5.4). It has been observed that the presence of an auxiliary ligand along with Et-BTP, has increased the solubility of Et-BTP as well as the extracted species, with significant increase in the extraction/ separation behaviour. Two auxiliary ligands namely, alpha-bromo carboxylic acid and chlorinated cobalt dicarbollide (CCD) have been exercised here along with Et-BTP.

Table 5.4 Solubility of Et-BTP in different organic diluents

Diluent	Solubility	Diluent	Solubility
n-Dodecane	Insoluble ^a	1-Octanol	Insoluble ^b
Toluene	Insoluble	Cyclohexanol	Very soluble
Tert-butyl benzene	Insoluble	Hexone	Very soluble
Tri-iso-propylbenzene	Insoluble	Pentanol	Very soluble ^c
1-Decanol	Insoluble	Benzyl alcohol	Very soluble ^c
Nitrobenzene	Partly soluble ^b	NPOE	Insoluble ^b

^a Soluble in presence of alpha-bromo carboxylic acid

^b Soluble in presence of CCD

^c Diluent is partially miscible with aqueous phase

5.2.2.2. Role of Alpha-Bromo Carboxylic Acids and Chlorinated Cobalt Dicarbollide (CCD) as Auxiliary Ligands

BTP ligands have different solubilities in organic medium as discussed above. Alpha-bromo-carboxylic acids as the auxiliary ligands assist the solubilization of the BTP ligands in organic medium and also solubilise the metal complexes with BTP by contributing as the counter anion (Table 5.5). For Et-BTP ligand, alpha bromo octanoic acid in n-dodecane is suitable as the organic phase which gives significant extraction of Am^{3+} and good separation from Eu^{3+} . But stripping of Am^{3+} from the loaded solvent is difficult which complicates for further applications.

Table 5.5 Data of Am^{3+} and Eu^{3+} extraction and their separation with 0.02 M Et-BTP+0.4 M α -bromo-octanoic acid for different aqueous feed solutions

Aqueous phase	D_{Am}	D_{Eu}	S.F.
0.01 M HNO_3	930	343	2.71
0.1 M HNO_3	240	5.3	45.3
0.3 M HNO_3	20.4	0.21	97.1
1 M HNO_3	28.6	0.31	92.3
2 M HNO_3	55.3	0.24	230
0.1 M AHIBA	121	310	0.39
0.01 M EDTA	0.62	0.69	0.90

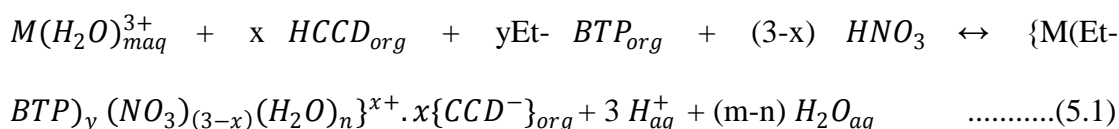
Chlorinated cobalt dicarbollide (CCD) as auxiliary ligands also plays a good role as an auxiliary ligand with good solubility and extractability of Am^{3+} . 0.005 M CCD along with 0.02 M Et-BTP in nitrobenzene medium or in 2-nitrophenyl octyl ether (NPOE) medium acts as a good extractant of Am^{3+} and separates it from Eu^{3+} . On the other hand, it also shows a good stripping of Am^{3+} from loaded solvent. Therefore, CCD has been used in subsequent use in SLM studies. The extraction, stripping and separation behaviour using CCD as an auxiliary ligand have been given in Table 5.6.

Table 5.6 Distribution ratio (D) of Am^{3+} and Eu^{3+} and their separation factors

Organic phase	Aqueous phase	D_{Am}	D_{Eu}	S.F.
0.02 M Et-BTP in benzyl alcohol+ tBu-benzene	Dist. water	0.45	-	-
	0.5 M HNO_3	0.15	-	-
0.02 M Et-BTP + 0.005 M	Dist water	> 500	22.2	-

CCD in nitrobenzene	0.01 M HNO ₃	> 500	3.1	-
	0.1 M HNO ₃	28.7	0.3	96
	0.5 M HNO ₃	1.03	0.04	26
	1.0 M HNO ₃	1.12	0.04	28
	0.01 M EDTA (pH 3.5)	< 0.001	< 0.001	-
0.02 M Et-BTP + 0.005 M CCD in NPOE	0.1 M HNO ₃	114	0.23	495
	0.01 M EDTA (pH 3.5)	< 0.01	< 0.01	-

It is obvious from the above studies (Table 5.6) that 0.1M HNO₃ is the optimum feed acidity and 0.01M EDTA is the optimum strip solution. The extraction mechanism in the CCD medium can be written as,



Distribution ratio 'D_M' of the metal ions can be defined as

$$D_M = [\{M(Et - BTP)_y (NO_3)_{(3-x)}(H_2O)_n\}^+ \cdot x\{CCD^-\}]_{org} / [M(H_2O)_m^{3+}]_{aq} \quad ..(5.2)$$

And the extraction constant K_{ex} can be written as

$$K_{ex} = \frac{[\{M(Et-BTP)_y (NO_3)_{(3-x)}(H_2O)_n\}^+ \cdot x\{CCD^-\}]_{org} \cdot [H^+]_{aq}^3}{[M(H_2O)_m^{3+}]_{aq} [HCCD]_{org}^x [Et-BTP]_{org}^y [HNO_3]_{(3-x)aq}^{(3-x)}} \quad \dots(5.3)$$

Taking logarithm of equation (5.3) can be changed into

$$\log D = \log K_{ex} + 3pH + x\log[HCCD]_{org} + y\log[Et-BTP] + (3-x)\log[HNO_3]_{aq} \quad \dots\dots(5.4)$$

x and y are found out from the slope of logD vs. log[HCCD]_{org.} and logD vs. log[Et-BTP] respectively keeping other parameters constant.

5.2.2.3. Effect of Variation of CCD Concentration

CCD concentration has been varied in the range of 0.001-0.005 M while keeping the Et-BTP concentration fixed at 0.02 M in nitrobenzene medium (aqueous feed acidity has been kept fixed at 0.1 M HNO₃ in all these studies). D_{Am} has been

determined in all these cases. Slope of $\log D$ vs. $\log [\text{HCCD}]_{\text{org.}}$ plot (Fig.5.8) has been found to be 1 indicating that one CCD molecule comes in the complexation reaction. It has been assumed in these studies that the tripositive charge of Am^{3+} has been neutralised by two nitrate groups.

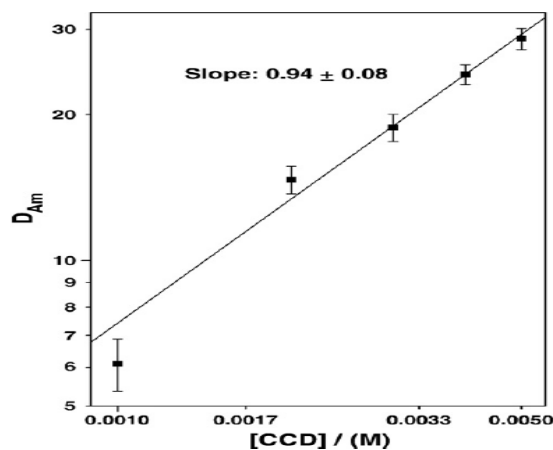


Fig.5.8 Effect of variation of CCD concentration on the extraction of Am^{3+}

5.2.2.4. Effect of Variation of Et-BTP Concentration

Concentration of Et-BTP has been varied in the range of 0.004-0.02 M, keeping the CCD concentration fixed at 0.001M in nitrobenzene medium. The aqueous phase acidity has been kept as 0.1 M HNO_3 as before. D_{Am} has been measured in all these cases. Slope of $\log D_{\text{Am}}$ vs. $\log [\text{Et-BTP}]_{\text{org.}}$ plot (Fig.5.9) has been found to be 1 indicating that one Et-BTP molecule is involved in the complexation reaction.

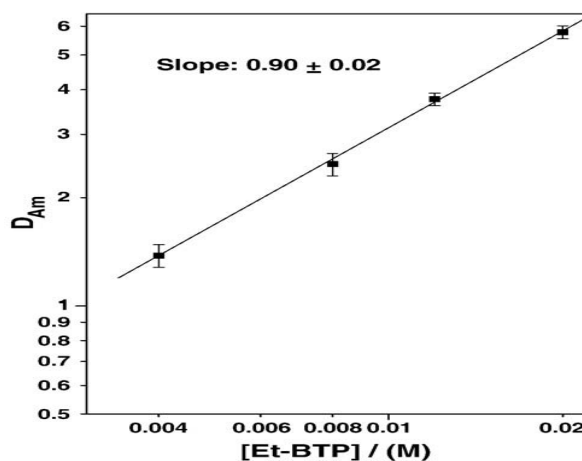


Fig.5.9 Effect of the variation of Et-BTP concentration on the extraction of Am^{3+}

5.2.3. Separation Studies of Rare Earths and Actinides using Ethyl-Bis-Triazinyl Pyridine (Et-BTP) by Supported Liquid Membrane (SLM) Technique

SLM studies for the separation of lanthanides and actinides have been carried out by the method described in chapter 2. The optimised parameters as obtained from the solvent extraction studies like the diluent used with Et-BTP, feed and strip conditions etc. have been utilised for the liquid membrane studies as described below. It has been found from the solvent extraction studies that NPOE is an optimum diluent for Et-BTP + CCD mixture (as described in section 5.2.2.1.), but transportation of Am^{3+} is not facilitated through SLM due to high viscosity of NPOE. Therefore, a mixture of NPOE and n-dodecane has been taken for SLM studies which show facile transport of Am^{3+} through the membrane. Moreover, mere EDTA can't serve as an optimum stripping agent (0.01M EDTA as obtained from solvent extraction studies) due to its precipitation in presence of nitric acid which comes from the feed solution through the membrane. Therefore, a mixture of chloroacetate buffer and EDTA has been taken as the stripping agent to avoid the precipitation of EDTA for the SLM studies. Transport of Am^{3+} has been facilitated by chloroacetate buffer and EDTA as the stripping agent (Fig.5.10).

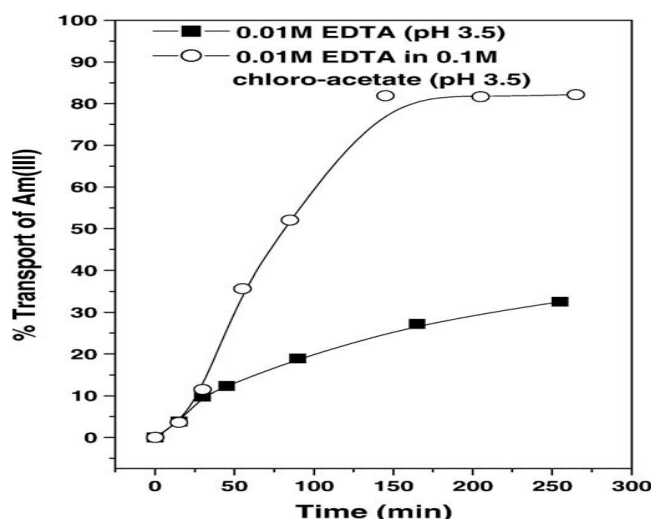


Fig.5.10 Am(III) transport studies with i) only EDTA and ii) EDTA+chloroacetate buffer as the stripping agent. Feed: 0.1 M HNO_3 ; Organic phase: 0.02 M Et-BTP+0.005 M CCD in nitrobenzene.

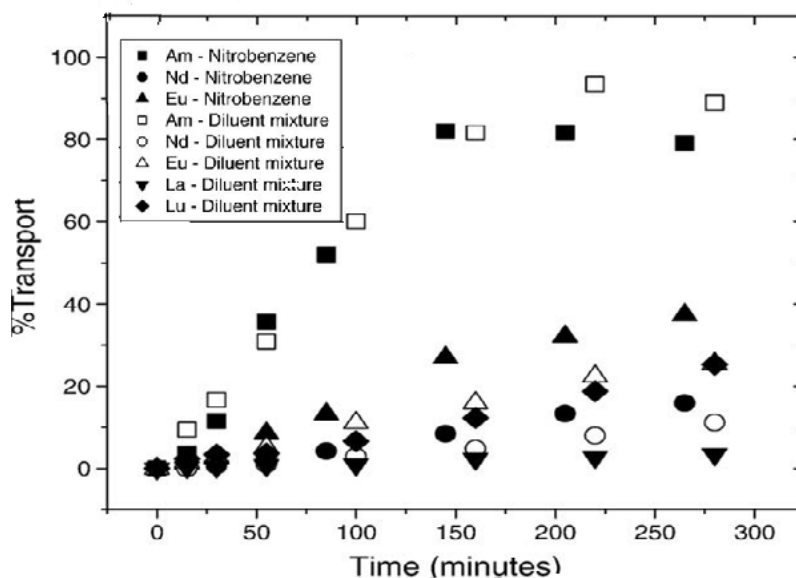


Fig.5.11 Transport of Am^{3+} , La^{3+} , Eu^{3+} , Nd^{3+} and Lu^{3+} using (0.02 M Et-BTP+ 0.005M CCD) ligands in (nitrobenzene + n-dodecane) diluent mixture. Feed: 0.1M HNO_3 ; Strip: 0.01 M EDTA in chloroacetate buffer (pH=3.5).

Transport studies have also been carried out for ^{241}Am , ^{152}Eu , ^{147}Nd , ^{177}Lu and ^{140}La using 0.02 M Et-BTP along with 0.005M CCD as ligands in the mixture of nitrobenzene and n-dodecane diluents. It is observed that Am^{3+} has been transported efficiently and separated well from the rare earths (i.e. La^{3+} , Nd^{3+} , Eu^{3+} , Lu^{3+}) (Fig.5.11).

5.3. Conclusion

DHAFSG seems to be a potential candidate to separate rare earth elements from uranium. Complexation of rare earth elements with DHAFSG is stronger than that of uranium which is reflected in their loading capacity values. Separation of rare earth elements from uranium using DHAFSG is not possible by variation of pH of the eluent solution. Different eluting reagents have been studied for their separation. It has been observed that complete separation of uranium and rare earth elements is possible by two steps of elution: in the first step, complete removal of uranium using

0.01M sodium carbonate reagent and in the second step, complete desorption of rare earth elements using 0.02M hydrochloric acid reagent.

Et-BTP on the other hand also seems to be a potential candidate to separate actinides from lanthanides using both solvent extraction as well as membrane techniques. Et-BTP selectively binds with actinides (e.g. Am^{3+}) compared to lanthanides (e.g. Eu^{3+}) in presence of CCD as the auxiliary ligand. Back-extraction (stripping) of actinides is not possible by mere variation of acidity of nitric acid of the strip solution because it is difficult to break the strong Et-BTP-CCD- Am^{3+} complex. Therefore, a complexing agent e.g. EDTA has been used for the back-extraction of loaded Am^{3+} (which is present in the organic phase) into the aqueous phase.

References

1. Development of very-high-density low-enriched-uranium fuels, J. L. Snelgrove, G. L. Hofman, M. K. Meyer, C. L. Trybus, T. C. Wiencek, Nuclear Engineering and Design, 1997, 178, 119-126.
2. Fuels for research and test reactors, status review, ANL-83-5, D. Stahl, 1982, DE83 014267.
3. Standard specification for nuclear-grade, sinterable uranium dioxide powder, ASTM C753-16a, ASTM international, West Conshohocken, PA, 2016.
4. Indian Minerals Yearbook 2015 (Part-III: Mineral Reviews), 54th Edition: Rare Earths, 2016.
5. U.S. Geological Survey, Mineral Commodity Summaries 2011, U.S. Department of Interior, 2011.
6. Lanthanide complexation in aqueous solutions, G. R. Choppin, Journal of the Less-Common Metals, 1984, 100, 141-151.
7. Prospects for solvent extraction processes in the Indian context for the recovery of base metals: a review, V. Kumar, S. K. Sahu, B. D. Pandey, Hydrometallurgy, 2010, 103, 45-53.
8. Separation of Nd (III), Dy(III) and Y(III) by solvent extraction using D_2EHPA and EHEHPA , M. Mohammadi, K. Forsberg, L. Kloo, J. M. De La Cruz, Å. Rasmuson, Hydrometallurgy, 2015, 156, 215-224.

9. A brief review on solvent extraction of uranium from acidic solutions, J. R. Kumar, J. S. Kim, J. Y. Lee, H. S. Yoon, *Separation & Purification Reviews*, 2011, 40, 77-125.
10. Sequential separation of lanthanides, thorium and uranium using novel solid phase extraction method from high acidic nuclear wastes, Ch. S. K. Raju, M. S. Subramanian, *Journal of Hazardous Materials*, 2007, 145, 315-322.
11. Separation of uranium and thorium from rare earths for rare earth production-A review, Z. Zhu, Y. Pranolo, C. Y. Cheng, *Minerals Engineering*, 2015, 77, 185-196.
12. Sequential separation of actinides and lanthanides by extraction chromatography using a CMPO-TBP/XAD7 column, M. Yamaura, H. T. Matsuda, *Journal of Radioanalytical and Nuclear Chemistry*, 1999, 241, 277-280.
13. Solvent extraction process for separating actinide and lanthanide metal values, R. A. Hildebrandt, H. H. Hyman, V. Seymour, Patent US3049402 A.
14. Atlas of Eh-pH diagrams: intercomparison of thermodynamic databases, Geological Survey of Japan Open File Report No.419. National Institute of Advanced Industrial Science and Technology Research Center for Deep Geological Environments Naoto, Takeno, 2005.
15. Solution extraction of several lanthanides from nitric acid with isohexyl-BTP in [Cnmim][NTf₂] ionic liquid, Z. Long, D. Zhen, M. Guolong, Y. Weijin, *Journal Of Rare Earths*, 2015, 33, No. 11, 1182.
16. Liquid-liquid extraction and flat sheet supported liquid membrane studies on Am(III) and Eu(III) separation using 2,6-bis(5,6-dipropyl-1,2,4-triazin-3-yl)pyridine as the extractant, A. Bhattacharyya, P. K. Mohapatra, T. Gadly, D. R. Raut, S. K. Ghosh, V. K. Manchanda, *Journal of Hazardous Materials*, 2011, 195, 238-244.
17. Ethyl-bis-triazinylpyridine (Et-BTP) for the separation of americium (III) from trivalent lanthanides using solvent extraction and supported liquid membrane methods, A. Bhattacharyya, P. K. Mohapatra, A. Roy, T. Gadly, S. K. Ghosh, V. K. Manchanda, *Hydrometallurgy*, 2009, 99, 18-24.

Separation and Enhanced Recovery of Palladium using Dithio Diglycol Amide (DTDGA) Ligand

6.1 Introduction

Palladium is a valuable metal which is applied in various fields e.g. catalysis, pharmaceuticals, electronics, telecommunication, heat and corrosion resistance apparatus, petroleum industry, dental alloys, jewellery etc. [1-3]. But the natural abundance of palladium in the earth crust is too low to meet the present growing demand. This has generated the need of exploring the separation and recovery of palladium from secondary resources. Among the various secondary resources of palladium the major ones include spent catalysts from automotive and petroleum industries and high level waste (HLW) from nuclear industry [4-9].

Different ligands have been proposed for extraction of palladium. Palladium is a soft metal and has a preference for co-ordination with ligands containing soft donor atoms like 'S'. Several extractants have been so far reported by researchers for the extraction of palladium. Ligands like 2-hydroxy-4-s-octanoyldiphenyl-ketoxime [10], dialkyl sulphoxides [11], 8-hydroxyquinoline [12], dioctyl sulphides [13], 4-acylpyrazolone [14], pyridine-carboxamides [15], Cyphos-IL-101 [16], and bis-(2,4,4-trimethyl pentyl)-phosphinodithioic acid [17], tertiary and quaternary amines (tri-n-octylamine, tri-n-octylmethyl ammonium chloride (TOMAC) and tri-n-octylmethyl ammonium nitrate (TOMAN) [18-19] α -benzoinoxime (ABO) [20] and benzoyl methylene triphenyl phosphorane (BMTTP) [21] have been exploited worldwide. Large scale implication of these ligands are affected by several limitations like pH sensitivity, chemical stability, slower kinetics of extraction, poor solubility in

paraffinic diluents, instability in acidic medium etc. These limitations has been overcome by exploring a sulphur based ligand, namely, N, N, N',N''-tetraoctylthiodiglycolamide (TOTDGA) in HCl medium [22-23]. This ligand has shown high extractability and selectivity for palladium over other metal ions. With the idea of increasing the extractability of palladium with less ligand inventory, the incorporation of second S atom has been attempted. This led us to the design of the molecule N,N,N',N'-tetra(2-ethylhexyl)dithiodiglycolamide (DTDGA). DTDGA has shown remarkable extractability and selectivity for palladium over other metal ions present [5]. The chelation of palladium with DTDGA occurs through more than one donor sites of thio-etheric sulfur and amidic moiety placed appropriately in the ligand which provides high selectivity and extractability for palladium [24]. DTDGA molecule possesses two thioetheric 'S' atoms as compared to the single 'S' atom in TOTDGA molecule and, therefore, it is expected that this ligand will chelate more effectively and selectively with palladium for its recovery from various resources.

In the present chapter, separation and recovery of palladium from both hydrochloric acid and nitric acid medium by DTDGA ligand has been discussed. Solvent extraction method has been exploited for the recovery of palladium from hydrochloric acid medium. Various parameters used in the solvent extraction method like feed acidity, extraction kinetics, ligand concentration, effect of diluents, back extraction of palladium etc. have been optimised. Finally, the recovery of palladium from spent catalyst dissolver solution in hydrochloric acid medium has been demonstrated. In addition, membrane method also has been exploited for the recovery of palladium from nitric acid medium. Parameters like effect of nitric acid in the feed solutions, effect of DTDGA concentration, effect of membrane pore size, membrane

thickness, stability of membrane etc. have been optimised. At the end, selectivity of the ligand over other fission products using the membrane technique has been tested.

6.2. Results and Discussion

6.2.1. Solvent Extraction Studies with DTDGA Ligand

Solvent extraction studies for palladium from hydrochloric acid medium using DTDGA ligand have been performed. Following experiments have been carried out to establish the extraction parameters.

6.2.1.1. Extraction Kinetics

Fig. 6.1 shows the variation of percentage extraction (%E) of palladium as a function of contact time. It is evident from the figure that the kinetics of extraction is very fast, the extraction equilibrium being achieved in less than 5 minutes under the chosen experimental conditions.

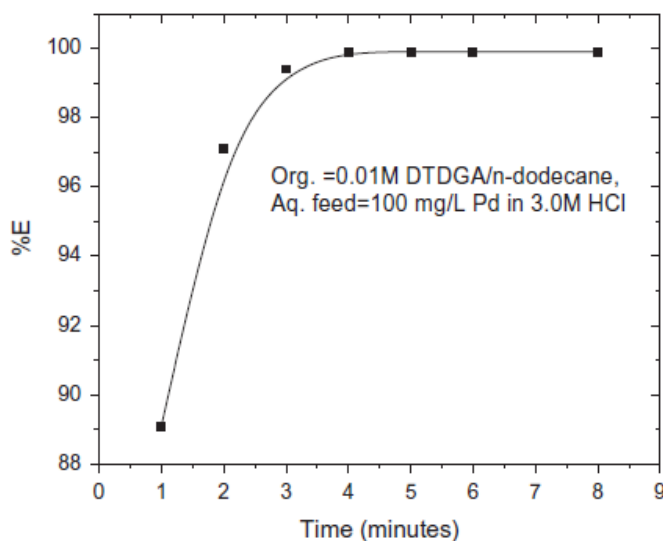


Fig.6.1 Extraction kinetics of palladium by DTDGA solvent

6.2.1.2. Effect of Feed Acidity

Influence of hydrochloric acid concentration (present in the feed solution) on the extraction of palladium has been studied by determining D_{Pd} at various concentrations of HCl (Fig. 6.2). It is observed that D_{Pd} increases with increase in HCl concentration up to 3M and no change in D_{Pd} has been observed on further increasing the HCl concentration. It suggests that the hydrochloric acid plays an

important role in extraction of palladium. It is therefore of importance to investigate the mode of participation of HCl in the extraction reaction. Fig. 6.3 shows that D_{Pd} remains unchanged with hydrochloric acid variation at a fixed ionic strength of chloride ion i.e. 3.0 M (H,Na)Cl. This indicates that HCl molecule itself does not participate in the complex formation reaction with palladium rather the chloride ions present in the feed solution participates in the complexation reaction which is reflected in the increase in D_{Pd} (cf. Fig. 6.2) with the increase in HCl concentration.

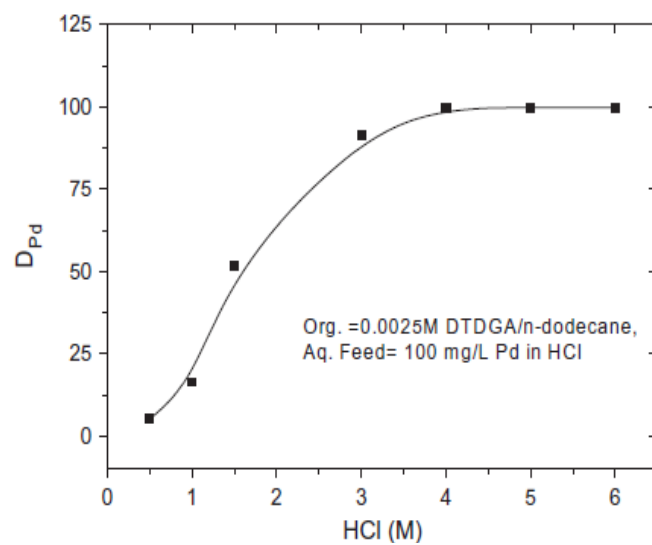


Fig.6.2 Extraction of palladium by DTDGA solvent with variation of feed acidity

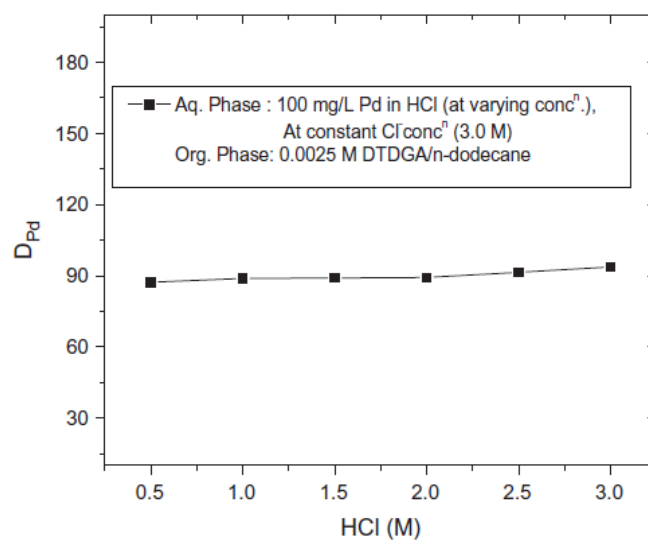


Fig.6.3 Variation of D_{Pd} at a fixed ionic strength of chloride ion

6.2.1.3. Effect of DTDGA Ligand Concentration

Since the extractability of Pd is very high with DTDGA, it is found to be difficult to determine the stoichiometry of Pd-DTDGA complex by using slope analysis method. Therefore, mole ratio plot method has been used to determine the stoichiometry. Fig. 6.4 shows the variation of concentration of palladium in the organic phase i.e. $[Pd]_{org}$. as a function of $[DTDGA]/[Pd]_{aq}$. From the figure it is evident that the concentration of palladium in the organic phase remains constant after $[DTDGA]/[Pd]_{aq} = 1$. This indicates the stoichiometry of DTDGA: Pd = 1.

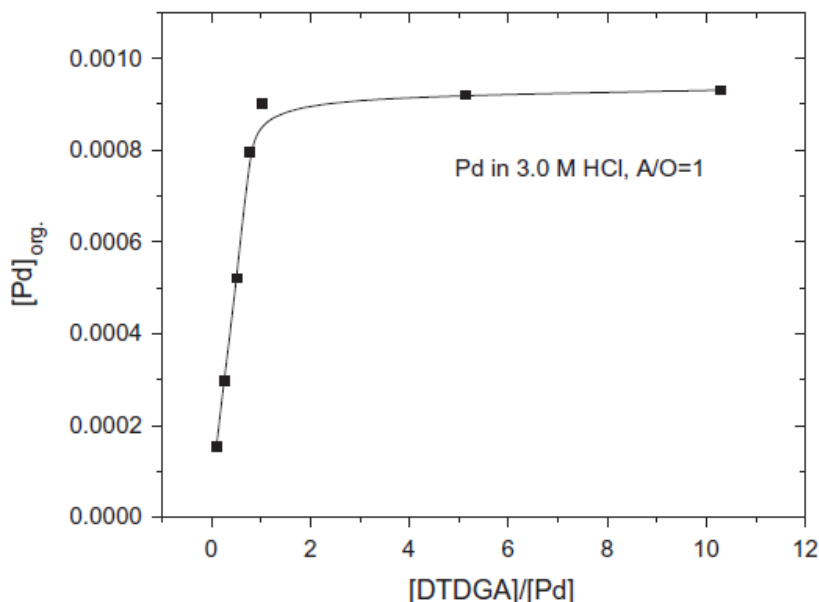
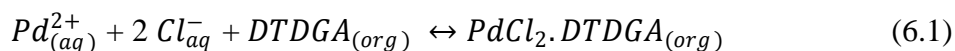


Fig.6.4 Mole ratio plot: variation of concentration of palladium in the organic phase with the change in $[DTDGA]/[Pd]_{aq}$

6.2.1.4 Effect of Diluents

The extraction behaviour of 10^{-3} M palladium in 3.0 M HCl with 0.0025 M DTDGA ligand dissolved in various diluents, namely, n-dodecane, toluene, isodecyl alcohol and CCl_4 has been investigated. Table 6.1 shows the variation of D_{Pd} in presence of different diluents. It is observed that as the polarity of the diluent

increases, the extractability of Pd decreases. Maximum extraction of palladium is obtained in the non-polar diluent, namely, n-dodecane. This could be attributed to the fact that palladium is extracted into the organic phase in the form of neutral molecule i.e. PdCl₂ and therefore, the non-polar diluents (e.g. n-dodecane) tend to facilitate the extraction.

Table 6.1 Effect of diluents on the extraction of palladium

Sr. No.	Diluent	D _{Pd}
1	n-Dodecane	109.1
2	Isodecyl alcohol	6.5
3	Toluene	2.7
4	CCl ₄	8.6

6.2.1.5 Back Extraction of Palladium from Loaded DTDGA

Back extraction of Pd from the loaded organic has been carried out using various reagents, namely, de-ionised water (at pH 7), ammonia solution (4%, v/v), 0.025 M EDTA solution and 0.01 M thiourea in 0.1 M HCl. The organic phase obtained after equilibrating 0.0025M DTDGA ligand (dissolved in n-dodecane) with the aqueous phase containing 10⁻³ M palladium dissolved in 3.0 M HCl, has been contacted with the above stripping solutions. Table 6.2 shows the percentage back extraction of palladium in a single contact. It is evident that with deionized (DI) water and 0.025 M EDTA solution, very less back extraction is achieved. With ammonia solution (4%, v/v), about 47% back extraction is achieved in a single stage with slight turbidity in the aqueous phase. Palladium is found to be quantitatively recovered using a solution of 0.01 M thiourea in 0.1 M hydrochloric acid.

Table 6.2 Back extraction studies

Sr. No.	Stripping solution	Recovery (%)
1	Water, pH ~ 7	6.3
2	Ammonia solution (4%, v/v) ^a	46.5
3	0.025 M EDTA solution	1.8
4	0.01 M Thiourea in 0.1 M HCl	98.8

^a slight turbidity observed in aqueous phase

6.2.1.6 Extraction Behavior of DTDGA from SSCD Solution

DTDGA/n-dodecane solvent system has been tested for the separation of palladium from spent catalyst dissolver solution, SSCD. Fig. 6.5 shows the distribution ratio of the elements present in SSCD at 3.0 M hydrochloric acid concentration by equilibrating it with 0.0025 M DTDGA/n-dodecane. Very high extractability of palladium with almost negligible extraction of other elements has been observed. Thus, a very high separation factor is obtained for palladium over other elements present in SSCD solution. Therefore, 0.0025 M DTDGA/n-dodecane can be used to selectively separate palladium from SSCD solution.

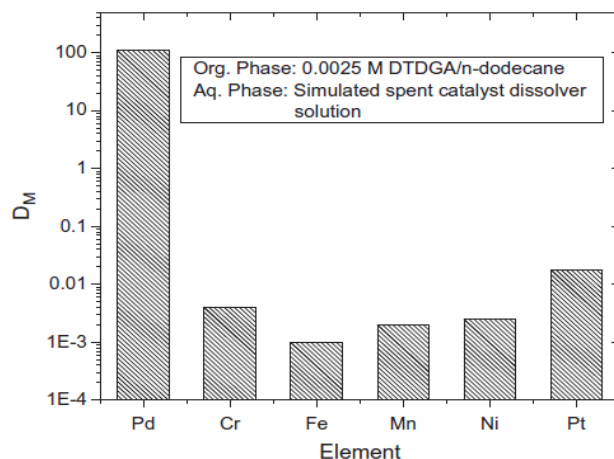


Fig.6.5 Distribution ratio of elements present in SSCD solution

6.2.2. Membrane Studies with DTDGA Ligand

Membrane separation studies for palladium from nitric acid medium using DTDGA ligand have been executed. Results of the experiments carried out to establish the extraction parameters have been discussed below.

6.2.2.1. Effect of Feed Nitric Acid Concentration

To understand the role of feed acidity (i.e. the concentration of nitric acid in the feed solution) in the transport rate of palladium using 0.025M DTDGA as carrier in membrane technique, nitric acid concentration in the feed solution has been varied from 1M to 6M. As evident from Fig.6.6, near quantitative transport of Pd (> 99%) in

120 min time interval in all these cases has been observed. The reason behind initial increase in transport rate from 1M HNO₃ to 2M HNO₃ is due to increase in nitrate ion assisted complexation of Pd with DTDGA at the feed-membrane interface as explained in Eq.6.2. Now with further increase in acidity the effect of acid transport from feed solution to the receiving phase became significant. After 120 min of operation, the acidity of 3M HNO₃ decreased to 2.9M whereas the acidity of 6M HNO₃ became 5.7M. Increasing acid transport caused a decrease in free DTDGA concentration in the membrane phase due to the formation of DTDGA.HNO₃ complex. This effect caused a decrease in transport of Pd at higher acidities which offset the effect of increasing nitrate concentration in the feed. These two effects balance each other out to make the transport rate nearly constant at higher acidities from 3M HNO₃. Permeability co-efficient values for Pd at different nitric acid concentrations are given in Table 6.3. So DTDGA as a carrier molecule is very efficient for transport of Pd with a very low ligand inventory.

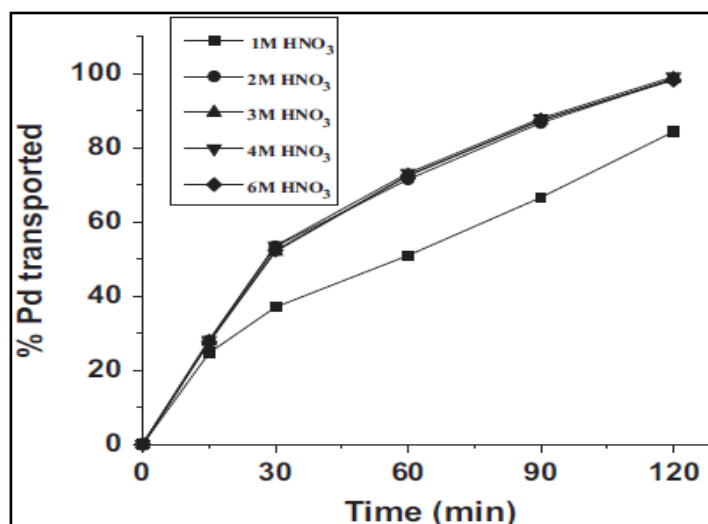


Fig.6.6 Effect of nitric acid concentration in feed solution

6.2.2.2 Effect of DTDGA Concentration

One of the major advantages of SLM technique that uses very low ligand inventory. Earlier we mentioned that a very low concentration of DTDGA (0.025M in n-dodecane) is sufficient to achieve quantitative transport of Pd. In order to optimize the DTDGA concentration, we have varied DTDGA concentration in the SLM method. During these studies, feed acidity has been maintained at 4.0M HNO₃ and stripping agent has been kept as 0.01M thiourea in 0.2 M HNO₃. The results are shown in Fig.6.6. Permeability coefficient values of Pd has also been shown in Table 6.3 for different concentrations of DTDGA. From Fig.6.7 it is evident that 0.025M DTDGA in n-dodecane is the optimized concentration of DTDGA for quantitative transport of Pd. The reason behind the increase in transport rate with increasing DTDGA concentration from 0.005M to 0.025M is increasing D_{Pd} which results in increase of Pd-DTDGA concentration in the feed-membrane interface. This causes an increase in membrane transport rate. Now, with further increase in DTDGA concentration from 0.025M to 0.05M, viscosity of the membrane phase also increases. As the transport of metal ion across a SLM is governed by Stokes-Einstein equation (being diffusion controlled):

$$D_0 = \kappa T / 6\pi R \eta \quad (6.3)$$

where D_0 is the diffusion-coefficient, κ is the Boltzmann constant, T is the absolute temperature (K), R is the ionic radius (Å) of metal ion and η is the viscosity of the organic phase. As evident from Eq. 6.3, D is inversely proportional to the viscosity of the organic phase, η . Therefore, with increasing DTDGA concentration from 0.025M to 0.05M the membrane transport is slowed down. So, 0.025M DTDGA can be chosen as the optimum concentration in the membrane phase during further studies.

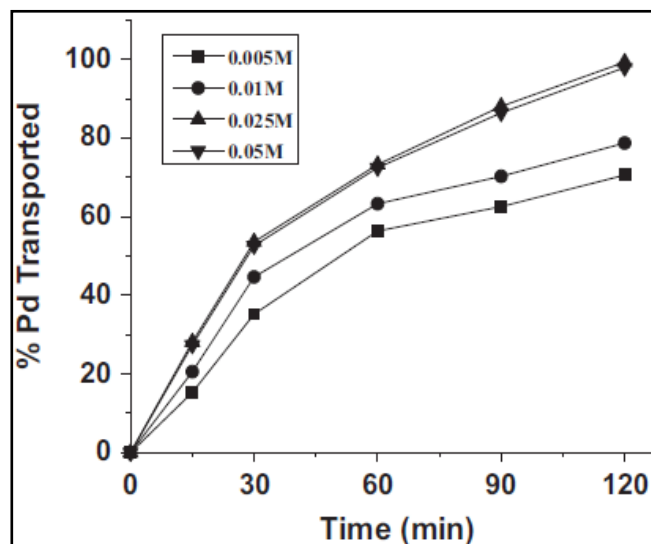


Fig.6.7 Effect of DTDGA concentration on the transport of palladium through membrane

6.2.2.3 Effect of Membrane Pore Size

During transport of metal ions across the organic phase in SLM system, various membrane parameters like membrane pore size, membrane tortuosity, pore structure, membrane thickness etc. have been varied to study their influences in the palladium transport rate. While studying metal ion transport across different membranes of different pore sizes, there are reports of different trends for different metal-carrier combination which are mainly govern by two opposing factors: i) increase in transport rate with increasing membrane pore size causes due to less resistance faced by diffusing metal-carrier complex, ii) the decrease with increasing membrane pore size is given by Laplace's equation:

$$F = (2\gamma/r)\cos\theta \quad (6.4)$$

where γ is the solvent-water interfacial tension, θ is the contact angle, r is the pore size and F is the trans-membrane pressure required to displace the carrier molecule from the membrane pores. Thus with increasing membrane pore size, it becomes easier to displace the carrier molecule from the membrane pores making the

membrane unstable against carrier leaching. This causes a decrease in transport rate with increasing membrane pore size.

To understand which of these factors will predominate in palladium-DTDGA system, the membrane pore sizes have been varied (0.2 mm, 0.45 mm, 1.2 mm, 5.0 mm) and studied the transport rates of palladium. During these studies, feed acidity has been kept as 4M HNO₃ and the organic phase has been kept as 0.025M DTDGA in n-dodecane. We have plotted the observed P values for four different membrane pore sizes in Fig.6.8. It is clearly understood from the figure that in the Pd-DTDGA system, the destabilizing effect of increasing membrane pore size is dominant resulting in continuous decrease in permeability co-efficient values as well as transport rates.

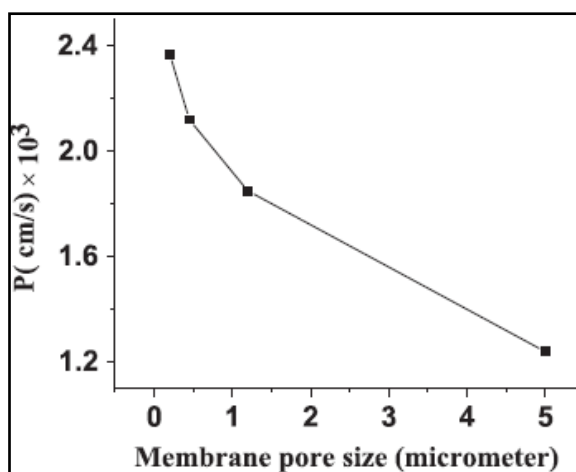


Fig.6.8 Effect of membrane pore size on the transport of palladium through the membrane

6.2.2.4. Membrane Thickness

Transport of metal ion across a SLM being diffusion controlled, the flux of the metal ion across the organic phase is dependent on the thickness of the membrane used Q which can be expressed by the following equation

$$P = D_{Pd} D_0 / d_0 \tau \quad (6.4)$$

where P is the permeability co-efficient, D_{Pd} is the distribution ratio of palladium, D_0 is the diffusion co-efficient, d_0 is the membrane thickness, τ is the tortuosity factor of the membrane. With increasing membrane thickness diffusional resistance of the membrane increases linearly resulting in decreased metal ion transport rate. To evaluate the diffusion co-efficient of Pd-DTDGA complex, membrane thickness has been varied. In this study, 4M HNO_3 as the feed acidity, 0.025M DTDGA in n-dodecane as the organic phase, PTFE membranes (having 0.2 mm pore size) as membrane support of variable thickness (prepared by laminating required number of membranes) have been considered. A stirring speed of 500 rpm has been maintained during these experiments to reduce the aqueous diffusion film thickness to the minimum value [25]. The permeability coefficient values with variation of DTDGA concentration along with the variation of feed acidity have been tabulated in Table 6.3.

Table 6.3 Permeability co-efficient (P) values for Pd(II) using DTDGA /n-dodecane organic phase

[HNO_3] (M)	$P \times 10^3$ (cm/s) ^a	[DTDGA] (M)	$P \times 10^3$ (cm/s) ^b
1	1.28	0.005	0.87
2	2.34	0.01	1.68
3	2.35	0.025	2.37
4	2.37	0.05	2.33
6	2.35	-	-

^a [DTDGA] = 0.025M ^b [HNO_3] = 4M

The effect of the thickness of membrane on the transport of palladium has been given in Fig.6.9. As evident from Fig.6.9, the transport rate for Pd(II) decreases with increase in membrane thickness (~99% in 120 min for 65 mm thicknesses to ~76%

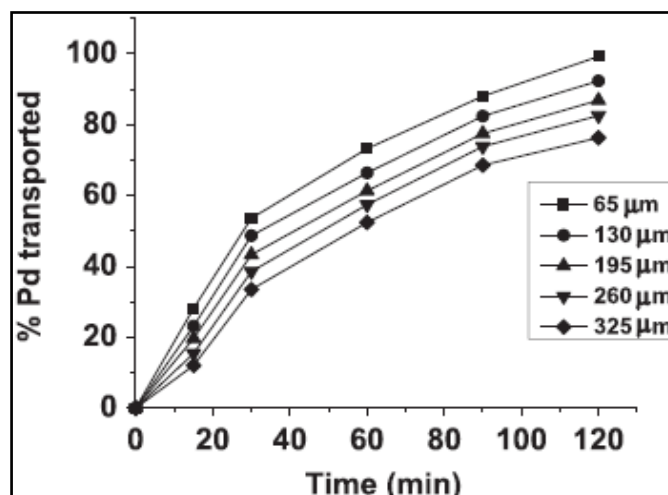


Fig.6.9 Effect of membrane thickness on the transport of palladium through the membrane

during same time interval for 325 mm thicknesses). Diffusion coefficient value has been calculated in a similar way using the plot of P vs. (1/ membrane thickness) from Eq. 6.4 and the value for Pd-DTDGA system was found to be $3.52 \times 10^{-5} \text{ cm}^2/\text{s}$.

6.2.2.5. Selectivity over other Fission Products

To investigate the selectivity of Pd(II) over other fission products by SLM technique, the transport study of Pd(II) has been carried out from a diluted HLW solution at 4M HNO_3 . Dilution of HLW has been carried out in nitric acid medium. From Fig.6.10 it is evident that none of the elements present in HLW has been transported to a significant level in the strip phase which indicates the excellent decontamination factor (DF) of the elements with respect to Pd (II) over 120 min of operation. The Pd (II) transport is observed to be ~99% during this time interval. Therefore, DTDGA provides an excellent possibility to separate Pd (II) from HLW with excellent DF over other fission products using SLM technique.

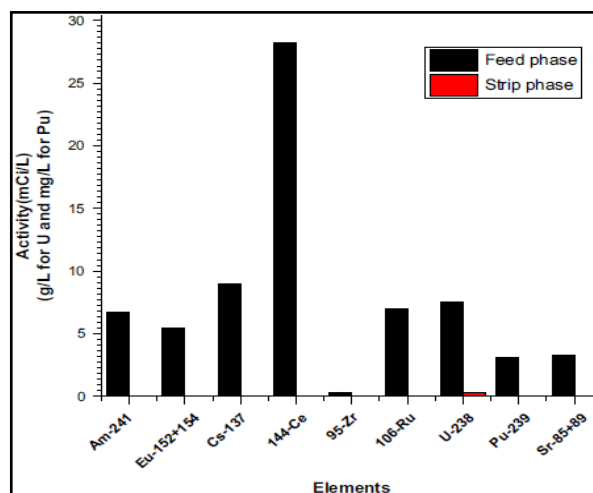


Fig.6.10 Transport behaviour of different elements using DTDGA carrier

6.2.2.6. Stability of Membrane

Instability of SLM with respect to carrier leaching is the major drawback which prohibits the large scale process application of this technique [26]. The reason behind the leaching out of the carrier can be aqueous solubility of the carrier, osmotic or hydro-static pressure gradient etc. The nature of the diluents also plays a very important role in the stability of SLM [27]. It is reported that diluents such as nitrobenzene and chloroform have shown poor stability whereas n-dodecane as diluent has given stable membrane over a period of 20 days using TODGA as carrier [28]. In case studies with n-dodecane diluent, the stability of the membrane in the SLM studies with DTDGA/n-dodecane as the organic carrier, transport experiments have been carried out for six consecutive cycles in which fresh solutions of feed and receiver phase have been added for each experiment. 0.025 M DTDGA in n-dodecane has been used as the organic phase (i.e. the carrier phase) and 4M HNO₃ as the feed acidity in the current study. Fig.6.11 clearly indicates the stability of the SLM containing DTDGA in n-dodecane as the carrier for six consecutive cycles of operation. Even after using the SLM for six cycles, ~97% transport of Pd is observed

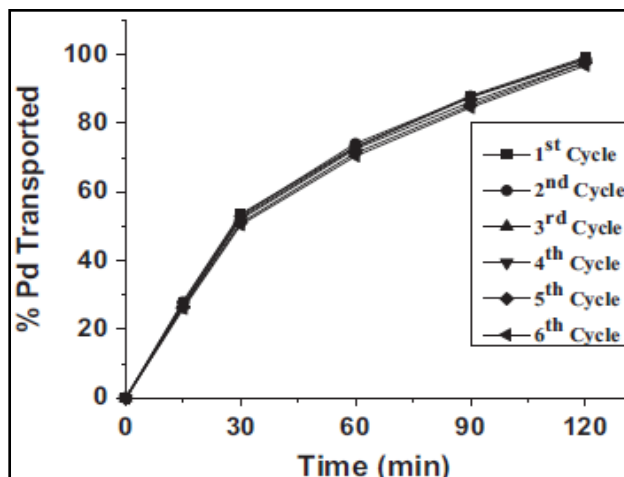


Fig.6.11 Stability of membrane for Pd (II) transport using DTDGA ligand in 120 min which is ~99% in the same time interval as observed in the first cycle of operation. This study provides us an option of long term reusability of SLM containing DTDGA as the ligand for palladium extraction from acidic medium.

6.3. Conclusion

DTDGA has proved to be a potential ligand for complexing with palladium both in hydrochloric acid medium and in nitric acid medium. In both the cases, it forms 1:1 complex with Pd(II) where the anions balance their charges forming neutral complexes during extraction. Solvent extraction technique has been tested for the separation of palladium from spent catalyst and membrane technique has been tested for the separation of palladium from high level waste. Both these techniques have given satisfactory separation of palladium over other metal ions present in the solutions. >99% back-extraction of palladium from the loaded DTDGA has been obtained in a single stage using 0.01M thiourea as the complexing agent. Therefore, complete separation and recovery of palladium is possible using DTDGA ligand.

References

1. Physical and chemical properties of bimetallic surfaces, J. A. Rodriduez, Surf.Sci. Rep., 1996, 24, 223-287.

2. Platinum Today, A. Cowley, M. Steel, Johnson Matthey Reports, London, 2007.
3. Encyclopedia of Electrochemistry, A. J. Bard, M. Stratmann, E. Gileadi, M. Urbakh, Thermodynamics and Electrified Interfaces, volume 1, Wiley-VCH, Weinheim, 2002.
4. N,N,N',N'-tetra-(2-ethylhexyl) thiodiglycolamide (T(2EH)TDGA): A novel ligand for the extraction of palladium from high level liquid waste (HLLW), R. Ruhela, J. N. Sharma, B. S. Tomar, S. Panja, S. C. Tripathi, R. C. Hubli, A. K. Suri, *Radiochim. Acta*, 2010, 98, 209-214.
5. Dithiodiglycolamide: novel ligand with highest selectivity and extractability for palladium, R. Ruhela, J. N. Sharma, B. S. Tomar, M. S. Murali, R. C. Hubli, A. K. Suri, *Tetrahedron Lett.*, 2011, 52, 3929-3932.
6. Recovery of platinum and palladium from deactivated catalysts, O. G. Gromov, G. N. Kunshina, A. P. Kuz'min, E. B. Seitenova, E. P. Lokshin, V. T. Kalinnikov, *Russ. J. Appl. Chem.*, 1999, 72, 1865-1868.
7. Recovery and separation of palladium from spent catalyst, M. A. Barakat, M. H. H. Mahmoud, Y. S. Mahrous, *Appl. Catal. A: Gen.*, 2006, 301, 182-186.
8. Hydrometallurgical recovery of nano-palladium from spent catalyst, M. A. Barakat, G. A. EL-Mahdy, M. Hegazy, F. Zahran, *Open Miner. Process. J.*, 2009, 2, 31-36.
9. Solvent extraction in hydrometallurgy, J. Rydberg, M. Cox, C. Musikas, G. R. Choppin, Springer, NY, 2004, 455-505.
10. Recovery palladium, gold and platinum from hydrochloric acid solution using 2-hydroxy-4-sec-octanoyl diphenyl-ketoxime, Y. F. Shen, W. Y. Xue, *Sep. Purif. Technol.*, 2007, 56, 278-283.
11. Solvent extraction of platinum-group metals from hydrochloric acid solutions by dialkyl sulphoxides, J. S. Preston, A. C. du Preez, *Solvent Extr. Ion Exch.*, 2002, 20, 359-374.
12. New 8-hydroxyquinoline derivative extractants for platinum group metals separation. Part 2. Pd(II) extraction equilibria and stripping, B. Cote, G. P. Demopoulos, *Solvent Extr. Ion Exch.*, 1994, 12, 393-421.

13. Phase-transfer catalysts in extraction kinetics: palladium extraction by dioctyl sulfide and KELEX 100, S. J. Al-Bazi, H. Freiser, *Inorg. Chem.*, 1989, 28, 417-420.
14. Association behavior of 4-acylpyrazolone derivative and tertiary amine of high molecular weight in antagonistic synergistic extraction of palladium, A. Zhang, G. Wanyan, M. Kumagai, *J. Solution Chem.*, 2004, 33, 1017-1028.
15. New pyridinecarboxamides for rapid extraction of palladium from acidic chloride media, I. Szczepanska, A. B. Resterna, M. Wisniewski, *Hydrometallurgy*, 2003, 68, 159-170.
16. Extraction of palladium(II) from chloride solutions with Cyphos_IL-101/toluene mixtures as novel extractant, A. Cieszynska, M. Wisniewski, *Sep. Purif. Technol.*, 2010, 73, 202-207.
17. Extraction of platinum and palladium with bis-(2,4,4-trimethyl pentyl)-phosphinodithioic acid, K. Saito, H. Freiser, *Anal. Sci.*, 1989, 5, 583-586.
18. Study of extraction of palladium from nitric acid solutions with nitrogen containing compounds, as applied to recovery to fission palladium from spent nuclear fuel of nuclear power plants-extraction and back washing conditions, E. A. Mezhov, V. A. Kuchmunov, V. V. Druzhenkov, *Radiochemistry*, 2002, 44, 135.
19. Study of extraction of palladium from nitric acid solutions with nitrogen containing compounds, as applied to recovery to fission palladium from spent nuclear fuel of nuclear power plants, Optimization of extraction process for palladium recovery and refining, E. A. Mezhov, V. A. Kuchmunov, V. V. Druzhenkov, *Radiochemistry*, 2002, 44, 146.
20. Separation of palladium from HLLW of PUREX origin by solvent extraction and precipi-tation methods using oximes, A. Dakshinamoorthy, P. S. Dharni, P. W. Naik, N. L. Dudwadkar, S. K. Munshi, P. K. Dey, V. Venugopal, *Desalination*, 2008, 232, 26.
21. Extraction of fission palladium (II) from nitric acid by benzoyl methylene triph-enyl phosphorane(BMTTP), M. Mohan Raj, A. Dharmaraja, K. Panchanatheswaran, K. A. Venkatesan, T. G. Srinivasan, V. Rao, *Hydrometallurgy*, 2006, 84, 118.
22. Palladium extraction with N,N,N',N'-tetra-noctyl-thiodiglycolamide, H. Narita, M. Tanaka, K. Morisaku, *Miner. Eng.*, 2008, 21, 483-488.

23. Rapid separation of palladium (II) from platinum(IV) in hydrochloric acid solution with thiodiglycolamide, H. Narita, M. Tanaka, K. Morisaku, T. Abe, *Chem. Lett.*, 2004, 33, 1144-1145.
24. Investigation of the extraction complexes of palladium(II) with novel thiodiglycolamide and dithio-diglycolamide ligands by EXAFS and computational methods, R. Ruhela, B. S. Tomar, A. K. Singh, R. C. Hubli, A. K. Suri, *Dalton Trans.*, 2013, 42, 7085-7091.
25. Facilitated transport of americium(III) from nitric acid media using dimethyldibutyltetradecyl-1,3-malonamide, S. Sriram, P. K. Mohapatra, A. K. Pandey, V. K. Manchanda, L. P. Badheka, *Journal of Membrane Science*, 2000, 177, 163.
26. Stability of supported liquid membranes: state of the art, A. J. B. Kemperman, D. Bargeman, T. V. D. Boomgaard, H. Strathmann, *Separation Science and Technology*, 1996, 31, 2733-2762.
27. Uranium pertraction across a PTFE flat sheet membrane containing Aliquat 336 as the carrier, P. K. Mohapatra, D. S. Lakshmi, D. Mohan, V. K. Manchanda, *Separation Science and Technology*, 2006, 51, 24-30.
28. Studies on uranium (VI) pertraction across a N,N,N',N'-tetraoctyldiglycolamide (TODGA) supported liquid membrane, S. Panja, P. K. Mohapatra, S. C. Tripathi, V. K. Manchanda, *Journal of Membrane Science*, 2009, 337, 274-281.

Separation of Lead, Zinc, Copper, Chromium from Aqueous Medium

7.1. Introduction

Heavy metals like lead, zinc, copper, chromium are present in different industrial wastes and process streams. These metals are highly hazardous to health causing organ failure as well as disorder to human body. Removal and re-use of these heavy metals from aqueous streams is beneficial to our society. Various methods for the removal of heavy metals from waste waters have been the subject of researches [1-4]. Precipitation [5-7], sorption, ion-exchange, reverse osmosis, membrane filtration [8-9], electrodeposition [10], cloud point extraction [11] and solvent extraction [12-15] are the common techniques for their separation and removal from aqueous streams. Many of these processes are not adoptable at large scale due to their high cost, low efficiency, disposal of huge amount of sludge etc. [16]. Precipitation is an easy technique but it produces a large amount of precipitated sludge which requires further treatment creating a secondary problem [17]. The cost of chemicals used for precipitation makes this process uneconomical. Compared to the high cost of the other techniques, solid phase extraction (SPE) e.g. sorption method is a low-cost method and also very simple to operate [18-22]. Sorbents in the SPE method should have the following criteria like: high surface area, good sorption properties including porosity, durability, and uniform pore distribution. In this regard, a number of sorbents for SPE method has been reported like amberlite XAD resins [19], [23], chitosan [24], diaion HP-2MG [25], benzophenone/naphthalene [26], chelex 100 [27], silica etc. The unique property of silica gel as a support material i.e. it does not shrink or swell in the

aqueous environment has made it a preferable structural material. Research on sorbents based on silica gel support has been reported [28-31]. However, the need of better sorbents still persists. In this chapter, the sorption and removal of heavy metals like lead, zinc, copper and chromium using functionalised silica gels like i) butanol functionalised silica gel (BFSG) and ii) amidopyridyl amine functionalised silica gel (APAFSG) have been discussed. These results have been compared with the sorption behaviour using alkali treated silica gel (ASG).

7.2. Results and Discussion

Synthesis and characterisation of BPFSG and AAPPFSG have been provided in chapter 2.

7.2.1. Sorption Extraction of Lead, Zinc, Copper and Chromium

Solutions containing Pb(II), Cu(II), Zn(II) and Cr(VI) metal ions, as obtained by dissolving lead nitrate, copper sulphate, zinc chloride and potassium dichromate in water respectively, have been equilibrated with a fixed measured quantity of alkali treated silica gel (ASG), butanol functionalised silica gel (BFSG) and amidopyridyl amine functionalised silica gel (APAFSG) separately (as described in chapter 2, section 2.3.0). Percentage extraction by sorption for these metal ions has been calculated using equation 2.3. The metal ion extraction ability by different ligand is very different and percentage extraction of metal ions by APAFSG, BFSG and ASG has been given in Fig. 7.1. This is due to the role of the donor atoms present in the sorbents and also the metal species present in the solution. ASG and BFSG act as oxygen donor ligands at the experimental pH 7. But there are two types of donor atoms e.g. nitrogen donor atom (amine group) and oxygen donor atom (amide group) which are present in APAFSG ligand. Therefore, APAFSG shows a high uptake of Pb(II). Extraction of Cu(II) is also reasonable (~27%) by APAFSG (Fig.7.1). Similar trend of sorption for Pb(II) and Cu(II) has been reported by N-donor ligand (amine group) by Aguado et al. as given in

Fig.7.2 [32]. The oxide ion present in ASG uptakes Pb(II), Cu(II) and Zn(II) more compared to Cr(VI) which is present as $\text{Cr}_2\text{O}_7^{2-}$ ion in the solution.

It is observed that uptake of Pb(II) and Cu(II) is more by N-donor ligands while, the uptake of Zn(II) is more by O-donor ligand. Uptake of Cr(VI) as $\text{Cr}_2\text{O}_7^{2-}$ ion has only been reported by ligands which act as cation exchangers. [33-35].

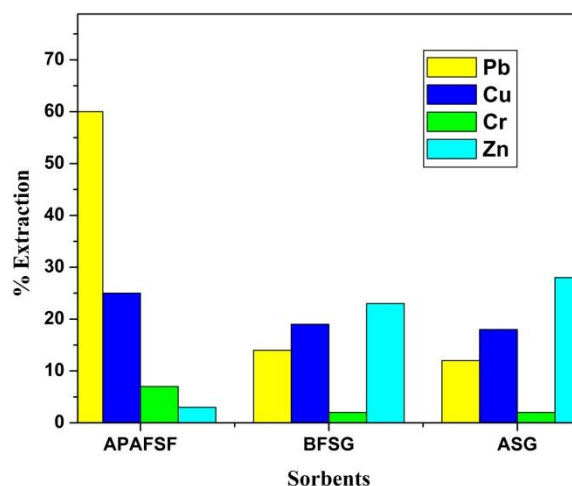


Fig.7.1 Percentage sorption of Pb(II), Cu(II), Cr(VI) and Zn(II) on APAFSG, BFGS and ASG

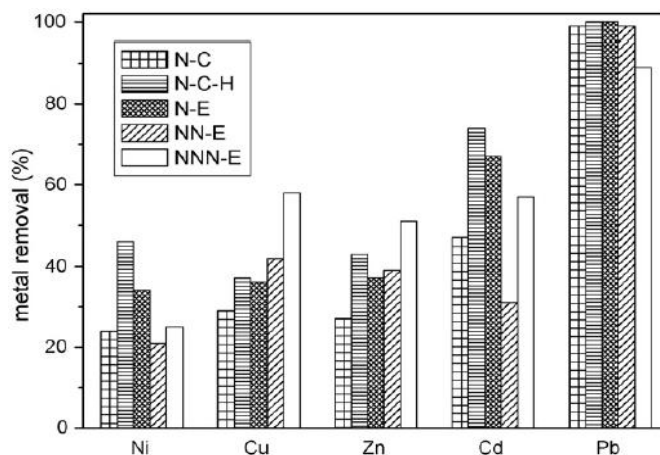
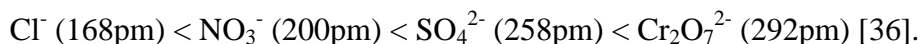


Fig.7.2 Percentage sorption of Pb(II), Cu(II), Cr and Zn(II) on amine functionalised sorbent

Moreover, APAFSG, since this ligand is a neutral ligand and therefore, extracts the metal ions in their neutral form. Therefore, the complexation reactions of the metal ions with APAFSG take place as their neutral complex where the anions balance the charges of these metal ions. Therefore, the counter ions of Pb(II), Cu(II),

Zn(II) i.e., nitrate, sulphate and chloride ions respectively present in the solutions play a dominant role in the complexation reactions with APAFSG. Therefore, the size of these anions and also the bulkiness around the binding sites in APAFSG ligand play a major role in the complexation reactions of Pb(II), Cu(II), Zn(II) and Cr(VI) (Fig.7.1). The reported ionic radius values increase in the order



and the order of complexation as observed is as (Fig.7.1) Pb(II) > Cu(II) > Cr(VI) > Zn(II). The bulky sulphate ion (ionic radius 258 pm, attached to the metal ion through the oxygen atom) which is attached to the copper ion (for the charge neutralisation) may pose some steric effect in the sorption of Cu(II) compared to the smaller nitrate ion (ionic radius 179 pm, attached to the metal ion through the oxygen atom) which is attached to Pb(II). The decrease in sorption of Zn(II) may be due to the bulky chloride ions (ionic radius 167 pm) which are directly attached to Zn(II) ion to neutralise its charges.

7.2.2. Loading Capacities

The loading capacities of Pb(II), Cu(II), Zn(II) and Cr(VI) on APAFSG, BFSG and ASG sorbents have been tabulated below. The reported loading capacities of Pb(II), Cu(II) and Cr(VI) on different sorbents have also been tabulated in Table 7.1.

Table 7.1 Loading capacities of Pb(II), Cu(II), Zn(II) and Cr(VI)

Ligand	Element	Loading Capacity mg/g	Reference (Nitrogen donor)	Reference (Oxygen donor)
N-donor				
APAFSG	Pb(II)	50		
	Cu(II)	25	30 [32]	
	Cr(VI)	7	10 [32]	
	Zn(II)	3		
O-donor				
BFSG	Pb(II)	14		12 [37]

	Cu(II)	19		15 [37]
	Cr(VI)	2		
	Zn(II)	23		
ASG	Pb(II)	12		
	Cu(II)	18		
	Cr(VI)	2		
	Zn(II)	28		

7.2.3. Comparison of Extraction of Metal Ions with other Sorbents

Different sorbents have been reported till now for the extraction and removal of these heavy metals from aqueous streams. Some of them have been enlisted below (Table 7.2).

Table 7.2 Sorption of Pb(II), Cu(II), Zn(II) and Cr(VI) by different sorbents

Material (Inorganic and Biomaterial)	Element	Loading Capacity (mg/g)	Reference
Chitosans			
Chitosan	Pb(II)	16	38
	Cu(II)	222	39
	Cr(VI)	273	40
	Cu(II)	17	38
	Cu(II)	4.7	41
	Cu(II)	13	42
Non cross-linked chitosan	Cr(VI)	80	43
	Cu(II)	85	43
Cross-linked chitosan	Cr(VI)	50	43
	Cu(II)	86	43
Crosslinked chitosan with glutaraldehyde	Cu(II)	60	44
Crosslinked chitosan with epichlorohydrin	Cu(II)	62	44
Crosslinked chitosan with ethylene glycol diglycidyl ether	Cu(II)	46	44
Zeolites			
Clinoptilolite	Cu(II)	1.64	45
	Pb(II)	1.6	45
	Cu(II)	3.8	46
	Pb(II)	6	46
	Pb(II)	1.4	47
	Pb(II)	62	48
Chabazite	Pb(II)	175	48
Chabazite–phillipsite	Cu(II)	5.1	48
	Pb(II)	6	48

	Zn(II)	0.04	49
	Cu(II)	0.37	49
Clay			
Kaolinite	Pb(II)	0.12	50
	Pb(II)	1.41	51
Illite	Pb(II)	4.29	51
Bentonite	Zn(II)	4.54	52
Peat	Zn(II)	11.12	53
	Cu(II)	12.07	53
Fly Ash	Cu(II)	1.39	54
Aluminium oxide	Cr(VI)	11.7	55
	Pb(II)	33	56
	Pb(II)	230	56
Industrial waste			
Lignin	Pb(II)	1865	57
	Zn(II)	95	57
Waste slurry	Pb(II)	1030	58
	Cr(VI)	640	58
Biomaterials			
Rice husk carbon	Cr(VI)	45.6	59
Triethylenetetramine treated sugarcane bagasse	Cu(II)	133	60
	Pb(II)	313	60
Carrot residues	Cu(II)	32.74	61
	Zn(II)	29.61	61

7.2.4. Thermodynamic Studies

Thermodynamic studies for the sorption of Pb(II), Cu(II), Cr(VI) and Zn(II) on APAFSG, BFSG and ASG have been carried out as described in chapter 2, section 2.2.2.7. $\ln D_M$ vs. $1/T$ has been plotted (D_M stands for the distribution ratio of the metal ion, T stands for temperature) for all the metal ions as shown in Fig.7.3. The enthalpy values have been tabulated in Table 7.3. Sorption of Pb(II), Cu(II) and Zn(II) on ASG takes place by oxide donor site and the sorption enthalpies are exothermic (Fig.7.3c). Sorption of Cr(VI) onto ASG is endothermic in nature which may be because of the coulombic repulsion faced by $Cr_2O_7^{2-}$ ion from the negative surface charge of ASG at pH 7. Similar observation is obtained in case of BFSG sorbent for $Cr_2O_7^{2-}$ ion (Fig.7.3b).

Sorption of Pb(II), Cu(II), Zn(II) and Cr(VI) on to APAFSG takes place via co-ordination complexes with the oxygen and nitrogen atoms present at the binding sites of APAFSG at pH 7. All the sorption reactions with APAFSG have been observed to be exothermic in nature (Fig.7.3a).

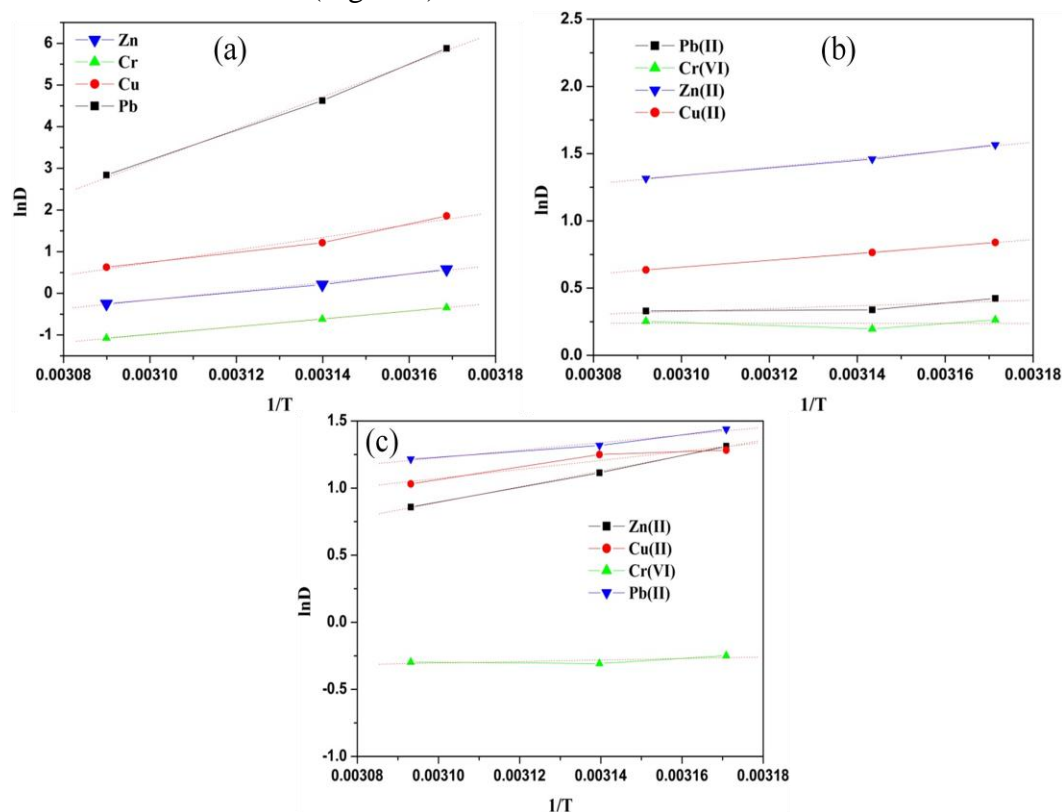


Fig.7.3 Thermodynamic studies of Pb(II), Cu(II), Cr(VI) and Zn(II) on (a) APAFSG, (b) BFGS and (c) ASG

Table 7.3 Enthalpy values of metal ligand complexes

Ligand	Metal ions	Enthalpy (ΔH) kcal/mol	Enthalpy of bare M^{2+} with triamine (ΔH) kcal/mol [Reference]
APAFSG	Pb(II)	-77	-8.2 [62]
	Cu(II)	-30	-13 [62]
	Zn(II)	-21.7	-7.3 [62]
	Cr(VI)	-20.6	
BPFSG	Pb(II)	-2	
	Cu(II)	-5	
	Zn(II)	-6.2	
	Cr(VI)	+0.06	
ASG	Pb(II)	-5.6	
	Cu(II)	-6.7	
	Zn(II)	-11.5	
	Cr(VI)	-0.11	

Theoretical studies on Cu(II) has been carried out by DFT method using with B3LYP/6-31G/LANL2DZ level of theory [63]. Kumar et. al. [63] has reported both square-pyramidal geometry and distorted octahedral geometry for Cu(II) complexes. Tetragonally distorted octahedral geometry, trigonal prismatic, trigonal bipyramidal, square-based pyramidal, tetrahedral geometries [64-67] and square planar geometry [68-69] are also reported for Cu(II) complexes. In this context, two possible geometries are possible for Cu(II) ion for binding with BFSG: i) two hydroxyl oxygen atoms can attach to Cu(II) providing tetrahedral geometry, ii) four hydroxyl oxygen atoms can attach to Cu(II) providing distorted octahedral geometry.

7.3. Conclusion

APAFSG ligand has shown a high sorption (about 60%) for Pb(II) from lead nitrate solution. Therefore, APAFSG can selectively extract and remove Pb(II) from its aqueous solution. Whereas, about 30% extraction of Cu(II) is observed using this ligand from copper sulphate solution. APAFSG acts as both N-donor and O-donor ligand. As it is a neutral ligand, it extracts Pb(II), Cu(II), Zn(II) and Cr(VI) as their neutral complexes at pH 7. Herein, the counter ions e.g. nitrate, sulphate and chloride ions balance the charges of the metal ions to form neutral metal species which form complexes with APAFSG. Therefore, the complexation reaction is also governed by the sizes of these anions which also play a major role.

BFSG and ASG on the other hand, act as O-donor ligands at pH 7. These ligands may get deprotonated at this pH and therefore, provides coulombic repulsion to Cr(VI) which is present as $\text{Cr}_2\text{O}_7^{2-}$ ion in the solution. Therefore, sorption of Cr(VI) is considerably less by these ligands.

References

1. Montmorillonite surface properties and sorption characteristics for heavy metal removal from aqueous solutions, C. O. Ijagbemi, M. H. Baek, D. S. Kim, *J. Hazard. Mater.*, 2009, 166, 538-546.
2. Adsorption of Zn (II) from aqueous solution by using different adsorbents, A. K. Bhattacharya, S. N. Mandal, S. K. Das, *Chem. Eng. J.*, 2006, 123, 43-51.
3. Mechanisms of heavymetal removal by activated sludge, F. Pagnanelli, S. Mainelli, L. Bornoroni, D. Dionisi, L. Toro, *Chemosphere*, 2009, 75, 1028-1034.
4. Characterization and properties of iron oxide-coated zeolite as adsorbent for removal of copper(II) from solution in fixed bed column, R. Han, L. Zou, X. Zhao, Y. Xu, F. Xu, Y. Li, Y. Wang, *Chem. Eng. J.*, 2009, 149, 123-131.
5. Preconcentrative separation of chromium (VI) species from chromium(III) by coprecipitation of its ethyl xanthate complex onto naphthalene, P. G. Krishna, J. M. Gladis, U. Rambabu, T. P. Rao, G. R. K. Naidu, *Talanta*, 2004, 63, 541-546.
6. Speciation of Cr (III) and Cr (VI) in aqueous samples by coprecipitation/slurry sampling fluorination assisted graphite furnace atomic absorption spectrometry, L. Wang, B. Hu, Z. Jiang, Z. Li, *Int. J. Environ. Anal. Chem.*, 2002, 82, 387-393.
7. Preconcentration of nickel and cobalt prior to their determination by graphite furnace atomic absorption spectrometry using the water-soluble polymer poly(vinylpyrrolidinone), N. Tokman, S. Akman, Y. Bakircioglu, *Microchim. Acta*, 2004, 146, 31-34.
8. Preconcentration-separation of heavy metal ions in environmental samples by membrane filtration-atomic absorption spectrometry combination, M. Soylak, I. Narin, U. Divrikli, S. Saracoglu, L. Elci, M. Dogan, *Anal. Lett.*, 2004, 37, 767-780.
9. Separation and preconcentration of cadmium ions in natural water using a liquid membrane system with 2-acetylpyridine benzoylhydrazone as carrier by flame atomic absorption spectrometry, M. D. G. Castro, M. D. G. Riaño, M. G. Vargas, *Spectrochim. Acta: Part B*, 2004, 59, 577-583.
10. Determination of europium (III) by graphite furnace atomic absorption spectrometry with preconcentration by 2-thenoyl trifluoroacetone phenanthroline modified electrode, H. B. He, W. J. Zhang, G. Z. Ma, H. X. Shen, *Chinese J. Anal. Chem.*, 2001, 29, 1125-1128.

11. Selective speciation of trace chromium through micellemediated preconcentration, coupled with micellar flow injection analysis-spectrofluorimetry, E. K. Paleologos, C. D. Stalikas, S. M. T. Karayanni, M. I. Karayannis, *Anal. Chim. Acta*, 2001, 436, 49-57.
12. Multivariate optimization of solvent extraction of Cd(II), Co(II), Cr(VI), Cu(II), Ni(II), Pb(II) and Zn(II) as dibenzyl dithiocarbamates and detection by AAS, M. Camino, M. G. Bagur, M. S. Vinas, D. Gazquez, R. Romero, *J. Anal. Atom. Spectrom.*, 2001, 16, 638-642.
13. Solvent extraction and HPLC determination of copper, iron, nickel and mercury in water and fishes as 2-pyrrolaldehyde-4-phenyl-3-thiosemi-carbazone as derivatizing reagent, M. Y. Khuhawar, S. N. Lanjwani, *J. Chem. Soc. Pakistan*, 2001, 23, 157-162.
14. Determination of iron in natural and mineral waters by flame atomic absorption spectrometry, S. Tautkus, L. Steponeniene, R. Kazlauskas, *J. Serb. Chem. Soc.*, 2004, 69, 393-402.
15. Extractive preconcentration and determination of nickel in water and wastewater samples by atomic absorption spectrometry, S. Tautkus, *Chem. Anal. (Warsaw)*, 2004, 49, 271-276.
16. Removal of Cd(II), Cr(VI), Fe(III) and Ni(II) from aqueous solutions by an *E. coli* biofilm supported on kaolin, C. Quintelas, Z. Rocha, B. Silva, B. Fonseca, H. Figueiredo, T. Tavares, *Chem. Eng. J.*, 2009, 149, 319-324.
17. Modified activated carbon for the removal of copper, zinc, chromium and cyanide from wastewater Lotfi Monser, Nafaa Adhoum, *Separation and Purification Technology*, 2002, 26, 137-146.
18. Determination of Cu, Ni and Pb in aqueous medium by FAAS after preconcentration on 2-aminothiazole modified silica gel, I. L. de Alcântara, P. S. Roldan, M. A. L. Margionte, G. R. Castroa, C. C. F. Padilha, A. O. Florentino, P. M. Padilha, *J. Braz. Chem. Soc.*, 2004, 15, 366-371.
19. Column preconcentration/separation and atomic absorption spectrometric determinationsof some heavy metals in table salt samples using Amberlite XAD-1180, M. Soylak, A. U. Karatepe, L. Elci, M. Dogan, *Turk. J. Chem.*, 2003, 27, 235-242.

20. Uptake of heavy metal ions by carbonaceous material obtained from industrial waste lignin using microwave irradiation, A. R. Chaudhari, L. P. Nagpurkar, J. D. Ekhe, *Asian J. Chem.*, 2003, 15, 917-924.
21. Preconcentration and separation procedures for the spectrochemical determination of platinum and palladium, B. G. Zylkiewicz, *Microchim. Acta*, 2004, 147, 189-210.
22. Preconcentration of trace and ultratrace amounts of platinum and palladium from real samples, T. P. Rao, S. Daniel, *Rev. Anal. Chem.*, 2003, 22, 167-189.
23. Column solid phase extraction of copper, iron and zinc ions at trace levels in environmental samples on Amberlite XAD-7 for their flame atomic absorption spectrometric determinations, M. Tuzen, M. Soylak, L. Elci, M. Dogan, *Anal. Lett.*, 2004, 37, 1185-1201.
24. Preparation and adsorption properties of modified chitosan, R. M. Wang, X. Xie, J. Q. Wang, S. J. Pan, Y. P. Wang, C. G. Xia, *Polym. Adv. Technol.*, 2004, 15, 52-54.
25. Column system using Diaion HP-2MG for determination of some metal ions by flame atomic absorption spectrometry, M. Tuzen, M. Soylak, *Anal. Chim. Acta*, 2004, 504, 325-334.
26. Preparation of 1-(2-pyridylazo)-2-naphthol functionalized benzophenone/naphthalene and their uses in solid phase extractive preconcentration/separation of uranium (VI), C. R. Preetha, T. P. Rao, *Radiochim. Acta*, 2003, 91, 247-251.
27. Solid phase extraction of Cu(II), Pb(II), Fe(III), Co(II) and Cr(III) on chelex 100 column prior to their flame atomic absorption spectrometric determinations, M. Soylak, *Anal. Lett.*, 2004, 37, 1203-1217.
28. Solid-phase extraction of ultratrace uranium(II) in natural waters using octadecyl silica membrane disks modified by tri-*n*-octylphosphine oxide and its spectrophotometric determination with dibenzoylmethane, M. Shamsipur, A. R. Ghiasvand, Y. Yamini, *Anal. Chem.*, 1999, 71, 4892-4895.
29. On-site preconcentration and trace metal ions determination in the Okavango Delta water system, Botswana, G. M. Sawula, *Talanta*, 2004, 64, 80-86.

30. Solid phase extraction and flame atomic absorption spectrometric determination of trace amounts of zinc and cobalt ions in water samples, Y. Yamini, M. H. Hosseini, A. Morsali, *Microchim. Acta*, 2004, 146, 67-72.
31. Silica gel coated with schiff's base: synthesis and application as an adsorbent for cadmium, copper, zinc, and nickel determination after preconcentration by flame atomic absorption spectrometry, F. Shemirani, A. A. Mirroshandel, M. S. Niasari, R. R. Kozani, *J. Anal. Chem.*, 2004, 59, 228-233.
32. Aqueous heavy metals removal by adsorption on amine-functionalized mesoporous silica, J. Aguado, J. M. Arsuaga, A. Arencibia, M. Lindo, V. Gascón, *Journal of Hazardous Materials*, 2009, 163, 213-221.
33. Selective capture of hexavalent chromium from an anion-exchange column of metal organic resin-alginate composite *Chem. Sci.*, 2016, 7, 2427.
34. The role of some compounds on extraction of chromium(VI) by amine extractants, *Journal of Hazardous Materials*, 2005, 117, 213-219.
35. Comparison of liquid-liquid extraction of Cr(VI) from acidic and alkaline solutions by two different amine extractants, N. E. El-Hefny, *Separation and Purification Technology*, 2009, 67, 44-49.
36. Thermochemical Radii of Complex Ions, H. K. Roobottom, H. Donald, B. Jenkins, J. Passmore, L. Glasser, *Journal of Chemical Education*, 1999, 76, 1570-1573.
37. Solid phase extraction of lead (II), copper (II), cadmium (II) and nickel (II) using gallic acid-modified silica gel prior to determination by flame atomic absorption spectrometry, F. Xie, X. Lin, X. Wu, Z. Xie, *Talanta*, 2008, 74, 836-843.
38. Adsorption of Cu(II) and Ni(II) by pelletized biopolymer, C. P. Huang, Y. C. Chung, M. R. Liou, *J. Hazard. Mater.*, 1996, 45, 265-277
39. Equilibrium Studies for the Sorption of Metal-Ions onto Chitosan, G. McKay, H. S. Blair, A. Findon, *Ind. J. Chem.*, 1989, 28A, 356-360.
40. Hexavalent chromium interaction with chitosan, P. Udaybhaskar, L. Iyengar, A. V. S. P. Rao, *J. Appl. Polym. Sci.*, 1990, 39, 739-747.
41. Comparison study of copper ion adsorption on chitosan, Dowex A-1, and Zerolit 225, W. S. W. Ngah, I. M. Isa, *J. Appl. Polym. Sci.*, 1998, 67, 1067-1070.

42. Proceedings of the Second Asia-Pacific Symposium, Asian Institute of Technology, A. P. Annachatre, N. N. Win, S. Chandkrachang, W. J. Stevens, M. S. Rao, S. Chandkrachang, Bangkok, Thailand, 1996, 169-173.
43. Adsorption of Cu(II) and Cr(VI) ions by chitosan: kinetics and equilibrium studies, R. Schmuhl, H. M. Krieg, K. Keizer, *Water S.A.*, 2001, 27, 1-7.
44. Removal of copper (II) ions from aqueous solution onto chitosan and cross-linked chitosan beads, W. S. W. Ngah, C. S. Endud, R. Mayanar, *Reactive Functional Polym. J.*, 2002, 50, 181-190.
45. Removal of heavy metals and other cations from waste water using Zeolites, M. J. Zamzow, B. R. Eichbaum, *Sep. Sci. Tech.*, 1990, 25, 1555-1569.
46. Performance of natural zeolites for the treatment of mixed metal-contaminated effluents, S. K. Ouki, M. Kavanagh, *Waste Manage. Res.*, 1997, 15, 383-394.
47. Lead and Cadmium Removal by Ion Exchange, E. Malliou, M. Malamis, P. O. Sakellarides, *Water Sci. Technol.*, 1992, 25, 133-138.
48. Effects of conditioning and treatment of chabazite and clinoptilolite prior to lead and cadmium removal, S. K. Ouki, C. R. Cheeseman, R. Perry, *Environ. Sci. Technol.*, 1993, 27, 1108-1116.
49. Use of natural chabazite-phillipsite tuff in wastewater treatment from electroplating factories in Jordan, K. M. Ibrahim, T. N. E. Deen, H. Khoury, *Environ. Geol.*, 2002, 41, 547-551.
50. Studies on the removal of some toxic metal ions. Part II (removal of lead and cadmium by montmorillonite and kaolinite), S. K. Srivastava, R. Tyagi, N. Pal, *Environ. Technol. Lett.*, 1989, 10, 275-282.
51. Adsorption of Lead Nitrate on Thai-Kaolin and Ball-clay, V. Chantawong, N. W. Harvey, V. N. Bashkin, *Asian J. Energy Environ.*, 2001, 1, 33-48.
52. Mixed adsorbent for Cu (II) removal from aqueous solutions, K. K. Panday, G. Prasad, V. N. Singh, *Environ. Technol. Lett.*, 1986, 7, 547-554.
53. Batch metal removal by peat. Kinetics and thermodynamics, T. Gosset, J. L. Trancart, D. R. Thevenot, *Water Res.*, 1986, 20, 21-26.
54. Removal of chromium from water by adsorption process, K. K. Panday, G. Prasad, V. N. Singh, *Water Res.*, 1985, 19, 869-873.
55. Aluminum oxide as adsorbent for removal of hexavalent chromium from aqueous waste, D. C. Gupta, U. C. Tiwari, *Ind. J. Environ. Health*, 1985, 27, 205-215.

56. Removal of lead and cadmium by hydrous iron and aluminium oxide, S. K. Srivastava, G. Bhattacharjee, R. Tyagi, N. Pant, N. Pal, *Environ. Technol. Lett.*, 1988, 9, 1173-1185.
57. Studies on the uptake of lead and zinc by lignin obtained from black liquor - A paper industry waste material, S. K. Srivastava, A. K. Singh, A. Sharma, *Environ. Technol.*, 1994, 15, 353-361.
58. Adsorption of heavy metal ions on carbonaceous material developed from the waste, S. K. Srivastava, R. Tyagi, N. Pant, *Water Res.*, 1989, 23, 1161-1165.
59. Studies on Chromium Removal by Rice Husk Carbon, K. Srinivasan, N. Balasubramanian, T. V. Ramakhrisna, *Indian J. Environ. Health*, 1988, 30, 376-387.
60. Adsorption of heavy metal ion from aqueous single metal solution by chemically modified sugarcane bagasse, O. K. Junior, L. V. A. Gurgel, J. C. P. de Melo, V. R. Botaro, T. M. S. Melo, R. P. de Freitas Gil, L. F. Gil, *Bioresour. Technol.*, 2006, 98, 1291-1297.
61. Comparison for biosorption modeling of heavy metals (Cr(III), Cu(II), Zn(II)) adsorption from wastewater by carrot residues, B. Nasernejad, T. E. Zadeh, B. B. Pour, M. E. Bygi, A. Zamani, *Process Biochem.*, 2005, 40, 1319-1322.
62. Equilibria of complex formation between several bivalent metal ions and macrocyclic tri- and penta-amines, M. Kodama, E. Kimura. *J. Chem. Soc., Dalton Trans.*, 1978, O, 1081-1085.
63. DFT studies of structural and some spectral parameters of copper(II) complexes with N,N,N',N''-tetrakis (2-hydroxyethyl/propyl) ethylene diamine and tris(2-hydroxyethyl)amine, R. Kumar, S. Obrai, J. Mitra, A. Sharma, *Spectrochimica Acta Part A: Molecular and Biomolecular Spectroscopy*, 2013, 115, 244-249.
64. M. Beretta, E. Bouwman, L. Casella, B. Douziech, W.L. Driessen, L.G. Soto, E. Monzani, J. Reedijk, *Inorg. Chim. Acta*, 2000, 310, 41-50.
65. Jahn–Teller distortions of six-coordinate CuII compounds: cis or trans?, J. Echeverria, E. Cremades, A. J. Amoroso, S. Alvarez, *Chem. Commun.*, 2009, 4242-4244.
66. Synthesis, crystal structure and DFT analysis of a phenoxo bridged Cu (II) complex and an azide and μ 3-O mixed bridged trinuclear Cu (II) complex, S. Ray, S. Konar, A. Jana, K. Das, R. J. Butcher, T. K. Mondal, S. K. Kar, *Polyhedron*, 2013, 50, 51-58.

67. Dimeric and polymeric square-pyramidal copper(II) complexes containing equatorial-apical chloride or acetate bridges, N. R. Sangeetha, S. Pal, *Polyhedron*, 2000, 19, 1593-1600
68. Spectro-electrochemical and DFT studies of a planar Cu(II)-phenolate complex active in the aerobic oxidation of primary alcohols, P. U. Maheswari, F. Hartl, M. Quesada, F. Buda, M. Lutz, A. L. Spek, P. Gamez, J. Reedijk, *Inorg. Chim. Acta.*, 2011, 374, 406-414.
69. Some New Cu(II) Complexes Containing an on Donor Schiff Base: Synthesis, Characterization and Antibacterial Activity, T. Rosu, E. Pahontu, C. Maxim, R. Georgescu, N. Stanica, A. Gulea, *Polyhedron*, 2011, 30, 154-162.

Abstract

Name of the Student: Amrita Das

Enrolment No.: CHEM01201104009

Thesis Title: Synthesis of novel ligands for extraction of metal ions from aqueous medium and theoretical investigation for the extraction mechanism

Extraction and separation of metal ions from various resources are important for their usage in different industries as well as safe disposal of the industrial metal bearing process streams into the environment. Therefore, attempt was to recover metal ions from various resources. The metal ions of importance in different industries like uranium, zirconium, rare earths, palladium, lead, copper, zinc etc. were targeted to recover from aqueous streams. In this context, new novel ligands like phosphate functionalized silica gels, amine and amido pyridyl phosphate functionalized silica gel, 1,8-dihydroxyanthraquinone functionalized silica gel etc. were synthesized, characterized and tested for the ability to extract, separate and recover the metal ions from different aqueous medium. Phosphate functionalized silica gels showed good extractability of uranium from aqueous nitric acid medium. Kinetics of the extraction was fast and equilibrium was attained within five minutes. All the phosphate functionalized silica gels have shown good loading capacities for uranium from nitric acid medium and also good re-usability upto few cycles. The recovery of uranium was > 99%. The functionalized silica gels have been tested for the recovery of uranium from simulated silicide fuel dissolver solution. Amine and amido pyridyl phosphate functionalized silica gel has shown a moderate separation of zirconium from hafnium from aqueous nitric acid medium under mild condition. Separation of zirconium from hafnium was also tested from simulated zircon ore dissolver solution. 1,8-dihydroxyanthraquinone functionalized silica gel has shown good binding with the rare earths compared to uranium in the nitric acid-sodium carbonate medium. Dithiodiglycolamide was able to extract palladium completely from hydrochloric acid medium. It was also tested for the recovery of palladium from simulated spent automobile catalyst dissolver solution. Studies have shown that the nitrogen donor ligands have a higher tendency to bind with the hazardous elements like lead, copper from aqueous medium than the oxygen donor ligands; but zinc ions bind stonger with the oxygen donor ligands. The complexation and binding of the metal ions with the ligands have been studied at molecular level. All the complexes have been modeled, their geometries were optimized, binding energies were calculated and the bond vibrational frequencies were matched with the experimental data. The theoretical results give details information about the complexes of the metal ions and also help in further designing of new selective ligands for the metal ions.

Summary and Conclusion

Industrial wastes create pollution to the environment due to the presence of toxic chemicals as well as metal ions. These metal ions also have their individual applications in various fields. Therefore, extraction and separation of these metal ions from the industrial aqueous streams is beneficial both as their re-usability as well as environmental concerns. In this regards, synthesis and characterisation of new ligands have been carried out to extract, separate and remove the metal ions of concern from the aqueous medium. Metal ions targetted in this present work are uranium, zirconium and hafnium, rare earth elements, palladium and heavy elements like lead, chromium, zinc and copper. Computational calculations on the metal-ligand complexes have been carried out to understand them at the molecular level which provides the binding pattern of the metal ions with different ligand.

The works carried out in the present thesis have been described below.

i) Phosphate functionalised silica gels namely, single phosphate functionalised silica gel (SPFSG), bi-phosphate functionalised silica gel (BPFSG), tri-phosphate functionalised silica gel (TPFSG) have been synthesised and characterised for the extraction of uranium from aqueous streams. Amine and amidopyridyl phosphate functionalised has also been synthesised, characterised for the sorption of uranium. SPFSG has been used for the extraction and sorption of uranium from nitric acid-sodium hydroxide medium at pH 1.0. Sorption kinetics is found to be fast for uranium and sorption takes place within five minutes with a sorbent dose of 5gL^{-1} . Sorption kinetics fits well in the pseudo second order kinetic model indicating that the sorption reaction is governed by the complexation reaction between the uranium species with

the ligand. Sorption isotherm follows Freundlich isotherm model indicating the presence of heterogeneous surface on SPFSG. Loading capacity on the SPFSG sorbent is high and it is 25 mg g^{-1} . SPFSG has shown very good re-usability. >99% recovery of uranium is possible from the loaded SPFSG in multiple stages. Selective sorption of uranium has been obtained from silicide fuel dissolver solution over iron(III), aluminium(III), calcium(II) and magnesium(II). Computational results match well with the experimental FT-IR results. The computed asymmetric vibrational frequencies (ν_{asym}) of bare and coordinated P=O are found within 35 cm^{-1} difference of the IR vibrational peaks. Theoretical calculations have confirmed the ratio of uranium (VI) with SPFSG sorbent is 1:2. Binding energy of the complex has been found to be $3.8 \text{ kcal mol}^{-1}$.

As the sorption experiments for uranium (VI) is not possible to carry-out in the nitric acid-sodium hydroxide medium above pH 4 due to the hydrolysis and precipitation of uranium at higher pH (higher than pH 4), the sorption experiments using BPFSG, TPFSG and AAPPFSG sorbents have been carried out for the sorption and extraction of uranium (VI) from nitric acid-sodium carbonate medium where uranium (VI) remains in the solution as their carbonate complexes. Sorption experiments using BPFSG, TPFSG and AAPPFSG have been carried out at pH 4.5. Sorption kinetics is fast for all these sorbents where the sorption equilibriums are attained within ten minutes with the sorbent dose of 2 g L^{-1} . Sorption kinetics follow pseudo second order kinetics model. Sorption isotherms follow Freundlich isotherm model. It is observed that sorption is high for AAPPFSG at pH less than pH 4.5 whereas, it decreases at higher pH than pH 5. This is due to the steric hindrance in the sorption of bulky uranium carbonate complexes on the AAPPFSG sorbent where the bulkiness is present around the binding site. Loading capacities of uranium (VI) on

BPFSG, TPFSG and AAPPFSG have been found to be 34mg g^{-1} , 36 mg g^{-1} and 38 mg g^{-1} respectively.

ii) Mono-phosphate functionalised silica gel (MPFSG) has been synthesised, characterised and applied for the extraction and separation of zirconium from hafnium in the nitric acid medium. In MPFSG sorbent, the phosphate group is directly attached to the solid silica surface where no flexible carbon chain is present. Since the separation of zirconium from hafnium is carried out in large scale using tri-butyl phosphate (TBP) solvent in the solvent extraction technique, trials have been taken for their separation using mono-, bi- and multiple phosphate functionalised silica gels in the nitric acid medium. In this respect, MPFSG, BPFSG and AAPPFSG sorbents have been tried for the extraction, separation and recovery of zirconium and hafnium in nitric acid medium. Sorption experiments have shown that sorption increases in the pH range 0.5-1.2, afterwards sorption for both zirconium and hafnium decreases, and then sorption increases above pH 1.6. These are the cumulative effects of the surface charge of the functionalised silica gels as well as the species of zirconium and hafnium present in the solution. Variation of pH of the feed solutions has also indicated that as the number of functional groups in the sorbent increases, the selectivity of the sorbent towards zirconium increases providing a better separation of zirconium from hafnium. Kinetics is fast for both zirconium and hafnium where the sorption equilibriums are attained within ten minutes with the sorbent dose of 1.2 gL^{-1} . Sorption rates become slower in the order of $\text{MPFSG} < \text{BPFSG} < \text{AAPPFSG}$. Kinetics is fast using MPFSG where there is no flexible carbon chain is present between the phosphate group and the silica surface. Whereas, a flexible carbon chain is present in case of BPFSG and in case of AAPPFSG, bulkiness around the binding sites is present which produces obstruction to the approaching metal ions to

AAPPFSG decreasing the kinetics rate. Kinetics data follow pseudo second order model in all these cases. This implies that all the reactions are governed by the complexation reactions between zirconium and hafnium with the sorbents. Sorption isotherms have shown that sorption of both zirconium and hafnium takes place better using AAPPFSG as well as using BPFSG. Loading capacities of zirconium on MPFSG, BPFSG and APPFSG have been obtained as 12.3, 16.7 and 16 mgg^{-1} respectively and for hafnium on MPFSG, BPFSG and AAPPFSG have been found to be 11.8, 15 and 14.2 mgg^{-1} respectively. Desorption of loaded zirconium and hafnium has been carried out by varying the pH of the eluent solutions in between pH 0.65 to 1.2. It has been observed that separation of zirconium from hafnium decreases as the pH increases. Separation is better obtained using AAPPFSG sorbent which has the maximum number of binding sites and which is also observed in the column studies.

iii) Rare earth elements are also formed during the fission reaction of uranium. Minor actinides are also produced during the fission reactions. During the reprocessing of spent fuel high level wastes (HLW) are generated which have very high radioactivity due to the presence of minor actinides which need to be removed before vitrification of HLW. It has been proposed that minor actinides need to be burnt at accelerator driven subcritical reactors (ADS) before the vitrification of HLW. But the presence of lanthanide elements (i.e. the rare earths) cause the deficiency of thermal neutrons inside the reactor due to their very high neutron absorption cross sections. Therefore, separation of lanthanides from minor actinides is an essential step before burning the minor actinides. Therefore, separation of minor actinides from lanthanides has been tried by both solvent extraction method as well as membrane separation method using ethyl-bis-triazinylpyridine (Et-BTP) as the solvent. Et-BTP is selective for actinides (e.g. Am^{3+}) compared to lanthanides (e.g. Eu^{3+}) in presence

of chlorinated cobalt dicarbollide (CCD). 0.02M Et-BTP and 0.005M CCD in 0.001M nitrobenzene has been found to be the suitable solvent from the solvent extraction studies. Feed acidity has been found to be 0.1M nitric acid as the optimised acidity for extraction. But the stripping of actinides from the loaded Et-BTP solvent is not possible by simple variation of acidity of the strip solution as it is difficult to break the actinide-Et-BTP-CCD complex. Therefore, EDTA has been used as the complexing agent for the back-extraction of the loaded metal ions (present in the organic phase) into the aqueous phase. 0.01M EDTA has been found to be the optimised strip solution. But, during the experiments in the supported liquid membrane (SLM) technique, EDTA in the strip solution precipitates in few minutes due to the transport of nitric acid from the feed solution along with Am^{3+} . This affects the transport of Am^{3+} in to the strip solution. To suppress the precipitation of EDTA in the strip solution, 0.1M chloro-acetate buffer has been introduced along with EDTA in the strip solution. The separation factor values of Am^{3+} over lanthanides like Nd^{3+} and Eu^{3+} have been found to be 11.7 and 4.2 respectively.

Sorbent like 1,8-dihydroxy anthraquinone functionalised silica gel (DHAFSG) has been synthesised, characterised and tried as the solid phase extractant for the extraction and separation of actinide (e.g. uranium(VI)) from rare earth elements (like Eu (III), Sm(III), Yb(III) and Y(III)). It has been found from the sorption studies that sorption of uranium as well as rare earth elements increase with the increase in the pH of the feed solution. The optimised pH obtained for the sorption studies is pH 6. Kinetics studies have shown that sorption equilibrium is attained within five minutes with a sorbent dose of 2 gL^{-1} for both actinide and rare earth elements. Kinetics data fit well in the pseudo second order kinetic model indicating that the sorption of both actinide and rare earth elements take place by complexation with DHAFSG in nitric

acid medium and the rate of complexation is the rate determining step in all these cases. Sorption isotherm studies have also been carried out for both actinide and rare earth elements. Isotherm data in all these cases fit well with the Freundlich isotherm model indicating that the surface of DHAFSG has heterogeneous sites for binding of metal ions. Loading capacities of rare earth elements have been found to be more on DHAFSG compared to uranium(VI) indicating a stronger binding of rare earth elements with DHAFSG. Loading capacity values for Eu(III), Sm(III), Yb(III), Y(III) and U(VI) on DHAFSG have been found to be 23, 20, 24, 21 and 15 mg g^{-1} . From the study of the effect of the variation of pH of feed solution on the sorption of both actinide and rare earth elements, it has been found that difference in the sorption of actinide is not very different from that of rare earth elements. This indicates that their separation is not possible to separate them by varying the pH of the eluent. Therefore, different eluent solutions have been tried like sodium carbonate, hydrochloric acid, oxalic acid, ethylenediamine tetraacetic acid (EDTA) etc. during their de-sorption studies. It has been found that separation of actinide from rare earth elements is possible in two steps: i) complete elution of uranium using 0.01M sodium carbonate solution, ii) complexing out the rare earth elements using 0.02M hydrochloric acid solution. Separation of actinide from rare earth elements is not possible using oxalic acid and EDTA as these reagents form complexes with both the rare earth elements as well as uranium. 0.01M oxalic acid elutes ~ 95% of the loaded rare earth elements along with 5% loaded uranium and 0.01M EDTA (pH >5) elutes ~90% loaded rare earth elements along with 70% loaded uranium.

iv) Palladium is produced in the fission reaction of uranium. During reprocessing of spent fuel it also comes in HLW and forms a separate phase during vitrification of HLW. Therefore, its separation from HLW is a mandate. Moreover, recovery of

palladium from spent automobile catalyst is also required because of its growing demand and poor availability in nature. In this context, extraction and separation of palladium has been tried using novel di-thiodiglycolamide (DTDGA) ligand from both HLW solution and spent automobile catalyst. Both the solvent extraction method and membrane separation method have been exploited for the extraction studies. Palladium has been extracted from spent catalyst dissolved in hydrochloric acid medium using DTDGA ligand. Kinetics of extraction of palladium is fast and equilibrium is attained within five minutes. Extraction of palladium increases as the feed acidity increases upto 3.0M hydrochloric acid concentration and then extraction becomes constant with the increase in feed acidity. To investigate the involvement of chloride ion in the complexation reaction, extraction studies have been carried out at a fixed ionic strength of 3.0M chloride ion. It has been found that extraction of palladium remains constant as long as the chloride ion concentration remains constant. The initial increase in the extraction of palladium with the increase in feed acidity is due to the increase in chloride ion concentration. These studies confirm that chloride ion takes part in the complexation reaction of palladium with DTDGA. The stoichiometry of the reaction has been found by mole ratio plot which has indicated a 1:1 stoichiometry of Pd: DTDGA. Therefore, the extracted complex has been found to be PdCl₂:DTDGA. As the extracted complex is a neutral one, extraction of palladium decreases as the polarity of the diluent increases and it has been observed that almost complete extraction is possible using n-paraffinic diluents. Back-extraction (i.e. stripping) of palladium from the loaded solvent has been obtained using 0.01M thiourea in 0.1M HCl which has shown >99% back-extraction of palladium in a single stage. A very high selectivity of DTDGA has been observed for palladium during its recovery from simulated spent catalyst dissolver (SSCD) solution over other metal

ions like iron, chromium, nickel and platinum present in the solution. This shows the applicability of this ligand for practical use.

Extraction and separation of palladium from HLW has been studied using membrane technique. The feed acidity has been varied from 1M nitric acid to 6M nitric acid. It has been observed that extraction of palladium increases when the feed acidity is increased from 1M nitric acid to 2M nitric acid as the nitrate ion takes part in the complexation reaction and palladium gets extracted as $\text{Pd}(\text{NO}_3)_2 \cdot \text{DTDGA}$ complex which was investigated earlier. Extraction of palladium does not increase much above 2M nitric acid and becomes almost constant. >99% extraction of palladium is obtained for the feed acidities 2M-6M. It has also been observed that after an extraction operation for about 120 minutes, the feed acidity decreases to 2.9M from initial 3M and to 5.7M from initial 6M. This is due to the transport of nitric acid from feed solution to through the organic phase and the $\text{DTDGA} \cdot \text{HNO}_3$ complex is formed decreasing the availability of free DTDGA for the extraction of palladium. Due to this effect extraction of palladium does not increase much above 2M of feed acidity. For optimising the DTDGA concentration for optimum transport of palladium with less viscosity of the solvent phase posing very less hindrance to palladium transport, DTDGA concentration has been varied from 0.005M to 0.05M in the paraffinic diluent like n-dodecane. It has been found that 0.025M DTDGA in n-dodecane is the optimized concentration of DTDGA for quantitative transport of palladium. Transport of palladium decreases as the thickness of the membrane increases. It has been observed that in 120 minutes of operation, ~99% palladium is transported keeping membrane thickness as 65 mm and that is ~76% using 325 mm of membrane thickness. It has been observed that >99% of Pd(II) is transported in 120 minutes of operation. Stability of membrane has been observed to be decreased after repeated use

of the membrane. This is due to the loss of organic solvent from the membrane pores due to the aqueous solubility of the carrier, osmotic or hydro-static pressure gradient etc. It has been found that after using the supported liquid membrane for six cycles (time of operation of each cycle has been kept as 120 min), transport of palladium has come down to ~97% which is ~99% in the first cycle of operation. These studies confirm that supported liquid membrane containing DTDGA ligand can be used for the palladium extraction from acidic medium.

v) Heavy elements like lead, chromium, zinc and copper come into aqueous body from different industrial waste streams. These elements are extremely hazardous to human health if inhaled or ingested. Therefore, efforts have been made for the extraction and removal of these heavy elements from the aqueous body. In this respect, butanol functionalised silica gel (BFSG) and aminopyridyl amine functionalised silica gel (APAFSG) have been synthesised and characterised and tested for the removal of these heavy elements from the aqueous streams. The results have been compared with the results obtained by using mere alkali treated silica (ASG). It has been observed that nitrogen donor APAFSG ligand selectively complexes with lead. Almost complete extraction of lead has been observed. Whereas, ~30% extraction of copper has been obtained using APAFSG. The oxygen donor ligands like BFSG and also ASG selectively extracts zinc(II) from the aqueous medium. Extraction of chromium(VI) is less probably due to the presence of dichromate ion in the solution which may face coulombic repulsion from the negative oxide ion present in the surfaces of BFSG and ASG.

From the studies carried out in the present work, it can be concluded that

i) Phosphate functionalised silica gels (SPFSG, BPFSG, TPFSG) as well as amido pyridyl phosphate functionalised silica gel (AAPPFSG) can be used for the

extraction of uranium by SPE method. AAPPFSG has also shown its ability to separate zirconium from hafnium and is a probable candidate for practical usage by SPE technique.

ii) DHAFSG sorbent is a good binder with rare earth elements and has shown its ability to separate rare earths from uranium by SPE method. Et-BTP solvent on the other hand, selectively binds with actinides in presence of CCD as an auxiliary ligand and separates well from lanthanides by both solvent extraction and membrane techniques.

iii) DTDGA solvent has shown to be a promising ligand to separate palladium from both simulated spent catalyst dissolver solution as well as high level waste and can be used for practical applications.

iv) APAFSG sorbent has shown to be a probable candidate to selectively bind and extract lead from aqueous solution.

v) Computational results have highlighted on the metal-ligand complexes at molecular level. This has focussed on the donating atom present in the ligand, the mode of co-ordination and also the ions/ molecules present in the first and second co-ordination spheres of the metal ions. This leads to the design of a more selective ligand for the metal ions of interest.

These ligands are proposed to be used for the scale up studies (upto bench scale) for demonstrating their applications.

Summary and Conclusion

Industrial wastes create pollution to the environment due to the presence of toxic chemicals as well as metal ions. These metal ions also have their individual applications in various fields. Therefore, extraction and separation of these metal ions from the industrial aqueous streams is beneficial both as their re-usability as well as environmental concerns. In this regards, synthesis and characterisation of new ligands have been carried out to extract, separate and remove the metal ions of concern from the aqueous medium. Metal ions targetted in this present work are uranium, zirconium and hafnium, rare earth elements, palladium and heavy elements like lead, chromium, zinc and copper. Computational calculations on the metal-ligand complexes have been carried out to understand them at the molecular level which provides the binding pattern of the metal ions with different ligand.

The works carried out in the present thesis have been described below.

i) Phosphate functionalised silica gels namely, single phosphate functionalised silica gel (SPFSG), bi-phosphate functionalised silica gel (BPFSG), tri-phosphate functionalised silica gel (TPFSG) have been synthesised and characterised for the extraction of uranium from aqueous streams. Amine and amidopyridyl phosphate functionalised has also been synthesised, characterised for the sorption of uranium. SPFSG has been used for the extraction and sorption of uranium from nitric acid-sodium hydroxide medium at pH 1.0. Sorption kinetics is found to be fast for uranium and sorption takes place within five minutes with a sorbent dose of 5gL^{-1} . Sorption kinetics fits well in the pseudo second order kinetic model indicating that the sorption reaction is governed by the complexation reaction between the uranium species with

the ligand. Sorption isotherm follows Freundlich isotherm model indicating the presence of heterogeneous surface on SPFSG. Loading capacity on the SPFSG sorbent is high and it is 25 mg g^{-1} . SPFSG has shown very good re-usability. $>99\%$ recovery of uranium is possible from the loaded SPFSG in multiple stages. Selective sorption of uranium has been obtained from silicide fuel dissolver solution over iron(III), aluminium(III), calcium(II) and magnesium(II). Computational results match well with the experimental FT-IR results. The computed asymmetric vibrational frequencies (ν_{asym}) of bare and coordinated P=O are found within 35 cm^{-1} difference of the IR vibrational peaks. Theoretical calculations have confirmed the ratio of uranium (VI) with SPFSG sorbent is 1:2. Binding energy of the complex has been found to be $3.8 \text{ kcal mol}^{-1}$.

As the sorption experiments for uranium (VI) is not possible to carry-out in the nitric acid-sodium hydroxide medium above pH 4 due to the hydrolysis and precipitation of uranium at higher pH (higher than pH 4), the sorption experiments using BPFSG, TPFSG and AAPPFSG sorbents have been carried out for the sorption and extraction of uranium (VI) from nitric acid-sodium carbonate medium where uranium (VI) remains in the solution as their carbonate complexes. Sorption experiments using BPFSG, TPFSG and AAPPFSG have been carried out at pH 4.5. Sorption kinetics is fast for all these sorbents where the sorption equilibriums are attained within ten minutes with the sorbent dose of 2 g L^{-1} . Sorption kinetics follow pseudo second order kinetics model. Sorption isotherms follow Freundlich isotherm model. It is observed that sorption is high for AAPPFSG at pH less than pH 4.5 whereas, it decreases at higher pH than pH 5. This is due to the steric hindrance in the sorption of bulky uranium carbonate complexes on the AAPPFSG sorbent where the bulkiness is present around the binding site. Loading capacities of uranium (VI) on

BPFSG, TPFSG and AAPPFSG have been found to be 34mg g^{-1} , 36 mg g^{-1} and 38 mg g^{-1} respectively.

ii) Mono-phosphate functionalised silica gel (MPFSG) has been synthesised, characterised and applied for the extraction and separation of zirconium from hafnium in the nitric acid medium. In MPFSG sorbent, the phosphate group is directly attached to the solid silica surface where no flexible carbon chain is present. Since the separation of zirconium from hafnium is carried out in large scale using tri-butyl phosphate (TBP) solvent in the solvent extraction technique, trials have been taken for their separation using mono-, bi- and multiple phosphate functionalised silica gels in the nitric acid medium. In this respect, MPFSG, BPFSG and AAPPFSG sorbents have been tried for the extraction, separation and recovery of zirconium and hafnium in nitric acid medium. Sorption experiments have shown that sorption increases in the pH range 0.5-1.2, afterwards sorption for both zirconium and hafnium decreases, and then sorption increases above pH 1.6. These are the cumulative effects of the surface charge of the functionalised silica gels as well as the species of zirconium and hafnium present in the solution. Variation of pH of the feed solutions has also indicated that as the number of functional groups in the sorbent increases, the selectivity of the sorbent towards zirconium increases providing a better separation of zirconium from hafnium. Kinetics is fast for both zirconium and hafnium where the sorption equilibriums are attained within ten minutes with the sorbent dose of 1.2 gL^{-1} . Sorption rates become slower in the order of $\text{MPFSG} < \text{BPFSG} < \text{AAPPFSG}$. Kinetics is fast using MPFSG where there is no flexible carbon chain is present between the phosphate group and the silica surface. Whereas, a flexible carbon chain is present in case of BPFSG and in case of AAPPFSG, bulkiness around the binding sites is present which produces obstruction to the approaching metal ions to

AAPPFSG decreasing the kinetics rate. Kinetics data follow pseudo second order model in all these cases. This implies that all the reactions are governed by the complexation reactions between zirconium and hafnium with the sorbents. Sorption isotherms have shown that sorption of both zirconium and hafnium takes place better using AAPPFSG as well as using BPFSG. Loading capacities of zirconium on MPFSG, BPFSG and APPFSG have been obtained as 12.3, 16.7 and 16 mgg^{-1} respectively and for hafnium on MPFSG, BPFSG and AAPPFSG have been found to be 11.8, 15 and 14.2 mgg^{-1} respectively. Desorption of loaded zirconium and hafnium has been carried out by varying the pH of the eluent solutions in between pH 0.65 to 1.2. It has been observed that separation of zirconium from hafnium decreases as the pH increases. Separation is better obtained using AAPPFSG sorbent which has the maximum number of binding sites and which is also observed in the column studies.

iii) Rare earth elements are also formed during the fission reaction of uranium. Minor actinides are also produced during the fission reactions. During the reprocessing of spent fuel high level wastes (HLW) are generated which have very high radioactivity due to the presence of minor actinides which need to be removed before vitrification of HLW. It has been proposed that minor actinides need to be burnt at accelerator driven subcritical reactors (ADS) before the vitrification of HLW. But the presence of lanthanide elements (i.e. the rare earths) cause the deficiency of thermal neutrons inside the reactor due to their very high neutron absorption cross sections. Therefore, separation of lanthanides from minor actinides is an essential step before burning the minor actinides. Therefore, separation of minor actinides from lanthanides has been tried by both solvent extraction method as well as membrane separation method using ethyl-bis-triazinylpyridine (Et-BTP) as the solvent. Et-BTP is selective for actinides (e.g. Am^{3+}) compared to lanthanides (e.g. Eu^{3+}) in presence

of chlorinated cobalt dicarbollide (CCD). 0.02M Et-BTP and 0.005M CCD in 0.001M nitrobenzene has been found to be the suitable solvent from the solvent extraction studies. Feed acidity has been found to be 0.1M nitric acid as the optimised acidity for extraction. But the stripping of actinides from the loaded Et-BTP solvent is not possible by simple variation of acidity of the strip solution as it is difficult to break the actinide-Et-BTP-CCD complex. Therefore, EDTA has been used as the complexing agent for the back-extraction of the loaded metal ions (present in the organic phase) into the aqueous phase. 0.01M EDTA has been found to be the optimised strip solution. But, during the experiments in the supported liquid membrane (SLM) technique, EDTA in the strip solution precipitates in few minutes due to the transport of nitric acid from the feed solution along with Am^{3+} . This affects the transport of Am^{3+} in to the strip solution. To suppress the precipitation of EDTA in the strip solution, 0.1M chloro-acetate buffer has been introduced along with EDTA in the strip solution. The separation factor values of Am^{3+} over lanthanides like Nd^{3+} and Eu^{3+} have been found to be 11.7 and 4.2 respectively.

Sorbent like 1,8-dihydroxy anthraquinone functionalised silica gel (DHAFSG) has been synthesised, characterised and tried as the solid phase extractant for the extraction and separation of actinide (e.g. uranium(VI)) from rare earth elements (like Eu (III), Sm(III), Yb(III) and Y(III)). It has been found from the sorption studies that sorption of uranium as well as rare earth elements increase with the increase in the pH of the feed solution. The optimised pH obtained for the sorption studies is pH 6. Kinetics studies have shown that sorption equilibrium is attained within five minutes with a sorbent dose of 2 gL^{-1} for both actinide and rare earth elements. Kinetics data fit well in the pseudo second order kinetic model indicating that the sorption of both actinide and rare earth elements take place by complexation with DHAFSG in nitric

acid medium and the rate of complexation is the rate determining step in all these cases. Sorption isotherm studies have also been carried out for both actinide and rare earth elements. Isotherm data in all these cases fit well with the Freundlich isotherm model indicating that the surface of DHAFSG has heterogeneous sites for binding of metal ions. Loading capacities of rare earth elements have been found to be more on DHAFSG compared to uranium(VI) indicating a stronger binding of rare earth elements with DHAFSG. Loading capacity values for Eu(III), Sm(III), Yb(III), Y(III) and U(VI) on DHAFSG have been found to be 23, 20, 24, 21 and 15 mgg^{-1} . From the study of the effect of the variation of pH of feed solution on the sorption of both actinide and rare earth elements, it has been found that difference in the sorption of actinide is not very different from that of rare earth elements. This indicates that their separation is not possible to separate them by varying the pH of the eluent. Therefore, different eluent solutions have been tried like sodium carbonate, hydrochloric acid, oxalic acid, ethylenediamine tetraacetic acid (EDTA) etc. during their de-sorption studies. It has been found that separation of actinide from rare earth elements is possible in two steps: i) complete elution of uranium using 0.01M sodium carbonate solution, ii) complexing out the rare earth elements using 0.02M hydrochloric acid solution. Separation of actinide from rare earth elements is not possible using oxalic acid and EDTA as these reagents form complexes with both the rare earth elements as well as uranium. 0.01M oxalic acid elutes ~ 95% of the loaded rare earth elements along with 5% loaded uranium and 0.01M EDTA (pH >5) elutes ~90% loaded rare earth elements along with 70% loaded uranium.

iv) Palladium is produced in the fission reaction of uranium. During reprocessing of spent fuel it also comes in HLW and forms a separate phase during vitrification of HLW. Therefore, its separation from HLW is a mandate. Moreover, recovery of

palladium from spent automobile catalyst is also required because of its growing demand and poor availability in nature. In this context, extraction and separation of palladium has been tried using novel di-thiodiglycolamide (DTDGA) ligand from both HLW solution and spent automobile catalyst. Both the solvent extraction method and membrane separation method have been exploited for the extraction studies. Palladium has been extracted from spent catalyst dissolved in hydrochloric acid medium using DTDGA ligand. Kinetics of extraction of palladium is fast and equilibrium is attained within five minutes. Extraction of palladium increases as the feed acidity increases upto 3.0M hydrochloric acid concentration and then extraction becomes constant with the increase in feed acidity. To investigate the involvement of chloride ion in the complexation reaction, extraction studies have been carried out at a fixed ionic strength of 3.0M chloride ion. It has been found that extraction of palladium remains constant as long as the chloride ion concentration remains constant. The initial increase in the extraction of palladium with the increase in feed acidity is due to the increase in chloride ion concentration. These studies confirm that chloride ion takes part in the complexation reaction of palladium with DTDGA. The stoichiometry of the reaction has been found by mole ratio plot which has indicated a 1:1 stoichiometry of Pd: DTDGA. Therefore, the extracted complex has been found to be PdCl₂:DTDGA. As the extracted complex is a neutral one, extraction of palladium decreases as the polarity of the diluent increases and it has been observed that almost complete extraction is possible using n-paraffinic diluents. Back-extraction (i.e. stripping) of palladium from the loaded solvent has been obtained using 0.01M thiourea in 0.1M HCl which has shown >99% back-extraction of palladium in a single stage. A very high selectivity of DTDGA has been observed for palladium during its recovery from simulated spent catalyst dissolver (SSCD) solution over other metal

ions like iron, chromium, nickel and platinum present in the solution. This shows the applicability of this ligand for practical use.

Extraction and separation of palladium from HLW has been studied using membrane technique. The feed acidity has been varied from 1M nitric acid to 6M nitric acid. It has been observed that extraction of palladium increases when the feed acidity is increased from 1M nitric acid to 2M nitric acid as the nitrate ion takes part in the complexation reaction and palladium gets extracted as $\text{Pd}(\text{NO}_3)_2 \cdot \text{DTDGA}$ complex which was investigated earlier. Extraction of palladium does not increase much above 2M nitric acid and becomes almost constant. >99% extraction of palladium is obtained for the feed acidities 2M-6M. It has also been observed that after an extraction operation for about 120 minutes, the feed acidity decreases to 2.9M from initial 3M and to 5.7M from initial 6M. This is due to the transport of nitric acid from feed solution to through the organic phase and the $\text{DTDGA} \cdot \text{HNO}_3$ complex is formed decreasing the availability of free DTDGA for the extraction of palladium. Due to this effect extraction of palladium does not increase much above 2M of feed acidity. For optimising the DTDGA concentration for optimum transport of palladium with less viscosity of the solvent phase posing very less hindrance to palladium transport, DTDGA concentration has been varied from 0.005M to 0.05M in the paraffinic diluent like n-dodecane. It has been found that 0.025M DTDGA in n-dodecane is the optimized concentration of DTDGA for quantitative transport of palladium. Transport of palladium decreases as the thickness of the membrane increases. It has been observed that in 120 minutes of operation, ~99% palladium is transported keeping membrane thickness as 65 mm and that is ~76% using 325 mm of membrane thickness. It has been observed that >99% of Pd(II) is transported in 120 minutes of operation. Stability of membrane has been observed to be decreased after repeated use

of the membrane. This is due to the loss of organic solvent from the membrane pores due to the aqueous solubility of the carrier, osmotic or hydro-static pressure gradient etc. It has been found that after using the supported liquid membrane for six cycles (time of operation of each cycle has been kept as 120 min), transport of palladium has come down to ~97% which is ~99% in the first cycle of operation. These studies confirm that supported liquid membrane containing DTDGA ligand can be used for the palladium extraction from acidic medium.

v) Heavy elements like lead, chromium, zinc and copper come into aqueous body from different industrial waste streams. These elements are extremely hazardous to human health if inhaled or ingested. Therefore, efforts have been made for the extraction and removal of these heavy elements from the aqueous body. In this respect, butanol functionalised silica gel (BFSG) and aminopyridyl amine functionalised silica gel (APAFSG) have been synthesised and characterised and tested for the removal of these heavy elements from the aqueous streams. The results have been compared with the results obtained by using mere alkali treated silica (ASG). It has been observed that nitrogen donor APAFSG ligand selectively complexes with lead. Almost complete extraction of lead has been observed. Whereas, ~30% extraction of copper has been obtained using APAFSG. The oxygen donor ligands like BFSG and also ASG selectively extracts zinc(II) from the aqueous medium. Extraction of chromium(VI) is less probably due to the presence of dichromate ion in the solution which may face coulombic repulsion from the negative oxide ion present in the surfaces of BFSG and ASG.

From the studies carried out in the present work, it can be concluded that

i) Phosphate functionalised silica gels (SPFSG, BPFSG, TPFSG) as well as amido pyridyl phosphate functionalised silica gel (AAPPFSG) can be used for the

extraction of uranium by SPE method. AAPPFSG has also shown its ability to separate zirconium from hafnium and is a probable candidate for practical usage by SPE technique.

ii) DHAFSG sorbent is a good binder with rare earth elements and has shown its ability to separate rare earths from uranium by SPE method. Et-BTP solvent on the other hand, selectively binds with actinides in presence of CCD as an auxiliary ligand and separates well from lanthanides by both solvent extraction and membrane techniques.

iii) DTDGA solvent has shown to be a promising ligand to separate palladium from both simulated spent catalyst dissolver solution as well as high level waste and can be used for practical applications.

iv) APAFSG sorbent has shown to be a probable candidate to selectively bind and extract lead from aqueous solution.

v) Computational results have highlighted on the metal-ligand complexes at molecular level. This has focussed on the donating atom present in the ligand, the mode of co-ordination and also the ions/ molecules present in the first and second co-ordination spheres of the metal ions. This leads to the design of a more selective ligand for the metal ions of interest.

These ligands are proposed to be used for the scale up studies (upto bench scale) for demonstrating their applications.